AN INVESTIGATION OF A PALAEOMAGNETIC POLARITY REVERSAL IN THE EASTERN BUSHVELD COMPLEX

by

NOLA NIXON

Submitted in partial fulfilment of the requirements
for the degree of

MASTER OF SCIENCE

in the Faculty of Science

UNIVERSITY OF PRETORIA

MAY 1988

It is amusing to reflect that if the pioneering paleomagnetists of the early fifties had known, or even suspected, the full complexity (chemical, mineralogical, textural, magnetic-structural) of the magnetic properties of rocks, they probably would have thrown up their hands, declared rocks inherently unreliable, and turned to lesser things. Ignorance, it would seem, can sometimes be a blessing.

J. Verhoogen

ABSTRACT

Palaeomagnetic and petrological investigations were undertaken near Roossenekal, at the contact between subzones A and B of the main zone in the eastern Bushveld Complex. Three rock-types were identified at the site; the upper mottled anorthosite, a two-pyroxene gabbro and a critical zone-associated noritic sill.

Twenty orientated core samples, which yielded fifty eight specimens, were obtained from the three rock-types for palaeomagnetic purposes. Additional samples were collected for petrographical and mineralogical studies.

Palaeomagnetic investigations comprised measurement of magnetization, magnetic susceptibility and anisotropy of susceptibilty of the specimens. Additionally, specimens were subjected to alternating field and continuous thermal demagnetization, to isolate the components of magnetization. Data obtained from Zijderveld stability diagrams, difference vectors, and great circle techniques facilitated the identification of magnetization components.

Petrographic procedures included microscopy under transmitted light, ore microscopy, electron microprobe and scanning electron microscope investigations. Electron microprobe work involved quantitative analysis of silicates and microscopic ore minerals, as well as qualitative analysis of sub-microscopic ore grains by using X-ray and backscattered electron images.

Mineralogical and palaeomagnetic data suggest that the differences in ore mineralogy, and in particular the relative quantities of the respective ore minerals, are responsible for the observed polarity differences in these rocks. The spurious behaviour of certain specimens, and the reversed polarity of the norite to that of the anorthosite/gabbro unit, is associated with hematite exsolutions in ilmenite. Ilmeno-hematite is thus linked to a partial self-reversal of magnetization at this site.

SAMEVATTING

Paleomagnetiese en petrologiese ondersoeke is onderneem naby Roossenekal, by die kontak tussen subsones A en B van die hoofsone van die Bosveld Kompleks. Drie gesteentetipes is hier onderskei; die boonste gevlekte anortosiet, ´n twee-pirokseen gabbro en ´n plaat geassosieerd met die kritieke sone.

Twintig georienteerde kerne, waaruit 58 monsters verkry is, is by die lokaliteit geneem vir paleomagnetiese ondersoeke. Hierdie monsters was verteenwoordigend van die drie gesteentetipes. Verdere monsters is verkry vir petrologiese en mineralogiese studies.

Paleomagnetiese ondersoeke het die meet van magnetisasie, magnetiese suseptibiliteit en anisotropie van suseptibiliteit behels. Monsters is met behulp van wisselveld- en deurlopende termiese demagnetisasie skoongemaak om magnetiese komponente te isoleer. Data wat verkry is vanaf Zijderveld stabiliteitsdiagramme, verskilvektore, en grootsirkeltegnieke is geinterpreteer om komponente van magnetisasie te identifiseer.

Petrografiese ondersoeke het mikroskopie onder deurvallende lig, ertsmikroskopie, elektron mikrosonde- en skandeer elektronmikroskopie-tegnieke ingesluit. Elektron-mikroskopie het die volgende behels: kwantitatiewe analise van silikate en mikroskopiese ertsminerale, en kwalitatiewe analise van sub-mikroskopiese ertskorrels deur middel van X-straal- en weerkaatste elektronbeelde.

Mineralogiese en paleomagnetiese data dui daarop dat die verskille in ertsmineralogie, en spesifiek die relatiewe hoeveelhede van die onderskeie ertsminerale, vir die waargenome polariteitsverskille tussen die gesteentetipes verantwoordelik is. Die onvoorspelbare gedrag van sommige monsters, en die omgekeerde polariteit van die noriet met betrekking tot die anortosiet/gabbro eenheid, is te wyte aan hematietuitskeidings in ilmeniet. Ilmeno-hematiet is dus geassosieer met ´n gedeeltelike selfomkering van magnetisasie by hierdie lokaliteit.

CONTENTS

LIST OF FIGURES

LIST OF TABLES

1. INTRODUCTION:

In 1959 Gough and van Niekerk isolated a direction of the natural remanent magnetization (NRM) of the mafic sequence of the Rustenburg Layered Suite of the Bushveld Complex. Subsequent palaeomagnetic investigations of the Bushveld Complex (Hattingh, 1983; 1986a; 1986b) have revealed that there is a strong correlation between magnetic signature and stratigraphic height in the layered succession. The investigation by Gough and van Niekerk did not reveal any mixed polarities, because the five sampling sites were all situated in the reversed polarity zone, or magnetic polarity zone B, defined by Hattingh (1983). Hattingh (op.cit.) divided the eastern and western Bushveld Complex into three distinct magnetic polarity zones; A, B and C. Zones A and C are normally magnetized, whereas magnetic polarity zone B is reversely magnetized with respect to the present day magnetic field. In the subdivision of the eastern Bushveld Complex, Hattingh separated zones A and B at the main mottled anorthosite layer in the Winnaarshoek Norite-Anorthosite. Magnetic polarity zones B and C were separated at an anorthosite layer in the Mapoch Gabbro-Norite. Stratigraphic nomenclature is according to S.A.C.S. (1980).

The present investigation was undertaken at the contact between zones A and B to determine whether it represents an apparent palaeomagnetic polarity reversal, or whether, alternatively, a geomagnetic field reversal or a self-reversal took place during the consolidation of these rocks.

It is generally accepted that the earth's magnetic field is generated by electrical currents circulating in the liquid part of the core, and that they are continually regenerated by a dynamo action (Tarling, 1983). According to this model, the boundary conditions for the dynamo are created by mass transfer in the lower mantle which produces undulations and variations in temperature at the core-mantle interface (Cox, 1980). The earth's present geomagnetic field consists of dipole and non-dipole components (Cox and Doell, 1960; Creer and Ispir, 1970); the palaeomagnetic record indicates that the magnitude of the non-dipole field vector increases dramatically with increasing latitude (Dodson, 1980). Based on palaeomagnetic investigations of

magnetic anomaly patterns recorded in the oceanic crust at spreading centres, it has been observed that the geomagnetic field has undergone changes in polarity on a random basis during at least the last 80 m.y. (Tarling, 1983, p. 200). The frequency of these reversals has been studied by authors such as Phillips (1977) and Fuller et al. (1979). According to the latter authors geomagnetic field reversals reflect an instability in the dynamo process. Several authors have reported the characteristics of the transitional field during a geomagnetic field reversal; recently Vadkovskii et al. (1980) confirmed that the intensity of the geomagnetic field during the transitional stage is greatly reduced. Hoffman (1982) reviewed geomagnetic field reversal models.

Approximately 500 cases of mixed polarity have been reported by Irving and Hastie (1975; in Morgan and Briden, 1981) in rocks of Precambrian age; Morgan and Briden found that a polarity reversal occurred in rocks of the Limpopo belt at between c. 2 000 m.y. and an unknown younger date. It is thus reasonable to assume that reversals have occurred throughout geological time, although they may not have been as frequent in Precambrian times (Morgan and Briden, 1981). There are indications that the earth's geomagnetic field is more stable after a reversed (R) to normal (N) reversal, than after a N-R reversal (Fuller et al., 1979). Excursions, on the other hand, represent departures of the geomagnetic field direction of more than 40^{o} from its normal direction. These last for 100 to 10 000 years, during which there is never a total reversal in polarity (Tarling, 1983, p. 211). According to Hoffman (1982) palaeomagnetic excursions closely resemble field behaviour at the onset of field reversals, and the possibility exists that excursions represent apparent failed reversals. Such an event, however, probably represents a time-interval which is too short to account for the polarity differences observed during this study. The c. 4 m.y.age difference between the critical zone (2054 $\pm$ 32 m.y.) and the Bushveld main zone (2058 $\pm$ 155 m.y.) as quoted by von Gruenewaldt et al. (1985) suggests this.

Complete and partial self-reversals have been reported in titanomagnetites in basaltic rocks by Schult (1968), Merrill and Grommé (1969), Nishida and Sasajima (1974), Kadzialko-Hofmokl and

Kruczyk (1976), Heller (1980), Hoffman and Shive (1982) and others. The classic self-reversal is that in the Haruna dacite, reported by Uyeda (1958). Reversals found in other rock types include the non-reproducible self-reversal in diorite (Merrill and Grommé, 1969), a self-reversal in shale containing pyrrhotite reported by Everitt (1962); more recently Champion and Christiansen (1984) reported occurrences of self-reversing magnetization associated with hemoilmenite in pyroclastic deposits, and Trukhin et al. (1984) found a self-reversal of thermoremanent magnetization (TRM) in kimberlite pipes. Neél (1951; in Tarling, 1983) proposed that a self-reversal could take place by means of magnetostatic exchange reactions between two sublattices in ferrimagnetic minerals. According to this hypothesis the direction of spontaneous magnetization would reverse when going from the high-temperature disordered state to the low-temperature ordered state, in which Ti-ions and vacancies preferentially occupy the six-fold sites. This is supported by Verhoogen (1962), who identified a large field in the TiO_2-FeO-Fe_2O_3 system in which self-reversal could take place. Subsequent to Neél's investigation Uyeda (1955) and Stacey (1963) questioned whether magnetostatic interactions were in fact strong enough to cause such a self-reversal. According to Heller (1980) there are three main self-reversal processes which depend on different physical mechanisms: firstly, a model proposed by Neél (1951), in which the direction of spontaneous magnetization in one phase reverses at a specific temperature and is associated with ionic ordering; secondly a two-phase model in which there is ionic migration across the boundary of the magnetic phases; and thirdly, a two-phase model in which magnetostatic interaction of electron spins between the two phases takes place. Verhoogen (1956, p. 208) estimated that this second process would take 100 000 to 1 000 000 years and that it would thus be non-reproducible in the laboratory. Many authors find that exchange interactions are only effective between nearest-neighbour atoms, and since oxygen atoms are always between the metal atoms, they can take part in this exchange coupling. This latter mechanism, which involves oxygen, is referred to as superexchange (Lindsley, 1976).

Uyeda (1958) found that certain members of the ilmenite-hematite series would become self-reversed even in a high applied field.

According to Morgan and Smith (1981) hematite exsolutions in ilmenite can cause a self-reversal, and Merrill (1975) found that the process of exsolution can result in a reversal of magnetization between the exsolved phase and the host mineral. Where magnetostatic interaction between two phases takes place, two minerals such as magnetite and pyrrhotite could take part in the interaction (Cox and Doell, 1960). Many authors have found that the mechanism of self-reversal in titanomagnetite is related to the fact that, in oxidized titanomagnetites rich in titanium (titanomaghemites), vacancies occur at cation positions in the spinel structure (for example, Schult, 1968). If it is assumed that the A-sublattice becomes larger than the B-sublattice during the oxidation process, then a resultant magnetization in the opposed direction will be produced (Schult, 1968).

A well defined relationship exists between titanomagnetite oxidation state and magnetic stability, which is partly due to the fact that oxidation processes result in a diminished effective grain size; this then results in an increase in the coercivity and stability of magnetization by the development of single-domain grains (Larsen and Strangway, 1966; Watkins and Haggerty, 1967). O´Reilly and Banerjee (1967) found that a high degree of low-temperature oxidation (about 390^{o} C) of titanomagnetites led to the decomposition of the metastable oxidation products and an increase in magnetization, due to the formation of secondary magnetite at these temperatures. More recently Tucker and O´Reilly (1980b) found that at an advanced stage of oxidation of titanomagnetite, fine-grained single-domain magnetite formed; this caused the crystals to carry an intense and stable magnetization with median destructive fields of tens of thousands of $A.m^{-1}$.

Any formation of new magnetic minerals under the Curie temperature of magnetite (T_c=578^{o}C (McElhinny, 1973)), and thus after the acquisition of a TRM, will give rise to a chemical remanent magnetization (CRM) as the crystallites grow through their critical blocking volumes (Tarling, 1983). Such chemical changes include deuteric alteration, post-deuteric alteration and oxidation and exsolution processes (Haggerty, 1976b). It is thus fundamental to this study to determine

whether the magnetic minerals are primary or secondary, or both, as apparent self-reversals can occur due to the acquisition of chemical remanences of differing ages and obviously at later stages than the acquisition of the TRM.

Grain size and domain-configuration are important in this investigation, to interpret the differences in magnetization in these rocks and to identify the carriers of remanence. Very fine grains of magnetic minerals are uniformly magnetized and are thus referred to as single-domain, whilst larger grains are subdivided into discrete magnetic domains by domain walls. It has been suggested by Lowrie and Fuller (1971) that the existence of a domain structure is energetically favoured in magnetite, before a grain is physically able to contain a domain wall. Consequently, they regard grains which are smaller than 0,03 micron as single-domain and those larger than 0,2 micron as multidomain, with an intermediate range in grain sizes of which the magnetization state is not clearly defined. The critical radius for the transition from single- to multidomain grains was found to be c. 0,7 micron by Soffel (1971). More recently O´Reilly (1976) confirmed that this transition occurs below 1 micron. According to Halgedahl and Fuller (1980), pseudo—single-domain grains of titanomagnetite (particles which are larger than the single-domain threshold size) can contribute greatly to remanence. During primary crystal growth the intensity of the TRM is drastically reduced by the development of one or more domains in opposite directions and the stability of the remanent magnetization is reduced, whilst the magnetic susceptibility and the induced magnetization of the rock is increased; this increases its ability to acquire a secondary magnetization (Soffel, 1971).

Palaeomagnetic studies have shown that in many igneous rocks the remanence is actually carried by the microscopic and sub-microscopic iron oxides. Evans et al. (1968) have shown that the 2 600 m.y. Modipe Gabbro (in Botswana) has a remanence that is carried almost entirely by single-domain magnetite exsolved out of pyroxene; Hargraves and Young (1969) have shown that submicroscopic magnetite exsolved out of feldspar in the Lambertsville Diabase is the carrier of the stable remanence. Murthy et al. (1971) found evidence for single-domain

magnetite in anorthosite whereas Davis (1981) reported that a stable remanence may be related to the exsolution of magnetite rods and spherules out of plagioclase in ocean floor gabbros. The shape anisotropy of magnetite rods and platelets which results in a stable remanence (Murthy et al., 1971), due to the fact that the critical size for the single-domain structure is greatly increased if the particles are elongated (McElhinny, 1973, p. 48), is also significant. Moon (1984) suggests that although an increase in elongation results in an increase in shape anisotropy and activation energy, this does not hold above a certain aspect ratio. Consequently, he concludes that classical single-domain behaviour is limited to a small number of grains, and that the stability of single-domain grains, especially those with a high length : width ratio, is controlled by the nucleation of domain walls. Coe (1979) found that shape anisotropy has a small average effect on the direction of TRM of subaerial basalts, but that it may have a substantial effect on the TRM direction of submarine basalts.

Previous accounts of the presence of magnetite needles in plagioclase in rocks of the Bushveld Complex are given by Groeneveld (1968), Molyneux (1970), von Gruenewaldt (1971) and Scharlau (1972). Hattingh (1983) reported the presence of needles of ore minerals in plagioclase and pyroxene grains. Ore minerals comprise less than 1% of the rocks studied in this investigation and their grains range from 1 to 50 micron in diameter and from 10 to 350 micron in length for the needles and platelets; the subhedral to euhedral grains are up to 600 micron in diameter. It was thus vital to consider the grain size, domain configuration, grain shape and the question of primary or secondary minerals in order to explain the differences in the magnetic signature of these rocks.

It is further important to determine whether a meaningful correlation can be found between petrological, mineralogical and palaeomagnetic data. In 1954 Balsley and Buddington found a close correlation between the composition and magnetic properties of a suite of North American igneous and metamorphic rocks, ranging in age from Precambrian to Triassic. Such polarity-petrology correlations have been found in basaltic rocks by Beck (1966), Watkins and Haggerty (1967), Wilson

and Watkins (1967), Ade-Hall and Wilson (1969), Hargraves and Peterson (1971) and Piper (1977). Both Watkins and Haggerty, as well as Ade-Hall and Wilson, found an apparent self-reversal in these investigations. In the latter cases it was found that the more highly oxidized minerals were more commonly associated with a reversed polarity. Piper (1977) suggested that the oxidation-polarity correlation implies that processes within the earth's core affect the chemistry of basaltic magmas fractionated from the uppermost part of the mantle. According to Cisowski (1980) there is a definite correlation between the intensity of saturation remanence of magnetic phases in a rock, and the abundance of these phases as well as their domain and oxidation states. Balsley and Buddington (1958) found that reversed magnetizations were associated with all rocks containing minerals in the ilmenite-hematite series in the form of solid solutions or intergrowths. Watkins and Haggerty (1965), Larsen and Strangway (1966) and Ade-Hall and Watkins (1970) did not find any polarity-petrology correlations.

2. SAMPLING METHODS AND LABORATORY PROCEDURES:

2.1 Sampling:

Nine core samples (M1-M9) for use in palaeomagnetic studies were drilled on the farm Kliprivier 73 JT, 15 km east of Roossenekal, on the Roossenekal-Lydenburg road. Figures 1 and 2 illustrate the position of the sampling site, M. Lithostratigraphic nomenclature is according to S.A.C.S. (1980), and the position of the Upper mottled anorthosite (Figure 2), is according to von Gruenewaldt (1971). Use was made of a portable petrol-driven drill to obtain core samples of 300 mm in length and 25 mm in diameter. Two distinct rock units, an upper mottled anorthosite and an underlying fine-grained norite (Figures 3-5), were initially identified and sampled. The samples were orientated during drilling by means of a sun-compass as described by Collinson (1983), which is accurate to within 1^{o} (Tarling, 1971).

Initial laboratory procedures comprised cutting the samples into specimens of 25 mm in length, producing a total of 45 specimens which were suitable for palaeomagnetic measurements. The remaining specimens, together with hand samples collected from the outcrop, were used for the preparation of polished thin sections for petrographical and mineralogical investigations.

Twelve additional specimens were obtained from Dr. P.J. Hattingh and Miss R. Blom; numbered H1-H5 and B1-B7 respectively. The use of these specimens became important at an advanced stage of the investigation when a third palaeomagnetically and petrographically distinct unit (Figure 3) was identified. The latter unit, a two-pyroxene gabbro, was extremely difficult to sample for palaeomagnetic purposes as it is laterally inconsistent and has an irregular upper and lower contact. Individual specimens of this unit could only be obtained from samples taken from the mottled anorthosite which happened to cut across the underlying two-pyroxene gabbro.

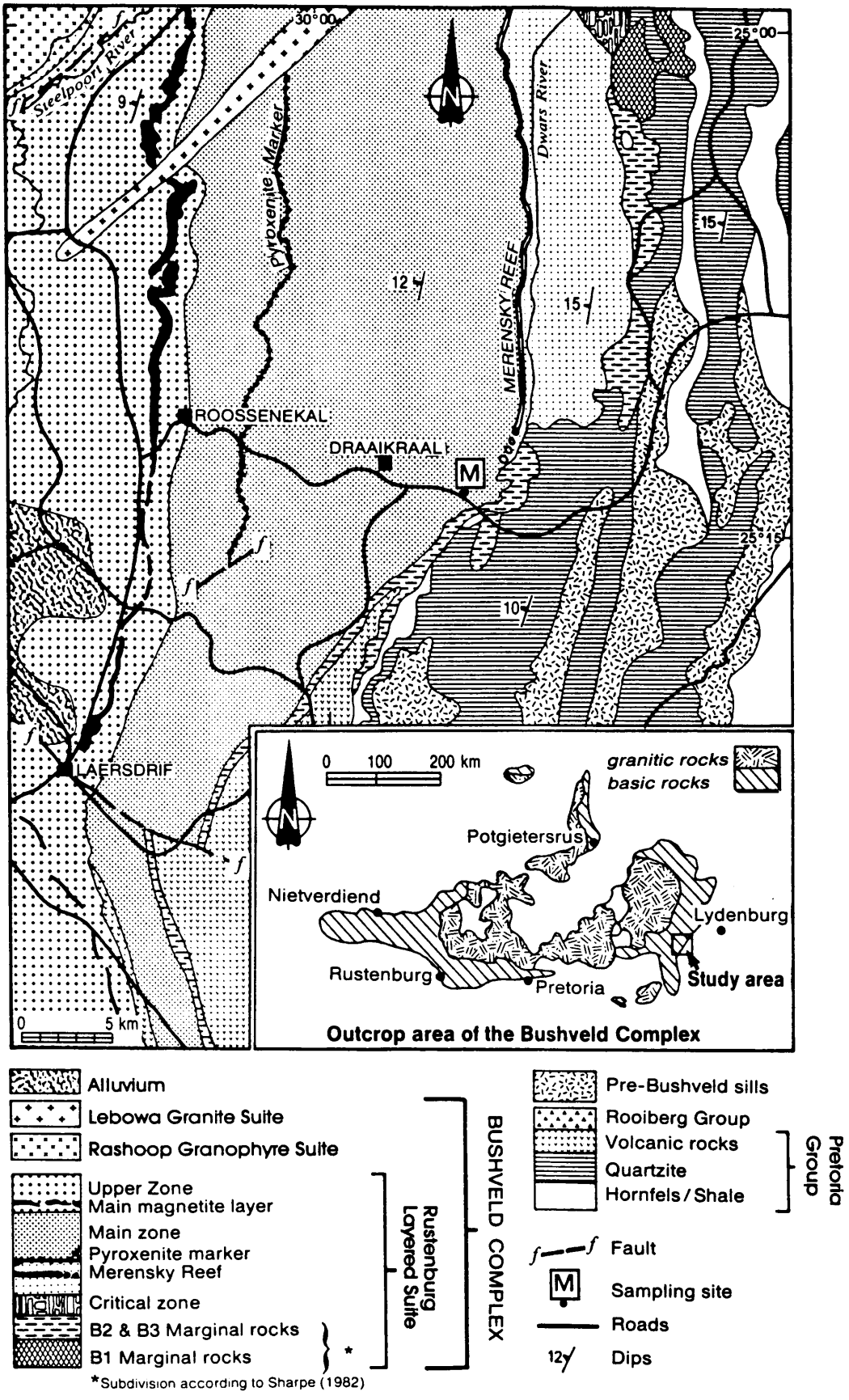

Figure 1: Geological map of part of the eastern Bushveld Complex. [Modified after Sharpe (1982)]

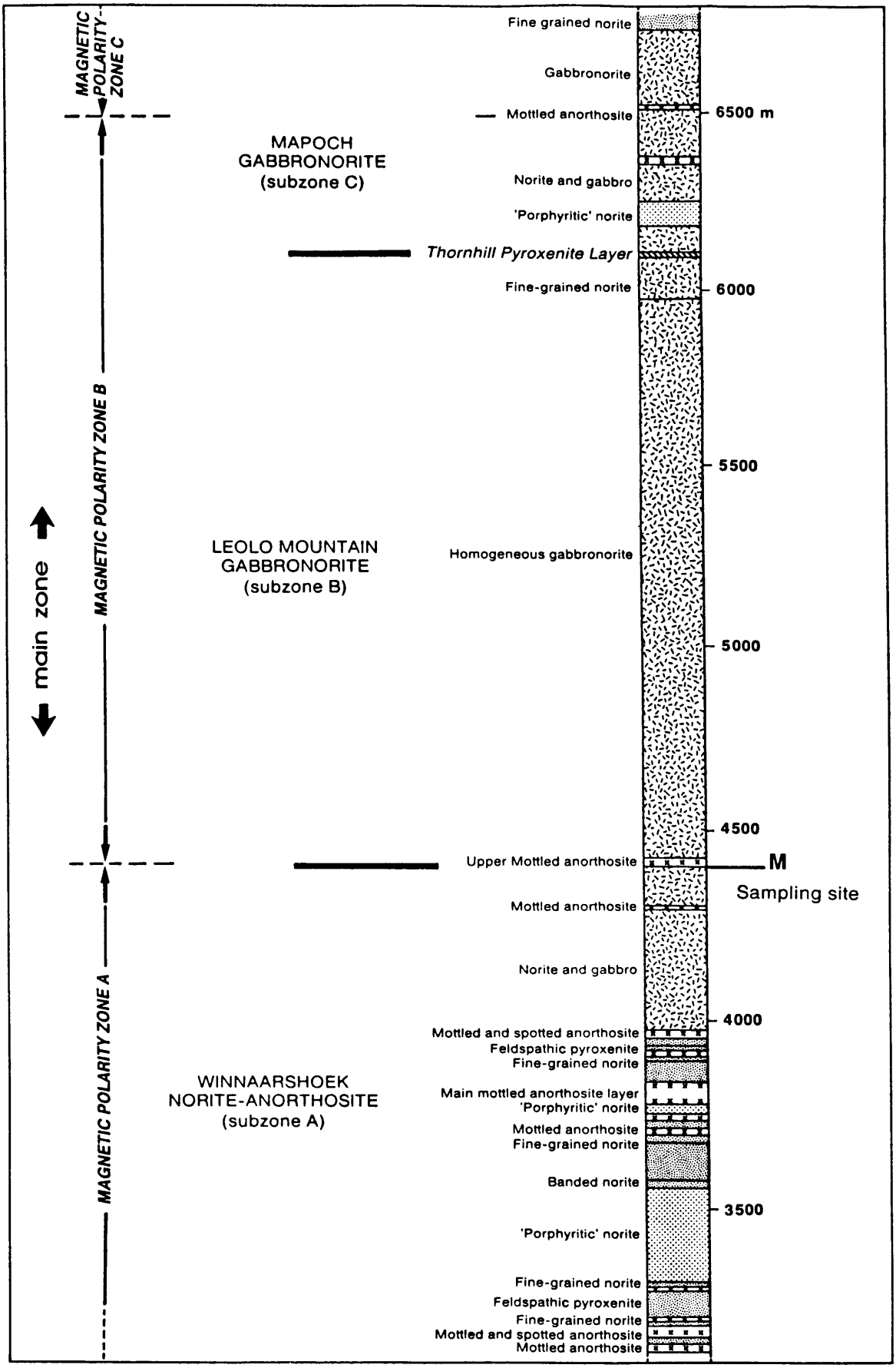

Figure 2: Suggested magnetic polarity zones. Hattingh (1983) puts the boundary between the magnetic polarity zones at the Main mottled anorthosite layer (3800m).

Figure 4(a): The Upper mottled anorthosite unit (a) underlain by the fine-grained norite (n). The intrusive two-pyroxene gabbro (g) contains slithers of anorthositic material.

(b): The contact between the mottled anorthosite and gabbro units indicating that mixing between the two rock-types took place.

:EA ENLARGED IN FIGURE 5a AREA ENLARGED IN FIGURE 5d AREA ENLARGED IN FIGURE 4

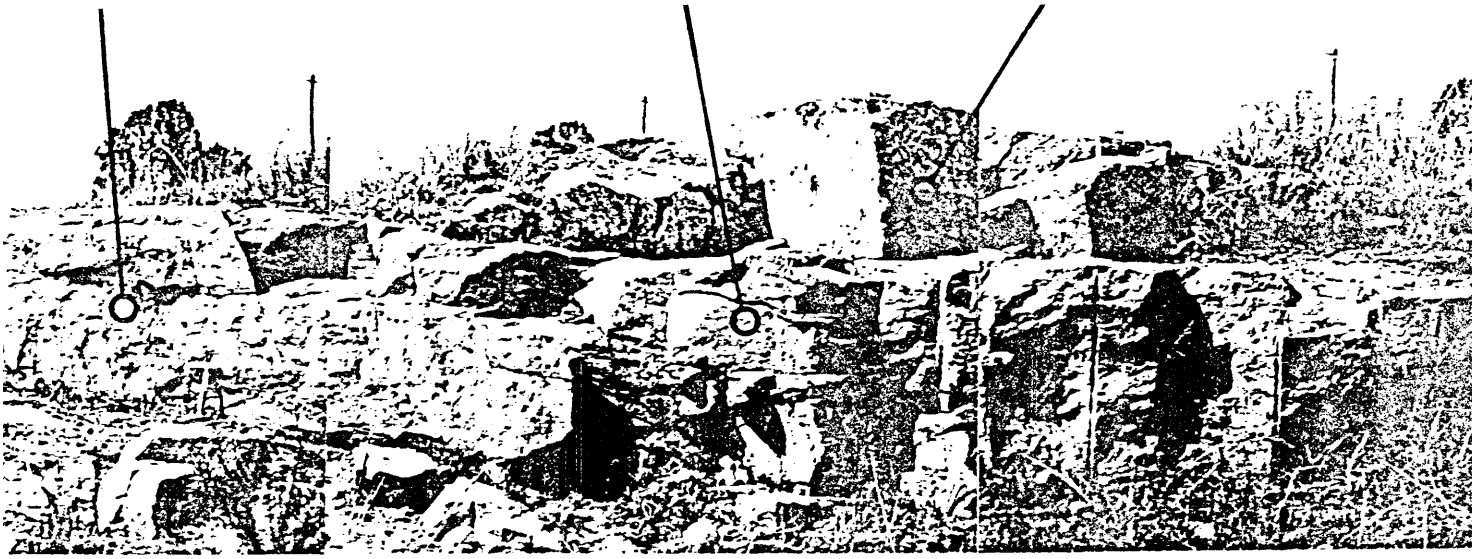

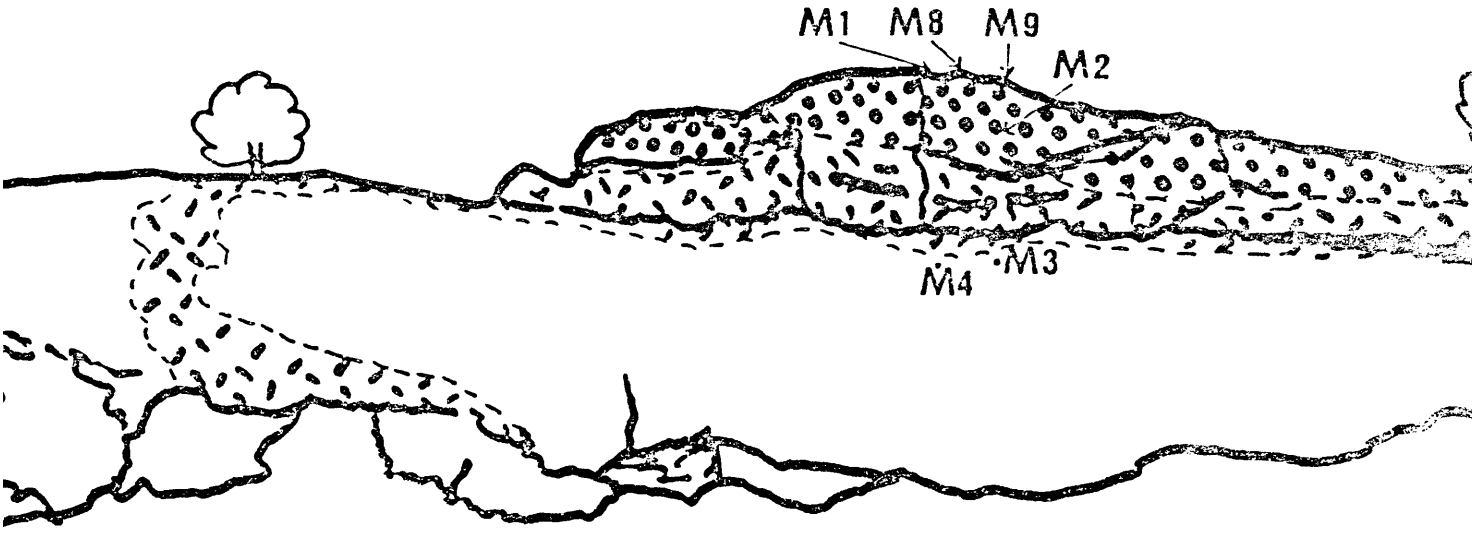

TCROP AT SITE M INDICATING POSITIONS OF SAMPLES AND

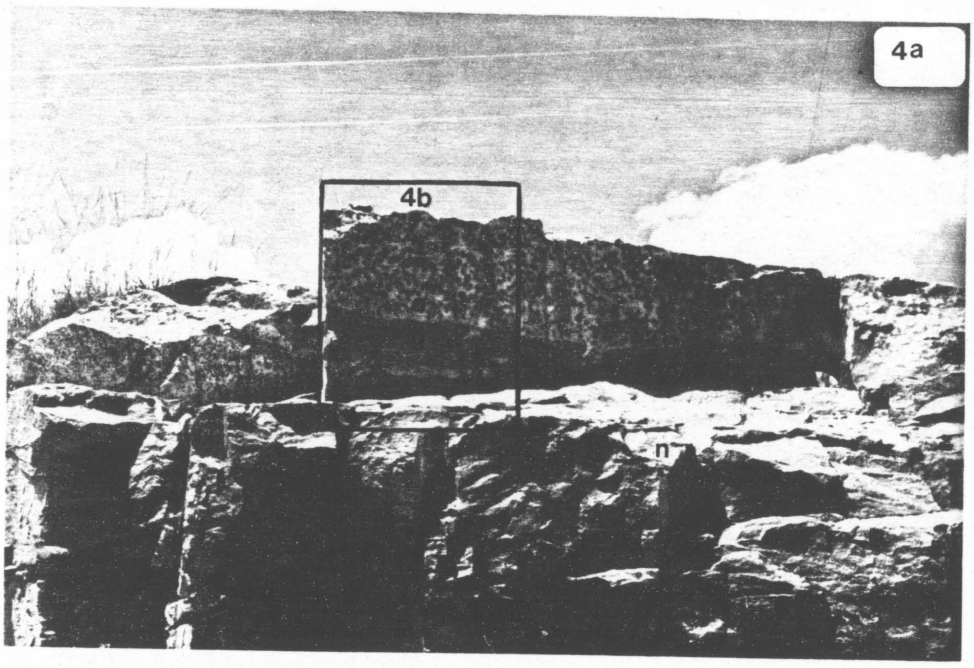

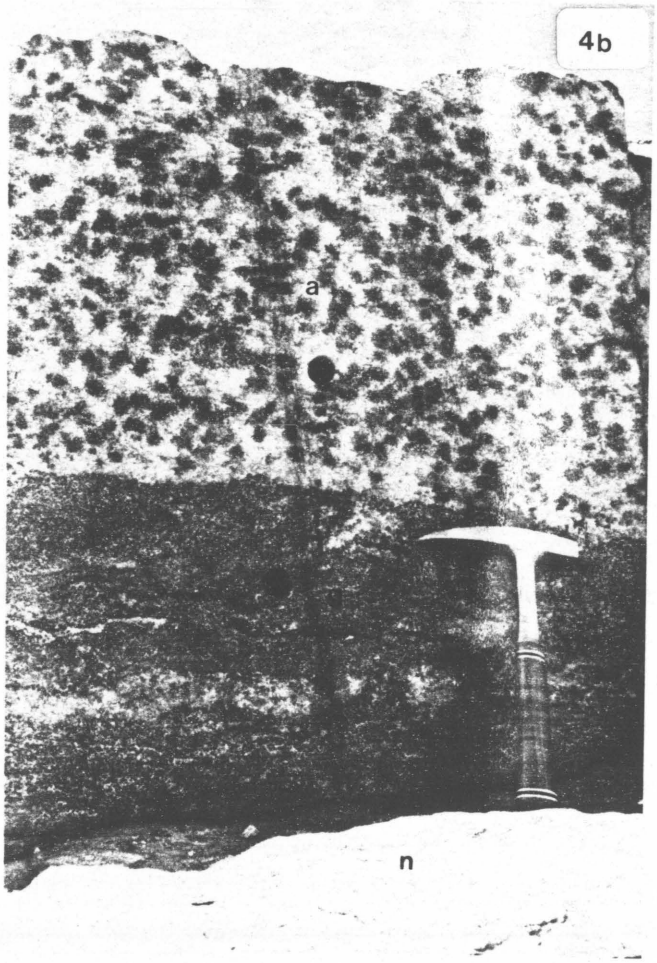

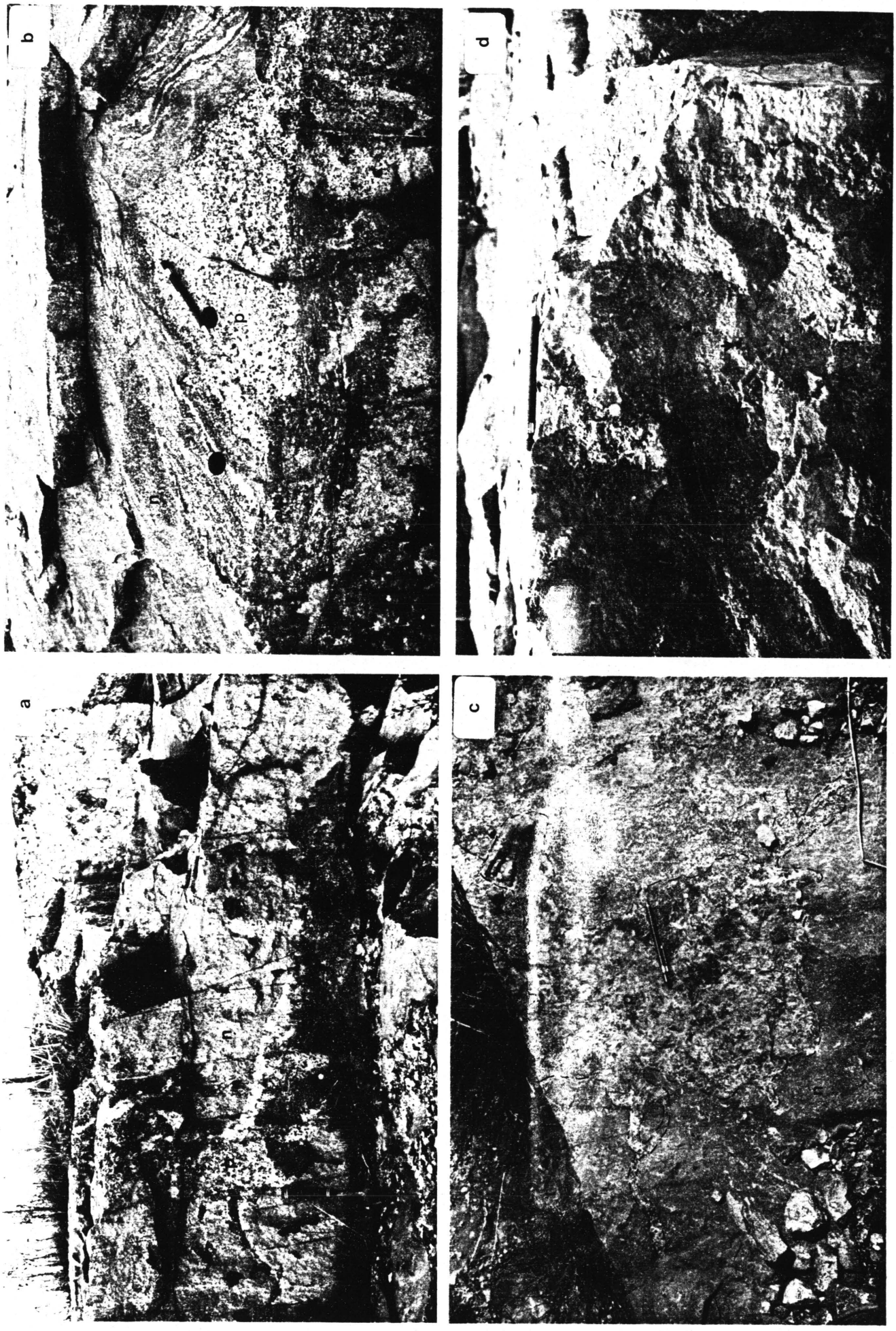

2.2 Laboratory procedures:

2.2.1 Palaeomagnetic laboratory procedures:

2.2.1.a Measurement of remanent magnetization, bulk susceptibility and anisotropy:

A Digico "Complete Results" fluxgate spinner magnetometer was used to measure the remanent magnetization of all the specimens. During remanent magnetization measurements the specimen is placed in six different orthogonal positions in the sample holder, enabling the computer to calculate the magnetization of the specimen along the three orthogonal directions. These results are then combined and are given in terms of total intensity of magnetization, declination and inclination of the resultant vector of remanent magnetization. The spinner magnetometer is designed to be resistant to induced field effects and ambient magnetic noise and it has a sensitivity of as low as $0,01 \times 10^{-5}$ A.m $^{-1}$. It was however found that measurements of magnetization intensities lower than $0,05 \times 10^{-5}$ A.m^{-1} could not be repeated accurately.

Use was made of a cryogenic magnetometer for the measurement of magnetization at an advanced stage of this study. This instrument comprises a ring that is maintained at liquid helium temperatures. A specimen which is placed in the ring causes a current to flow that is proportional to the magnetic moment along the axis of the ring. Measurement of the direction and total magnetization of a specimen is made by inserting the specimen in two different perpendicular orientations in the ring. The cryogenic magnetometer has a very high sensitivity and its detection limit is far below that of the Digico spinner magnetometer (Tarling, 1983). Use was made of the cryogenic magnetometer for measurement of specimens with low intensities of magnetization, particularly after they had been magnetically cleaned by means of alternating field or thermal demagnetization.

Bulk magnetic susceptibility and anisotropy of susceptibility measurements were made using a low-field susceptibility bridge which is attached to the Digico system. Selected specimens from each rock

type were used for this purpose. A single susceptibility reading is printed out during susceptibility measurements. The directions and intensity of magnetization of the three axes of the ellipsoid of susceptibility, which are proportional to the maximum, intermediate and minimum values, are calculated by means of a computer programme during anisotropy measurements. Very little use is made of the latter data, but the results are nevertheless presented.

2.2.1.b Alternating field demagnetization: (AF demagnetization)

Stepwise alternating field demagnetization of representative specimens from each rock type was done with the aid of an AF demagnetization unit which was built and assembled according to a description of McElhinny (1964) at the Geological Survey of South Africa. The specimen is placed on the axis of a coil and the earth's magnetic field is cancelled by Helmholtz coils to prevent anhysteritic magnetization (ARM). AF demagnetization is carried out by passing an alternating current through the coil, thus producing an alternating field along its axis. The sample is rotated about three mutually perpendicular axes to further reduce the effect of anhysteritic magnetization and to demagnetize the specimen as a whole. Measurements of the remanences of the specimens were made after successive demagnetizations in the applied alternating field with the aid of the spinner magnetometer. Maximum alternating fields of 130 mT were attained. Bulk AF demagnetization was done with selected specimens at intermediate field intensities.

2.2.1.c Thermal demagnetization:

Continuous thermal demagnetization of representative specimens from each rock type was done with a modified high temperature spinner magnetometer attached to the Digico computer. As the specimen is being heated, readings of the intensity and direction of magnetization of the specimen at selected temperatures are obtained. The manufacturers of the instrument suggest that the rock specimen will be 10-15^{o}C cooler than the thermocouple at lower temperatures, whilst at maximum temperatures it will be 10^{o}C higher than the thermocouple. No corrections for the latter were made during measurements. Maximum

temperatures of 650°C were reached during this investigation.

Stepwise thermal demagnetization of one specimen was done to investigate the repeated reversal in inclination of the magnetization vector. The specimen was heated and then allowed to cool in a field free space for 14 hours. Measurements of the magnetization were then made. The procedures were repeated at successively higher temperatures up to 650°C. After heating the specimen to 650°C it was allowed to cool in a low intensity field for 14 hours, after which the final measurements were made.

2.2.1.d Statistical analysis of palaeomagnetic results:

Statistical analysis of results from the samples was done to identify possible stable magnetization directions after sample means were determined from specimen analyses. Various sample means were grouped to yield means for the respective rock types.

It was proposed by Fisher (1953) that points on a sphere have a probable density distribution P given by

$$P = \frac{\kappa}{4\pi \sinh \kappa} \exp (\kappa \cos \psi)$$

where ψ is the angle between a point and the true mean of the vector population and κ is the precision parameter which determines the dispersion of the points. A best estimate k of the precision parameter κ (Fisher, 1953) is determined for the total number of specimens. Normally P is taken as 0,05 (McElhinny, 1973), and the probability that a direction will be observed which makes an angle ψ with the true mean direction is given by

$$\psi_{95} = \frac{140}{\sqrt{k}} \text{ degrees.}$$

Although κ is zero for a truly random population, the estimate k is never zero. Thus, according to Watson's randomness test for directions (1956), the length of a resultant vector R for a sample size N will be large if there is a preferred direction. If there is no preferred direction then the length of the resultant vector R will be small. Specific R_o values were tabulated by Watson (op. cit.) for various sample sizes. If values are smaller than these tabulated values they

indicate a random orientation of directions.

2.2.2 Petrographical and mineralogical methods:

A detailed petrographical study was made of polished thin sections of all the samples by means of a petrographical microscope. In addition use was made of reflected light to study the ore minerals microscopically under oil immersion. A 105 X objective was fitted to the microscope to facilitate this study. Powdered fractions of selected pyroxenes from the three rock types were mounted in immersions liquids and their refractive indices determined; the orientation of ore mineral inclusions was also investigated during this examination.

Following the above investigation electron microprobe work was undertaken with the aid of a JEOL Superprobe JCXA-733 X-ray microanalyser (computer controlled), which is attached to an energy-dispersive system [EDS] (KEVEX). Quantitative analyses were made of plagioclase, clinopyroxene and orthopyroxene by means of a wavelength dispersive system [accelerating voltage 20 kV, beam current 2×10^{-8} A, counting time 20 seconds (peak) and 10 seconds (background)]. It was attempted to determine the relative elemental composition of the ore minerals. This method proved to be unreliable for studying the ore needles, platelets and blebs due to the fact that the excitation area resulting from the electron beam includes the background (host) silicate mineral. To support this it can be illustrated that magnetite with a relative density of 5.2 will result in an excitation area of 3,0-3,4 micron for Fe $k\alpha$ (Merkle and Hatton, 1987, pers. comm.), which is far broader than the width of < 1 micron for the average needles / platelets. Qualitative analyses were thus made of these minute ore needles/platelets and blebs with the aid of backscattered electron images (BEI) and X-ray images. Furthermore it was attempted to use a scanning electron microscope (SEM) attached to an EDAX (energy dispersive analysis of X-rays) system to assist in a qualitative investigation of the ore minerals, and this proved to be much more successful for the qualitative study of microscopic to sub-microscopic ore minerals. The latter investigation was successful at an advanced stage of the study when rock chips were mounted in the SEM, thus

exposing the "needles" on the surface of the silicates. The elongated ore minerals could be viewed from above as well as side on. A three dimensional picture of these "needles" could thus be obtained, indicating that they are in fact laths and not needles.

3. THE MOTTLED ANORTHOSITE:

3.1 Introduction:

The mottled anorthosite unit at site M is regarded by the author as the Upper mottled anorthosite. This unit consists of two layers of mottled anorthosite; a 1,5 m thick upper layer and a 3 m thick lower layer (von Gruenewaldt, 1971), which are 10 m apart (von Gruenewaldt, 1973). The Upper mottled anorthosite occurs at a height of 1 275 m above the Merensky Reef, and it separates subzones A and B of the main zone (von Gruenewaldt, 1971). At site M only one layer of mottled anorthosite, which is at most 1,5 m thick, occurs in outcrop (Figure 4).

Hattingh (1983) indicated this site as the Main mottled anorthosite in the main zone. However, comparison with a map of the area (von Gruenewaldt, 1973), and the textural nature of the orthopyroxene grains indicates that this is in fact the Upper mottled anorthosite unit. At site M the orthopyroxene in the mottled anorthosite is intercumulus. According to von Gruenewaldt (1971, p. 68), orthopyroxene changes from cumulus to intercumulus at 1 000 m above the Merensky Reef, and although there is a break at 150 m above the first appearance of intercumulus orthopyroxene, from 1 200 m it is again intercumulus. The Main mottled anorthosite occurs at a height of 700 m above the Merensky Reef (von Gruenewaldt, 1971), and thus contains cumulus orthopyroxene.

At c. 1 200 m above the Merensky Reef, inverted pigeonite appears in small quantities in the layered sequence (von Gruenewaldt, 1973, p. 219) and it coexists with orthopyroxene for the next 1 000 m. The latter assemblage corresponds to the observed orthopyroxene in the mottled anorthosite of site M.

Four core samples M1, M2, M8 and M9 were taken from this unit for palaeomagnetic purposes. Their relative positions are indicated in Figure 3. From these samples 17 specimens were obtained, although 3 specimens had to be rejected as core sample M1 was apparently

incorrectly orientated during drilling. Furthermore, specimens H1, H4 and B7 were also included, bringing the total number of specimens from this rock to 20.

The mean intensity of magnetization of the mottled anorthosite is 4 434 x 10^{-3}A.m^{-1} (standard deviation = 2 375 x 10^{-3}, minimum intensity = 1 223 x 10^{-3}, maximum intensity = 8 541 x 10^{-3}). The rock is characterized by a consistent magnetization direction which was identified during magnetic cleaning. The latter magnetization direction, based on specimen measurements, corresponds to that isolated by Hattingh (1983, p. 54) as group Bmz3AF, the characteristic main zone direction, which was determined from multiple sites.

3.2 **Palaeomagnetic results:**

(a) Natural remanent magnetization (NRM):

NRM refers to the total remanence of a specimen which includes all the components of remanence which were acquired by natural processes. The NRM directions of the mottled anorthosite specimens are presented in Table I and Figure 6. The R_o value (Watson, 1956) of 5,98 indicates that there is no significant orientation of NRM directions.

Table I: NRM results from the mottled anorthosite.

Specimen	D ^{o}	I ^{o}
M2A	248,54	6,57
M2B	234,76	1,13
M2C	231,51	8,38
M8A	162,25	-28,01
M8B	196,68	-16,11
M8C	221,11	-36,31
M8D	229,95	- 6,49
M8E	221,14	- 4,61
M8F	232,45	- 9,95
M9A	240,52	10,78
M9B	232,35	8,85
M9C	248,54	11,19
M9D	239,70	4,54
M9E	241,72	14,02
	mean 230,45	mean - 3,03

with $\alpha_{95} = 22,82^{o}$, k = 4, $R^{o} = 5,98$

where D = declination of magnetization direction measured from north in a clockwise direction;

I = inclination of magnetization direction where upwards is negative and downwards is positive.

The mean magnetic susceptibility of the anorthosite is 6,5 x 10^{-3}SI (standard deviation = 2,3 x 10^{-3}). The magnetic susceptibility is a function of the size and number of magnetic grains which carry a remanence. The relatively low magnitude of anisotropy (Owens, 1974) of 0,27 (standard deviation = 0,12) suggests that the alignment of magnetic minerals due to their shapes did not significantly affect the direction of the remanence acquired by the rock during its magnetization in the ambient field.

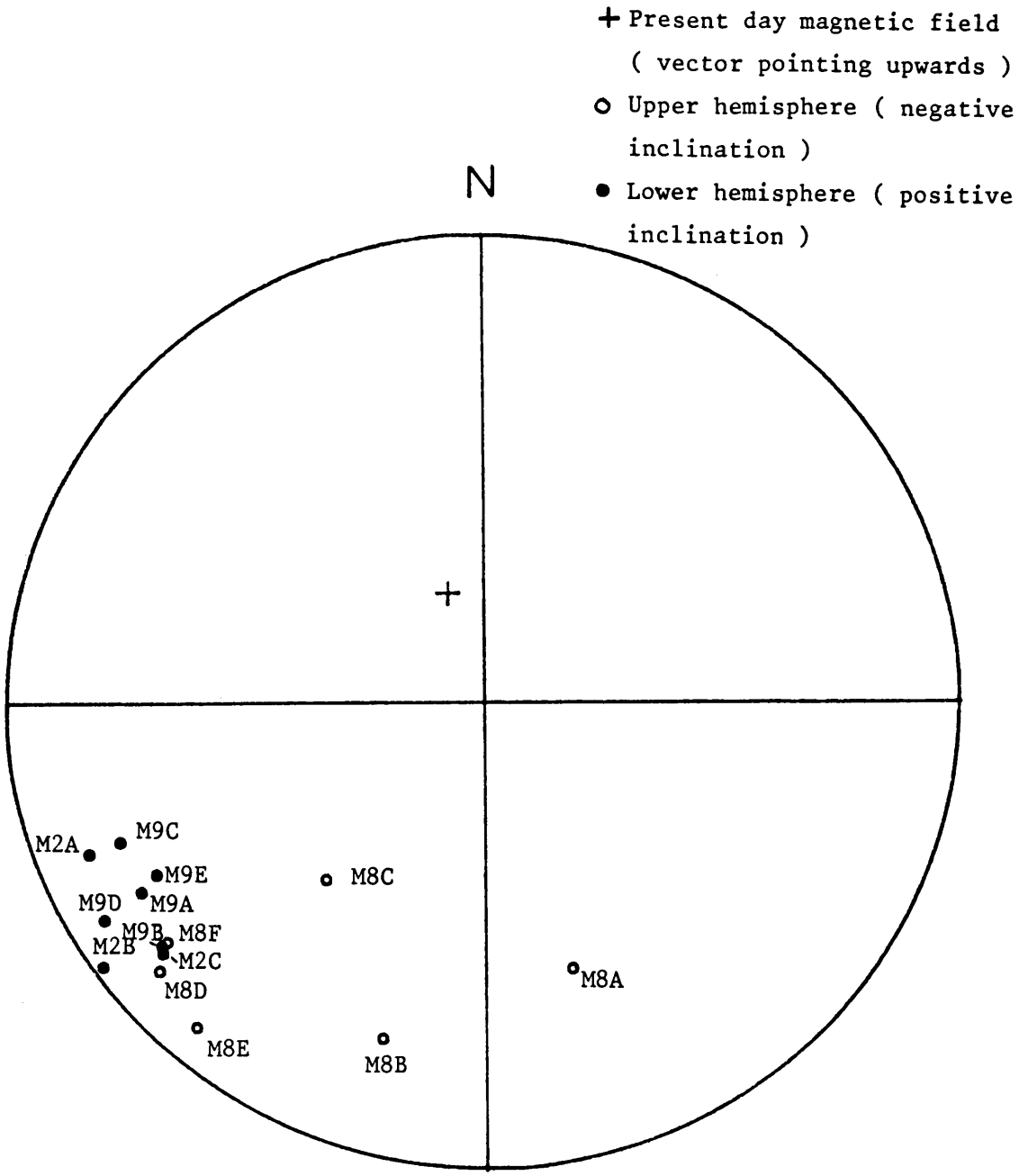

Figure 6: Stereographic projection of NRM directions of specimens from the mottled anorthosite.

(b) Alternating field demagnetization (AF demagnetization):

(i) Stepwise alternating field demagnetization:

An important aspect regarding the demagnetization process, is that demagnetization in multidomain grains is most likely achieved by wall motion, whilst domain rotation takes place in single domain grains (Lowrie and Fuller, 1971). The resultant vector movement involves the progressive removal or breaking down of components of magnetization with specific microscopic coercivities. Coercivity is a structure sensitive property which is controlled by defects in the crystal lattice. The latter defects create local energy perturbations which pin domain walls in the multidomain structure (Tucker and O´Reilly, 1980a). In single-domain magnetite the coercivity is dependent on the uniaxial anisotropy of the grain (Lowrie and Fuller, 1971). Thus, for an assemblage of single-domain grains, applied fields must overcome high energy barriers during demagnetization, whilst some demagnetization of multidomain remanence occurs at low field strengths.

Stepwise AF demagnetization was done on three specimens from the mottled anorthosite. The normalized intensity response curves are shown in Figures 7(b) and 8(b). A feature of these curves is that a soft component of magnetization is removed at low AF strengths as indicated by the dramatic drop in intensity after magnetic cleaning at 10 mT (Figure 7(b)). The subsequent increase in magnetic field intensity at field strengths higher than 10 mT (Figure 7(b)) indicates that an antipodal component of magnetization is removed here. The shape of the intensity response curves for these specimens is indicative of overlapping coercivity spectra, suggesting that two magnetization components are removed at fields greater than 10 mT. The difference in the shape of the intensity response curves for these two specimens can be attributed to different quantities of the magnetic carriers.

The typical behaviour of the resultant vectors during stepwise demagnetization is illustrated in Figures 7(a) and 8(a). The demagnetization paths of these specimens indicate that a consistent

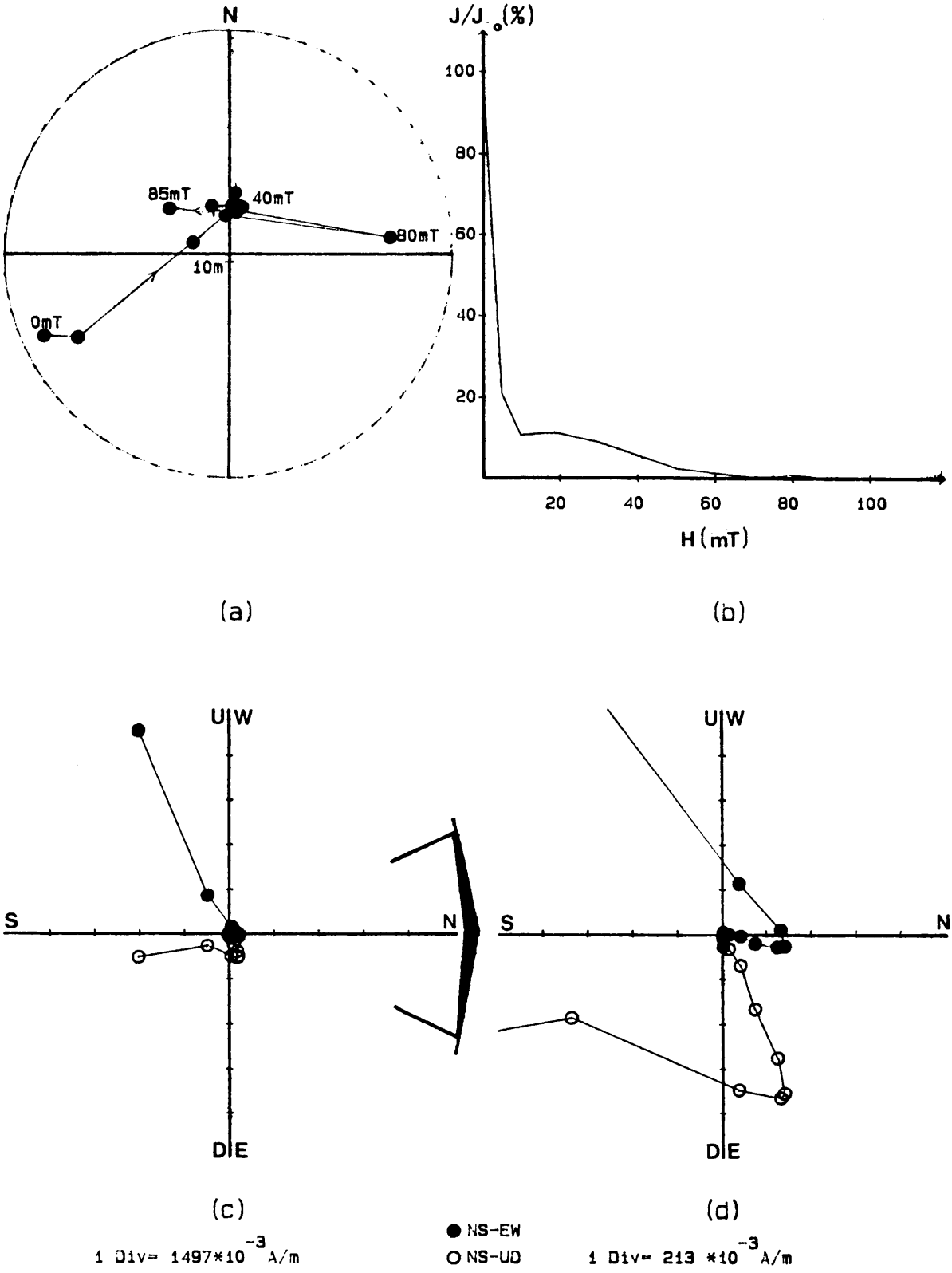

Figure 7: Stepwise AF demagnetization of specimen M2A.

(a) Resultant vectors (plotting convention as in Fig.6)

(b) Normalized intensity response curve.

(c) Zijderveld stability diagram.

(d) Magnification of Zijderveld diagram (c).

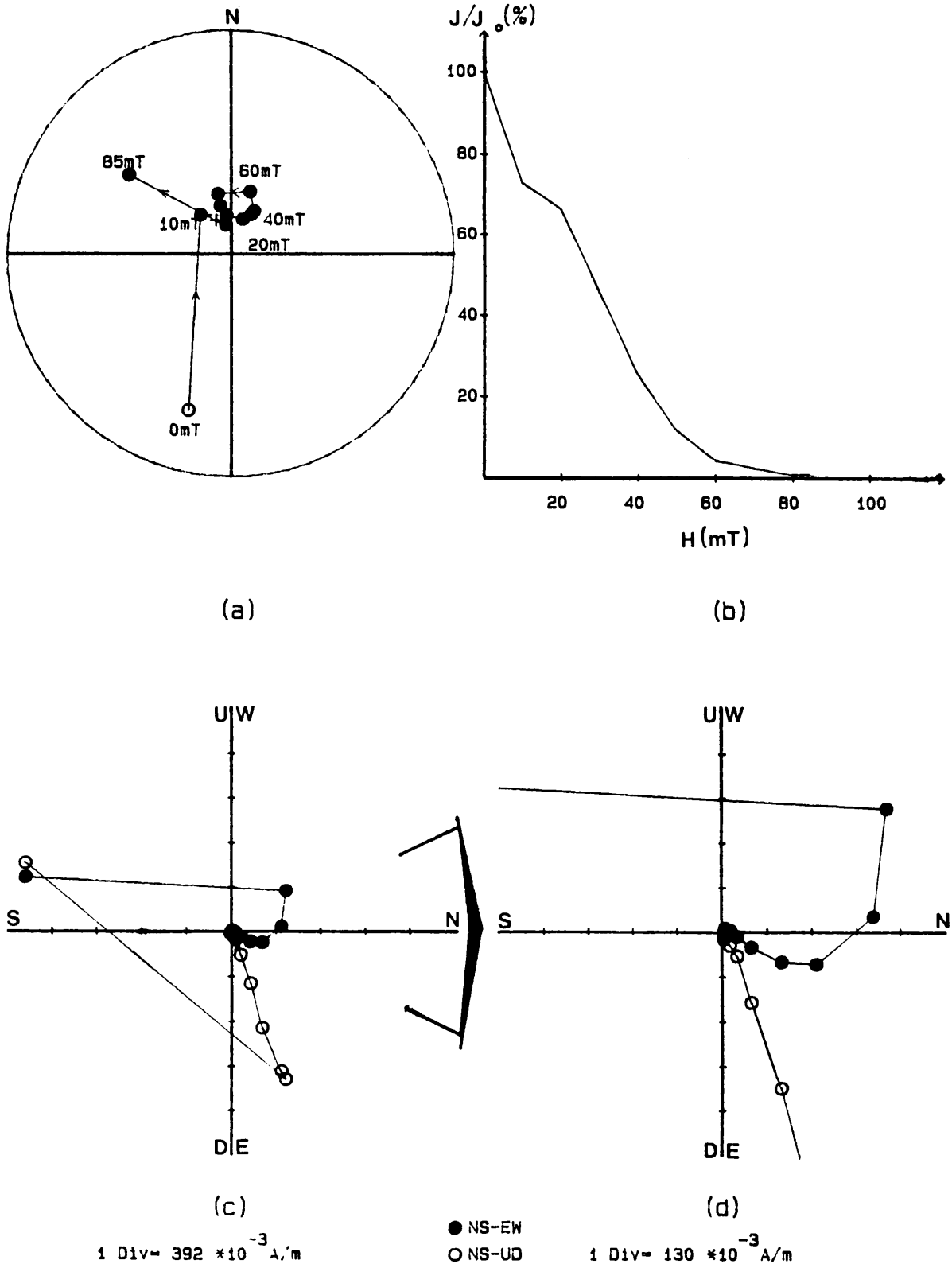

Figure 8: Stepwise AF demagnetization of specimen M8B.

(a) Resultant vectors (plotting convention as in Fig.6).

(b) Normalized intensity response curve.

(c) Zijderveld stability diagram.

(d) Magnification of Zijderveld diagram (c).

magnetization direction (mid-point) is reached at field intensities of between 15 and 70 mT. At fields stronger than 70 mT the vectors tend to diverge from this mid-point. The difference and resultant vectors converge at the stable mid-point (Figure 9), indicating that a single component of magnetization is being removed here (Halls, 1979).

Zijderveld stability diagrams (Zijderveld, 1967) for specimen M2A indicate that a low coercivity magnetization component is removed at low alternating fields of c. 10 mT (Figures 7(c),(d)). Furthermore, a single component of magnetization is only removed at high AF values. By fitting the best straight line to the final segment of the Zijderveld display (Kirschvink, 1980) in Figures 7(d) and 8(d), an estimated direction for this consistent component can be isolated. The estimated magnetization direction of this high coercivity component is the following:
D = 17,6° and I = 68,3°. The Zijderveld stability diagrams also suggest that a magnetization component is removed at intermediate alternating fields. The rounded breakpoints at these fields on the Zijderveld diagrams (Figures 7(d) and 8(d)) indicate overlapping coercivity spectra between the intermediate and high coercivity component.

It is thus evident that three components of magnetization are present in this rock, namely a soft secondary component which is removed at low field strengths, an intermediate coercivity component and a primary consistent high coercivity component which is removed at high fields. The intermediate component is antipodal to the primary magnetization component, and the presence of the soft component of magnetization is is not indicated in all the anorthosite specimens.

A further interesting feature of this rock is that two specimens (M2A and M9D) reversed their magnetization directions over a period of 18 months. The specimens had been demagnetized at alternating field strengths of 70 and 80 mT respectively. Eighteen months later the specimens had reversed inclinations and their intensities of magnetization had increased fourfold. The specimens were then cleaned magnetically at the same fields at which they had been 18 months previously. During redemagnetization at 80 mT, specimen M9D remained

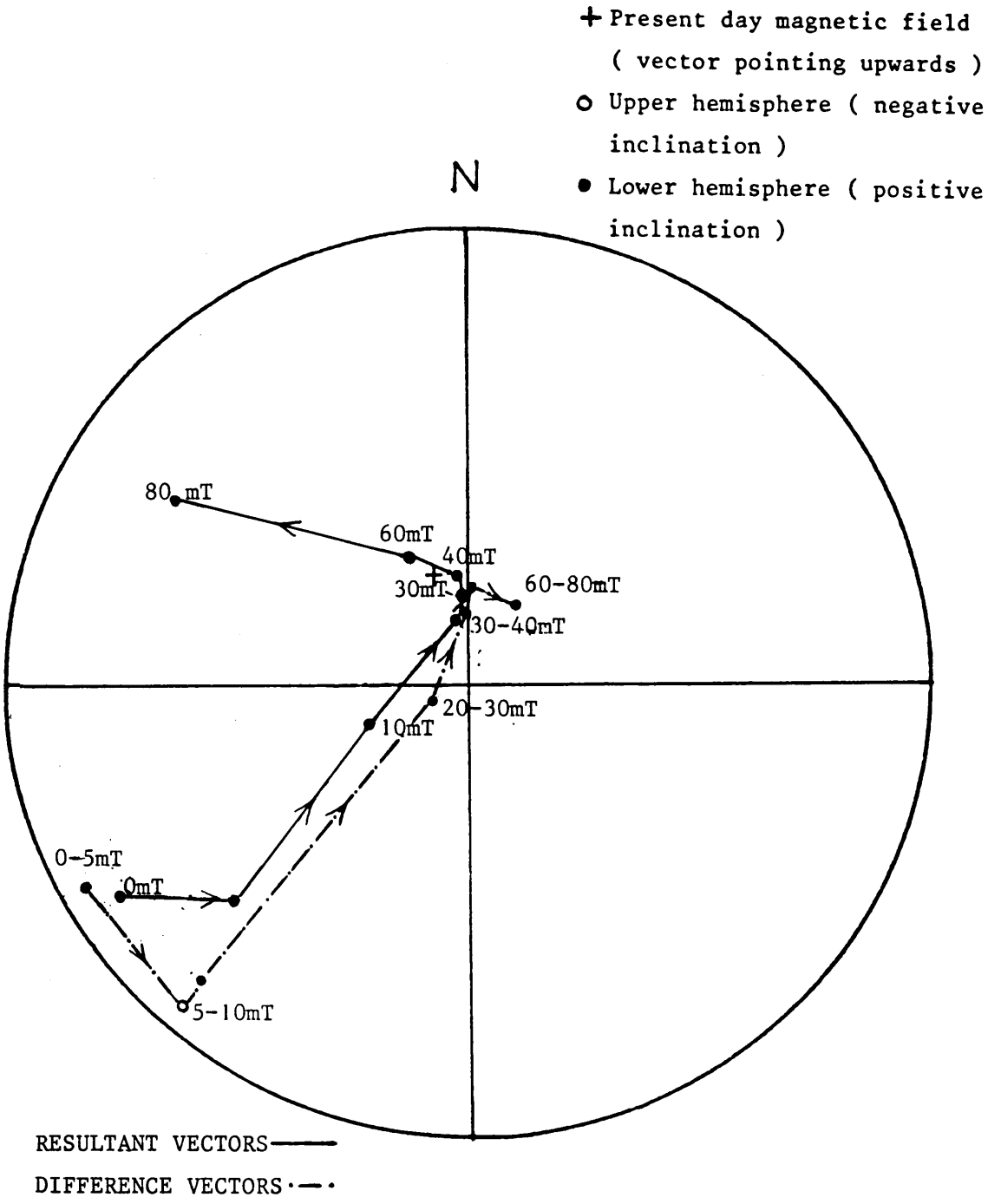

Figure 9: Resultant and difference vectors of specimen M9D during AF demagnetization.

reversed, whilst M2A reverted back to its original magnetization direction during AF cleaning at 70 mT. Specimen M9D was left overnight, and redemagnetized at 80 mT the next day. The inclination reversed back to the original positive sign, and the magnetization direction of the specimen stabilized. The intensity of magnetization of the specimen was also lower at this stage. Both specimens had repeatable magnetization directions after subsequent cleaning at higher AF strengths. An explanation for the change in magnetization of these specimens is that they acquired a time-dependant VRM (viscous remanent magnetization) over the 18 months period. According to Tivey and Johnson (1981) the acquisition of a VRM is strongly dependent on the size of the magnetic minerals, with both very large and very small grains being the most susceptible. However, the acquisition of a VRM which has a reversed direction of magnetization suggests that a more probable explanation may be that some form of self-reversal of magnetization has taken place. Due to the fact that the position of the stored samples with respect to the ambient magnetic field was not recorded, no further experimental work was undertaken to examine this possibility.

(ii) Bulk alternating field demagnetization:

Stepwise AF demagnetization of specimens was done to determine the optimum demagnetization field for the mottled anorthosite. Bulk cleaning was done at this optimum field. The results are presented in Figure 10. The directions of magnetization at an alternating field strength of 40 mT proved to be consistent, and the following results were obtained:
N = 7; D = 17,33°; I = 67,75°; α_{95} = 4,72°; k = 164; R_o=4,18, where N=number of specimens. Comparison with stepwise AF demagnetization results indicates that this direction represents the consistent, high coercivity component carried by these specimens.

(c) Continuous thermal demagnetization:

Continuous thermal demagnetization was done on four specimens of the mottled anorthosite. The normalized intensity response curves to thermal demagnetization (Figures 11(b), 12(b)) display a distributed

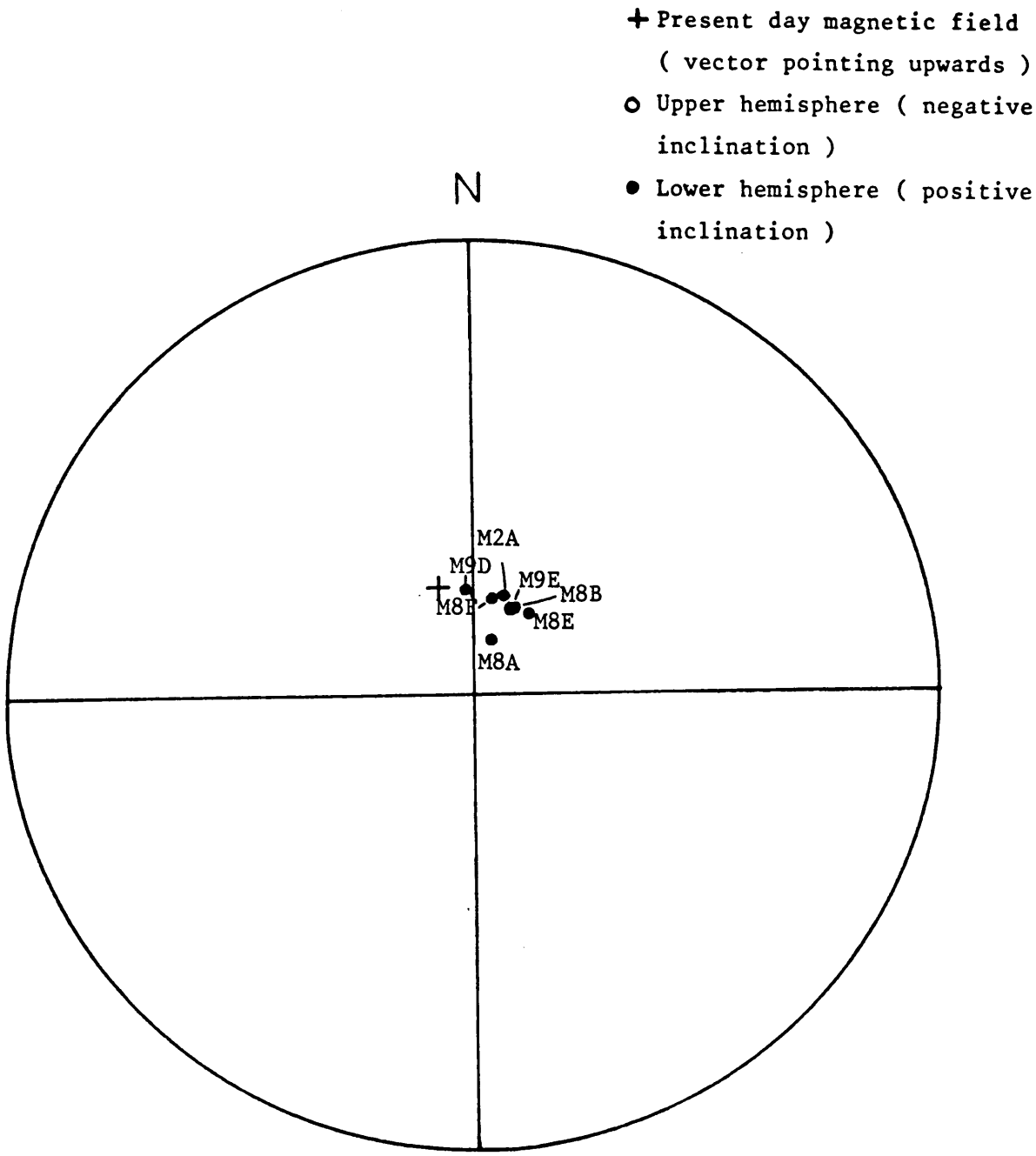

Figure 10: Directions of magnetization of specimens from the mottled anorthosite after bulk AF demagnetization.

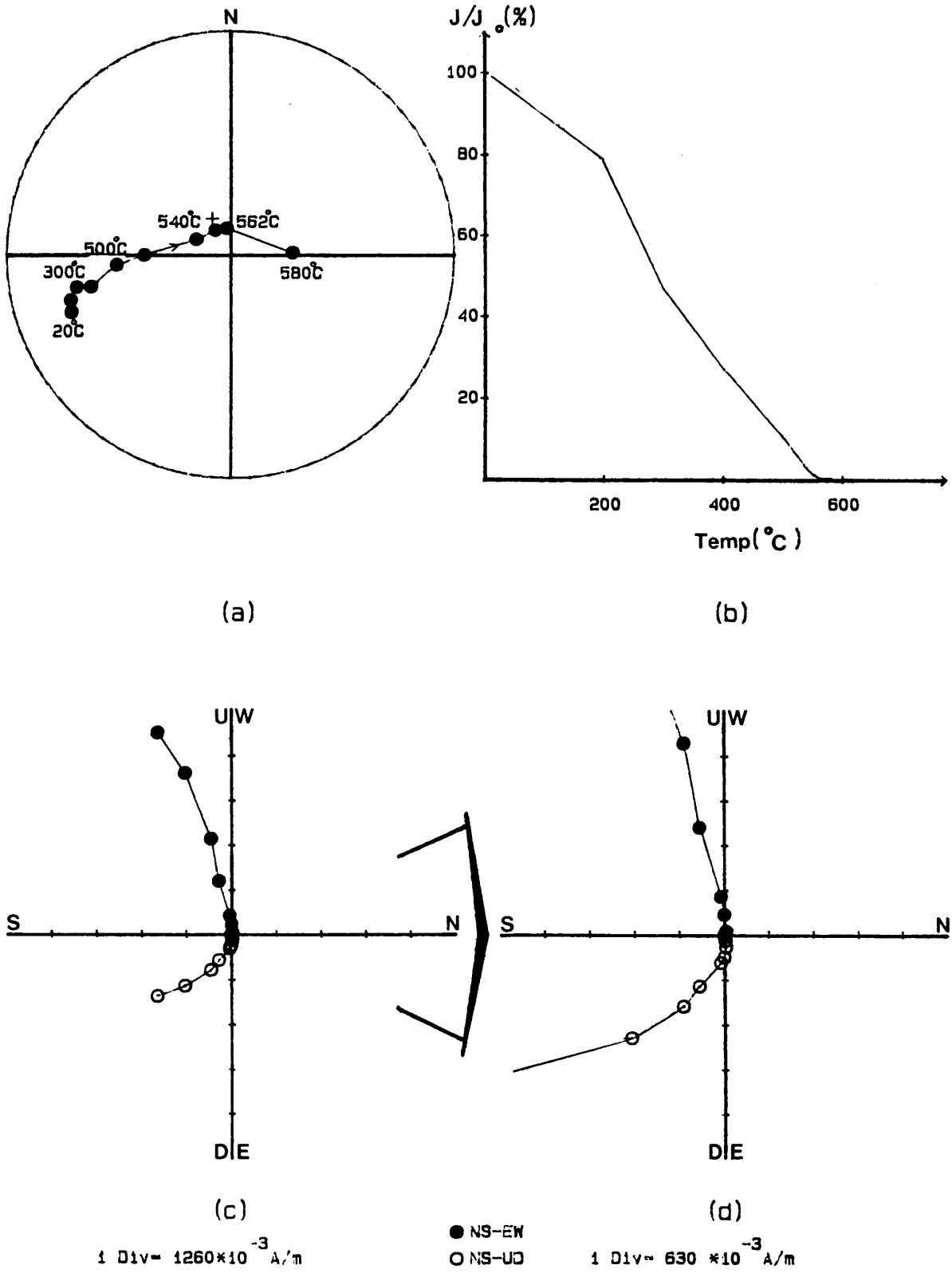

Figure 11: Response of specimen H1 to thermal demagnetization.

(a) Resultant vectors (plotting convention as in Fig.6).

(b) Normalized intensity response curve.

(c) Zijderveld stability diagram.

(d) Magnification of Zijderveld diagram (c).

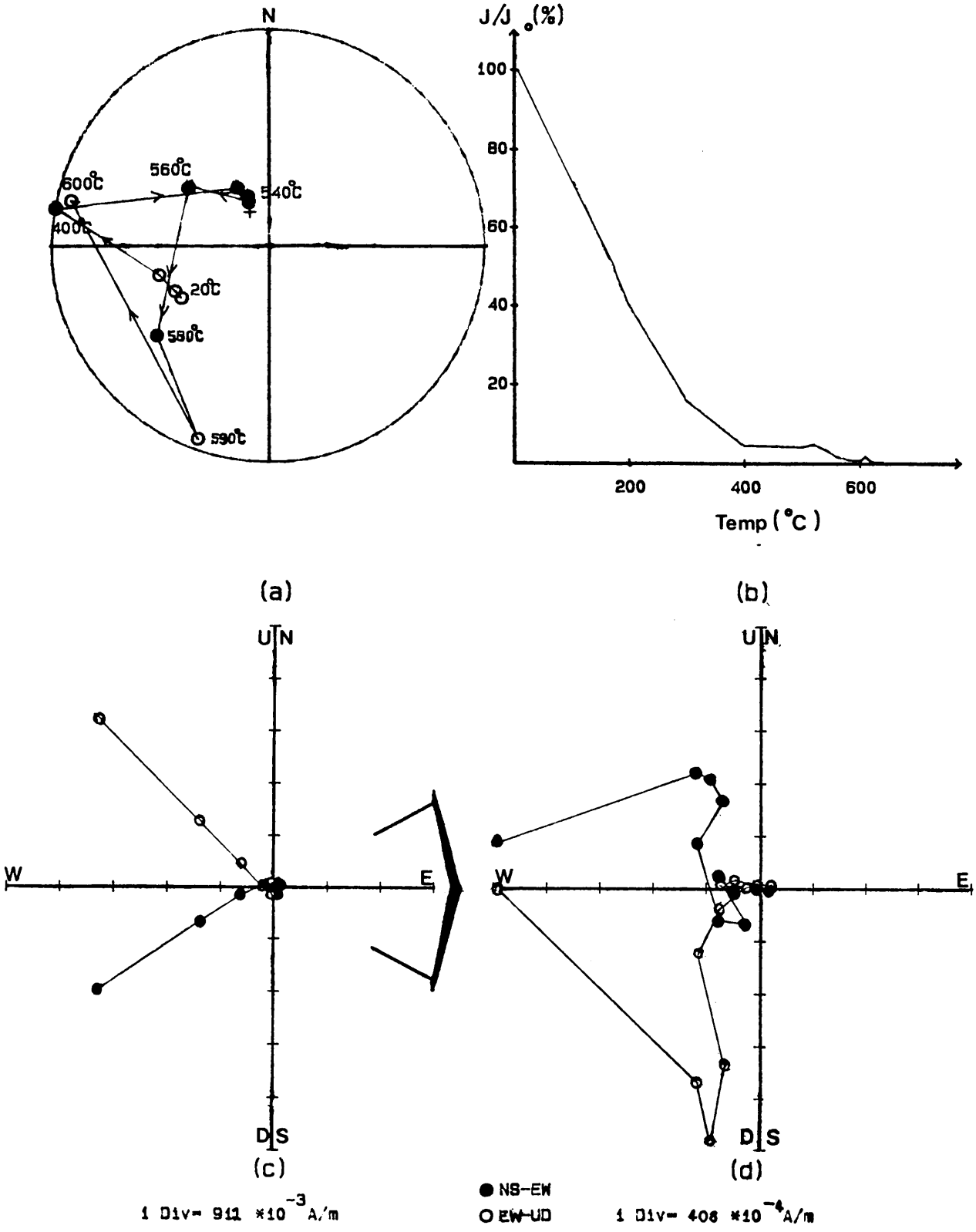

Figure 12: Response of specimen H4 to thermal demagnetization.

(a) Resultant vectors (plotting convention as in Fig.6).

(b) Normalized intensity response curve.

(c) Zijderveld stability diagram.

(d) Magnification of Zijderveld diagram (c).

blocking temperature range. Comparison with curves presented by Day (1975) suggests that these specimens may contain single-domain or pseudo single-domain magnetite grains. The increase in intensity at temperatures above 600°C (Figure 12(b)) is relevant, possibly indicating the presence of a component of magnetization with a high blocking temperature.

All the specimens which were thermally cleaned indicate vector movement towards the consistent magnetization direction identified during AF cleaning, at temperatures approaching the Curie point of magnetite (Figures 11(a),12(a)). Specimen H1 (Figure 11(a)) exhibits a progressive directional change towards the stable mid-point along an arc of a great circle, defining a circle of remagnetization (Halls, 1976). The corresponding Zijderveld diagrams (Figure 11(c),(d)) indicate however that more than one component of magnetization is possibly destroyed during thermal cleaning.

The resultant vectors for specimen H4 (Figure 12(a)) indicate that a component with an intermediate blocking temperature is present in this specimen. The antipodal nature of this component with respect to a magnetization component with a higher blocking temperature, is clearly indicated in Figure 12(d).

A magnetization component with an intermediate blocking temperature is indicated by Figure 11(d). This intermediate component has the following direction:
D = 263,0° and I = 46,5°, and the antipodal nature of this component is not illustrated clearly by this specimen, possibly due to overlapping blocking temperature spectra. Figure 13 indicates that the resultant and difference vectors correspond until temperatures approaching 400°C, suggesting that a single intermediate magnetization component is removed at temperatures in the vicinity of 400°C. Specimen H4 displays an unusual behaviour at high temperatures. Figure 12(d) indicates an intensity increase at these temperatures which may be attributable to the presence of a component of magnetization with a high blocking temperature. The behaviour of specimens H1 and H4 differs during thermal cleaning. It appears that all the anorthosite specimens do not contain a component with a low

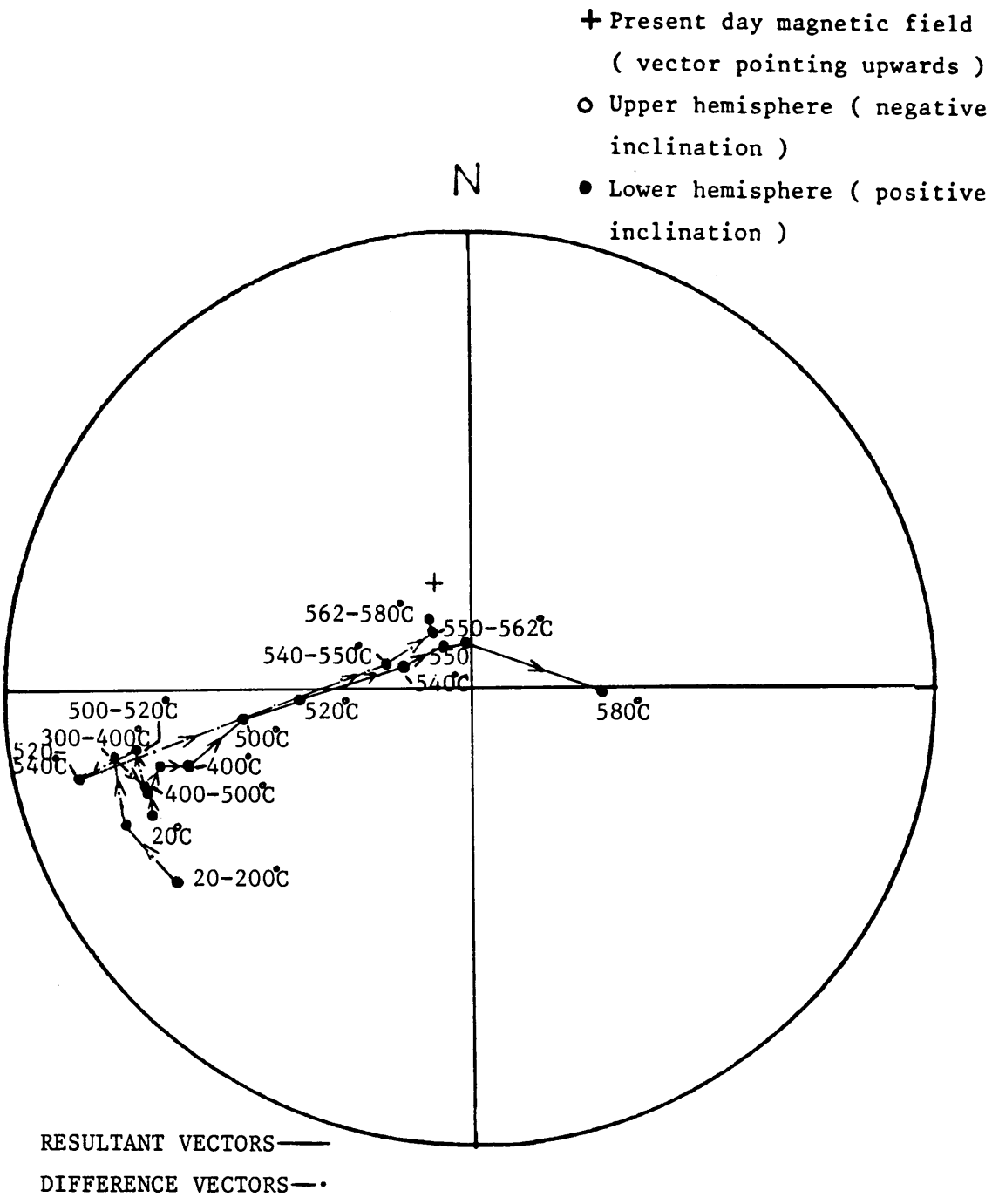

Figure 13: Resultant and difference vectors of specimen H1 during thermal demagnetization.

blocking temperature, and that the low to intermediate blocking temperature component is always present in these specimens. The latter component is significant because it has an antipodal direction to that of the primary magnetization direction.

3.3 Petrographical and mineralogical results:

(a) Petrography:

The mottled anorthosite consists of bent, interpenetrating cumulus plagioclase crystals with lesser amounts of intercumulus orthopyroxene and interstitial clinopyroxene as well as about 3 volume percent quartz and orthoclase. During microscopic inspection it was found that the interstitial quartz is optically continuous over large areas. Von Gruenewaldt (1973) suggested that this was an indication that the interstitial spaces are interconnected.

The plagioclase crystals, which are up to 45 mm in length, are twinned and zoning is common. According to von Gruenewaldt (1973) the zoning is usually less than 10 mol. percent An, and may be normal, reversed or oscillatory, and it is confined to the outermost rims of the crystals. The composition of An_{65} (Table II) corresponds with that found by von Gruenewaldt (1971, Folder III), and only central areas of crystals were analysed for this determination. Minute exsolved K-feldspar phases, which are apparently orientated parallel to the cleavage traces of the plagioclase, were found during microprobe investigations. Saussuritization of the plagioclase has taken place, and the rock is characterised by numerous cross-cutting serisitic veins. According to Molyneux (1970, p. 37) the saussuritization is a magmatic (deuteric) alteration.

The orthopyroxene, which is strongly pleochroic, has a composition of Fs_{42} (Table III). Coarse and fine exsolved blebs and lamellae of clinopyroxene occur in the orthopyroxene grains, indicating that this rock is in the orthopyroxene-pigeonite transition (von Gruenewaldt, 1971). These exsolutions are orientated in three crystallographic directions, and represent pre- and post inversion lamellae (von Gruenewaldt, 1970), as indicated in Figure 14. The interstitial

Table II: Electron microprobe analyses, structural formulae and molecular percentages of plagioclase in the mottled anorthosite.

Sample #		1PL1	1PL2	1PL3	1PL4	1PL5
SiO_2		52,32	52,23	52,99	52,60	51,75
Al_2O_3		30,43	30,52	30,20	30,52	30,61
FeO		0,45	0,42	0,37	0,48	0,39
MgO		0,01	-----	-----	0,01	0,01
CaO		13,07	12,76	12,87	13,17	13,22
Na_2O		3,79	3,70	3,89	3,71	3,60
K_2O		0,21	0,17	0,20	0,22	0,17
Total		100,28	99,80	100,52	100,71	99,75
Number of cations on the basis of 32(O)						
Si		9,48	9,49	9,56	9,48	9,43
Al		6,50	6,53	6,42	6,48	6,57
		15,98	16,02	15,98	15,96	16,00
Fe		0,07	0,06	0,06	0,07	0,06
Mg		----	----	----	----	----
Ca		2,54	2,48	2,49	2,54	2,58
Na		1,34	1,30	1,36	1,30	1,28
K		0,04	0,04	0,04	0,04	0,04
		3,99	3,88	3,95	3,95	3,96
mol%	An	64,8	64,9	64,0	65,5	66,2
	Ab	34,2	34,0	35,0	33,5	32,8
	Or	1,0	1,1	1,0	1,0	1,0

Table III: Electron microprobe analyses, structural formulae and Mg/(Mg+Fe) values for coexisting ortho- and clinopyroxenes in the mottled anorthosite.

	ORTHOPYROXENE		CLINOPYROXENE	
Sample #	1OPX1	1OPX2	1CPX1	1CPX2
SiO_2	52,32	52,28	51,96	51,72
TiO_2	0,15	0,20	0,36	0,44
Al_2O_3	0,67	0,60	1,28	1,35
FeO_T	26,69	25,45	10,61	11,30
MnO	0,56	0,59	0,25	0,23
MgO	19,45	19,35	12,81	12,71
CaO	0,89	1,18	22,17	21,33
Na_2O	0,01	0,01	0,22	0,24
K_2O	----	----	----	----
Cr_2O_3	----	0,01	----	----
Total	100,74	99,67	99,66	99,32
Number of cations on the basis of 6(O)				
Si	1,98	1,99	1,96	1,96
Al	0,02	0,01	0,04	0,04
	2,00	2,00	2,00	2,00
Al	0,01	0,01	0,02	0,02
Ti	----	0,01	0,01	0,01
Fe_T	0,84	0,81	0,34	0,36
Mn	0,02	0,02	0,01	0,01
Mg	1,10	1,10	0,72	0,72
Ca	0,04	0,05	0,90	0,87
Na	----	----	0,02	0,02
K	----	----	----	----
Cr	----	----	----	----
	2,01	2,00	2,02	2,01
$Mg/(Mg+Fe^{2+})$	0,57	0,58	0,68	0,67
Mol % Wo	2,0	2,5	46,0	44,6
Mol % En	55,6	56,1	36,7	36,9
Mol % Fs	42,4	41,4	17,3	18,5

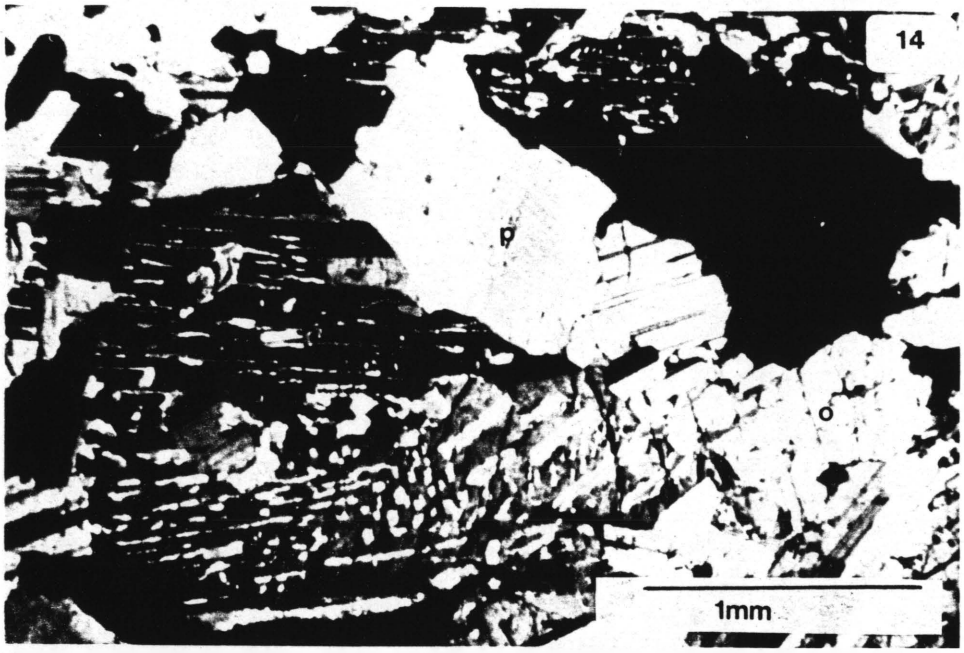

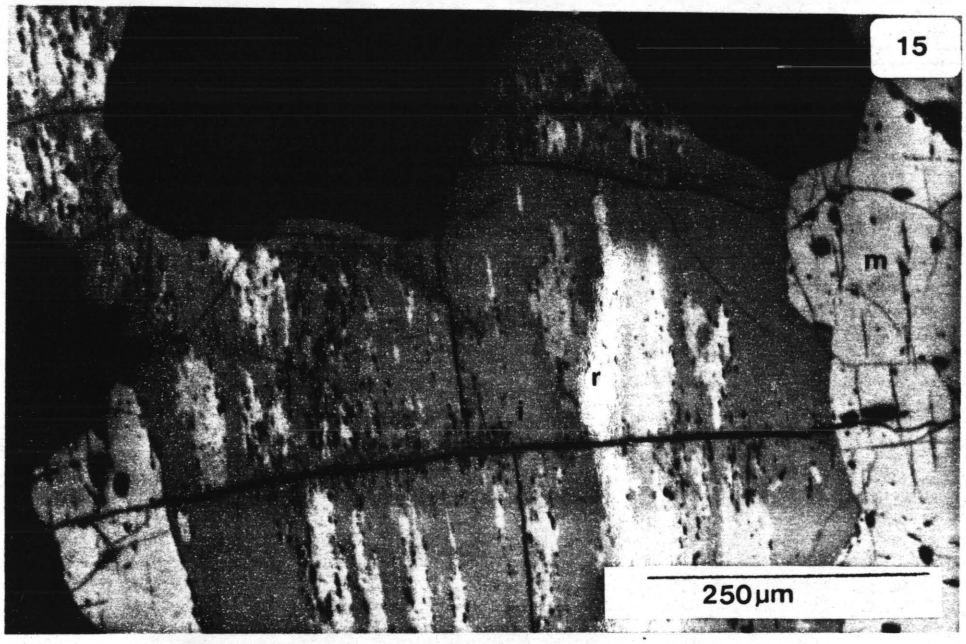

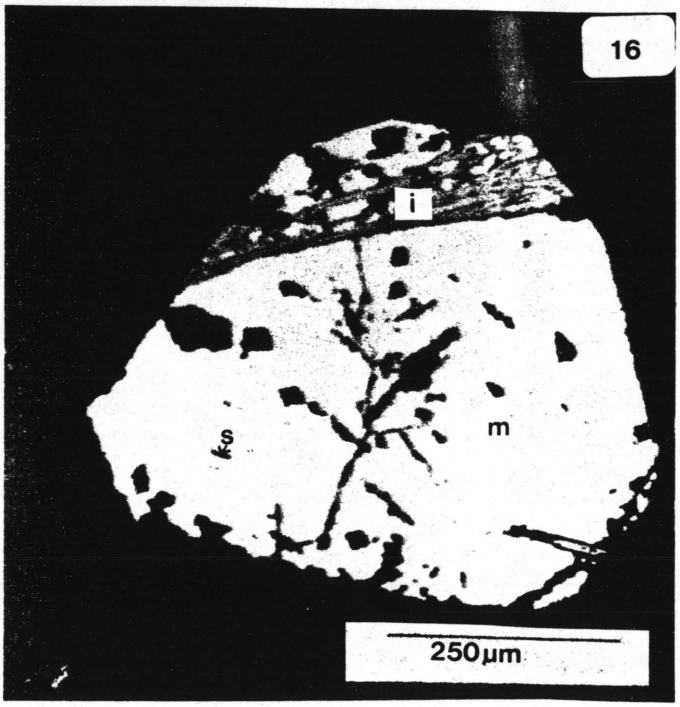

clinopyroxene ($Wo_{45}En_{37}Fs_{18}$, Table III) has a prominent parting parallel to (001) (malacolite parting) and generally has reaction rims of hornblende. Both the ortho- and clinopyroxene grains enclose plagioclase laths ophitically to subophitically. No difference in composition between the included and the larger cumulus plagioclase crystals was found. The orthopyroxene is more commonly altered than the clinopyroxene, and the alteration products include chlorite, a fibrous amphibole (uralite) and biotite.

After calculation of a structural formula for the ortho- and clinopyroxenes from microprobe analyses, it was found that the Fs-content of 42 for the orthopyroxene appeared to be far too high, in comparison with Fs_{35} found by von Gruenewaldt (1971, Folder III). Comparison of atomic percentages with molecular percentages indicated that the Fe-content was in fact so high and the results obtained from the calculation of the structural formulae, as well as the corresponding Mg /(Mg+Fe) values (Table III), supported this. A powdered fraction of the pyroxene in the rock was prepared and the refractive indices were determined. This, however, supported the previous findings. A comparison of the distribution coefficient of Mg and Fe in coexisting Ca-poor and Ca-rich pyroxenes (Kretz, 1963) in silicate systems confirmed that these two pyroxenes could however have crystallized together from the melt. This is taken as conclusive evidence that the determined Fs - content of the orthopyroxene is correct. Figure 17(a) after Kretz (1963) indicates the above mentioned equilibrium.

(b) Ore mineralogy:

Extremely small quantities of opaque minerals were found in the mottled anorthosite. Initial investigations indicated that ore minerals occur chiefly as tiny finely scattered grains and blebs which are associated with plagioclase, ortho- and clinopyroxene grains and cross-cutting serisitic veins, and that these represent remnants of larger originally euhedral ore grains.

Larger, partially resorbed, euhedral to subhedral ore grains of up to 500 micron in diameter occur interstitially between the silicate

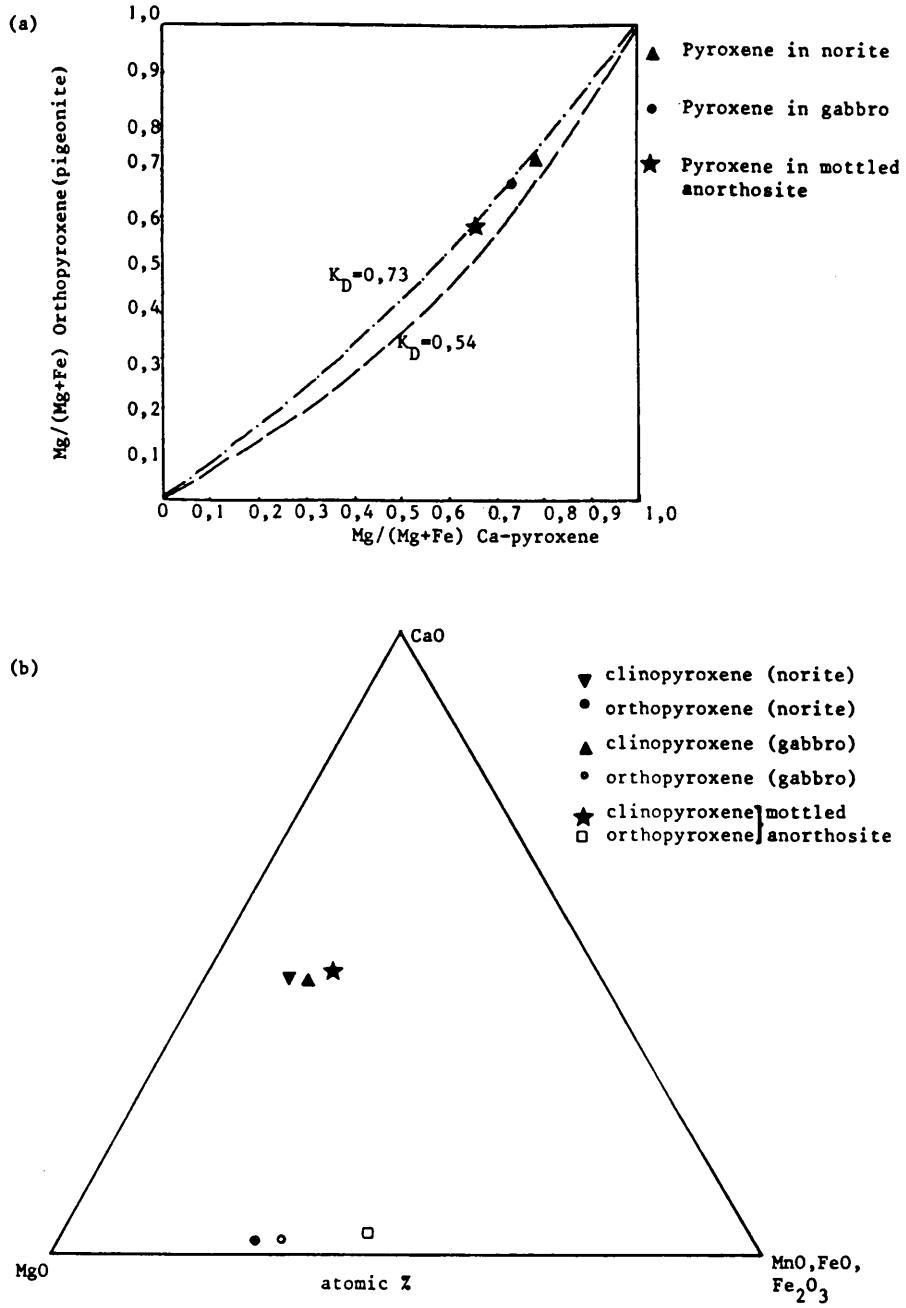

Figure 17(a): Distribution of Mg and Fe^{2+} between coexisting Ca-rich and -poor pyroxenes in the rocks from the study site.
Curve K_D=0,54 (metamorphic rocks);
curve K_D=0,73 (rocks crystallized from silicate melt) (after Kretz, 1963).

(b): Compositional plot of coexisting pyroxenes in the three rock types from the study site.

minerals , often associated with clinopyroxene. These grains are generally altered and surrounded by biotite which in turn is partially altered to chlorite. Microprobe investigations indicate that these interstitial euhedral to subhedral ore grains are mainly relatively pure unaltered magnetite with a very low Ti-content, and ilmenite. Table IV consists of analyses of these coexisting phases, and Figure 18(a) indicates their composition in the system $FeO.TiO_2.\frac{1}{2}Fe_2O_3$. The ilmenite contains minute orientated hematite exsolutions (less than 10 micron in length) in the central parts of the grains between larger patchy lenses of alteration (Figure 15).

Three types of ilmenite exsolution are found in the magnetite; trellis, composite and sandwich types (Buddington and Lindsley, 1964). Fine exsolved ilmenite lamellae (c . 10-50 micron in length) orientated along {111} of magnetite form trellis type exsolutions. These lamellae are oxidation-exsolution features (Haggerty, 1976b) and have tapered terminations. This type of exsolution represents an intermediate stage of oxidation during which the following reaction applies:

$$6\ Fe_2TiO_4 + O_2 = 6\ FeTiO_3 + 2\ Fe_3O_4$$

and f_{O_2} of $10^{-20.8}$ atm. at 600°C or $10^{-15.4}$ atm. at 800°C

(Haggerty, 1976b, Hg8).

Less frequently larger and coarser sandwich exsolutions of ilmenite which have sharply defined contacts with the host occur along one set of octahedral planes (Figure 16). These exsolutions are not parallel and do not have tapering terminations. It appears that sandwich laths may be the result of subsolidus oxidation at high temperatures or they may be primary inclusions (Haggerty, 1976b).

External composite exsolution types are recognized as subhedral inclusions of ilmenite which are frequently present in association with and adjacent to magnetite. They form well defined cuspate contacts with their magnetite hosts and no orientation along {100} or {111} could be recognised (Figure 19). According to Buddington and Lindsley (1964) composite intergrowths of ilmenite and magnetite may

Table IV: Electron microprobe analyses of coexisting ilmenite and magnetite in the mottled anorthosite.

	ILMENITE			
Sample #	MA1	MA2	MA3	MA4
SiO_2	0,04	0,02	0,06	0,04
TiO_2	46,87	47,26	46,47	47,81
Al_2O_3	0,02	0,03	0,03	0,02
Fe_2O_3	10,99	11,71	12,30	9,76
FeO	39,80	39,88	39,27	40,63
MnO	2,31	2,57	2,50	2,35
MgO	0,03	0,02	0,03	0,02
Cr_2O_3	----	----	----	0,01
V_2O_3	0,05	0,06	0,06	0,03
Total	100,11	101,55	100,72	100,67
Number of ions on the basis of 3(O)				
Si	----	----	----	----
Ti	0,89	0,89	0,88	0,91
Al	----	----	----	----
Fe^{3+}	0,21	0,22	0,23	0,19
Cr	----	----	----	----
V	----	----	----	----
	1,10	1,11	1,11	1,10
Fe^{2+}	0,84	0,83	0,83	0,86
Mn	0,05	0,05	0,05	0,05
Mg	----	----	----	----
	0,89	0,88	0,88	0,91

	MAGNETITE			
Sample #	MM1	MM2	MM3	MM4
SiO_2	0,08	----	----	----
TiO_2	0,04	0,05	0,04	0,04
Al_2O_3	0,25	0.09	0,02	0,04
Fe_2O_3	68,48	69,35	68,79	69,08
FeO	31,40	31,41	31,08	31,22
MnO	0,03	----	0,02	0,01
MgO	----	----	----	----
Cr_2O_3	----	----	----	----
V_2O_3	0,38	0,12	0,13	0,11
Total	100,66	101,22	100,08	100,50
Number of ions on the basis of 4(O)				
Si	----	----	----	----
Ti	----	----	----	----
Al	0,01	----	----	----
Fe^{3+}	1,97	1,99	1,99	1,99
Cr	----	----	----	----
V	0,01	----	----	----
	1,99	1,99	1,99	1,99
Fe^{2+}	1,00	1,00	1,00	1,00
Mn	----	----	----	----
Mg	----	----	----	----
	1,00	1,00	1,00	1,00

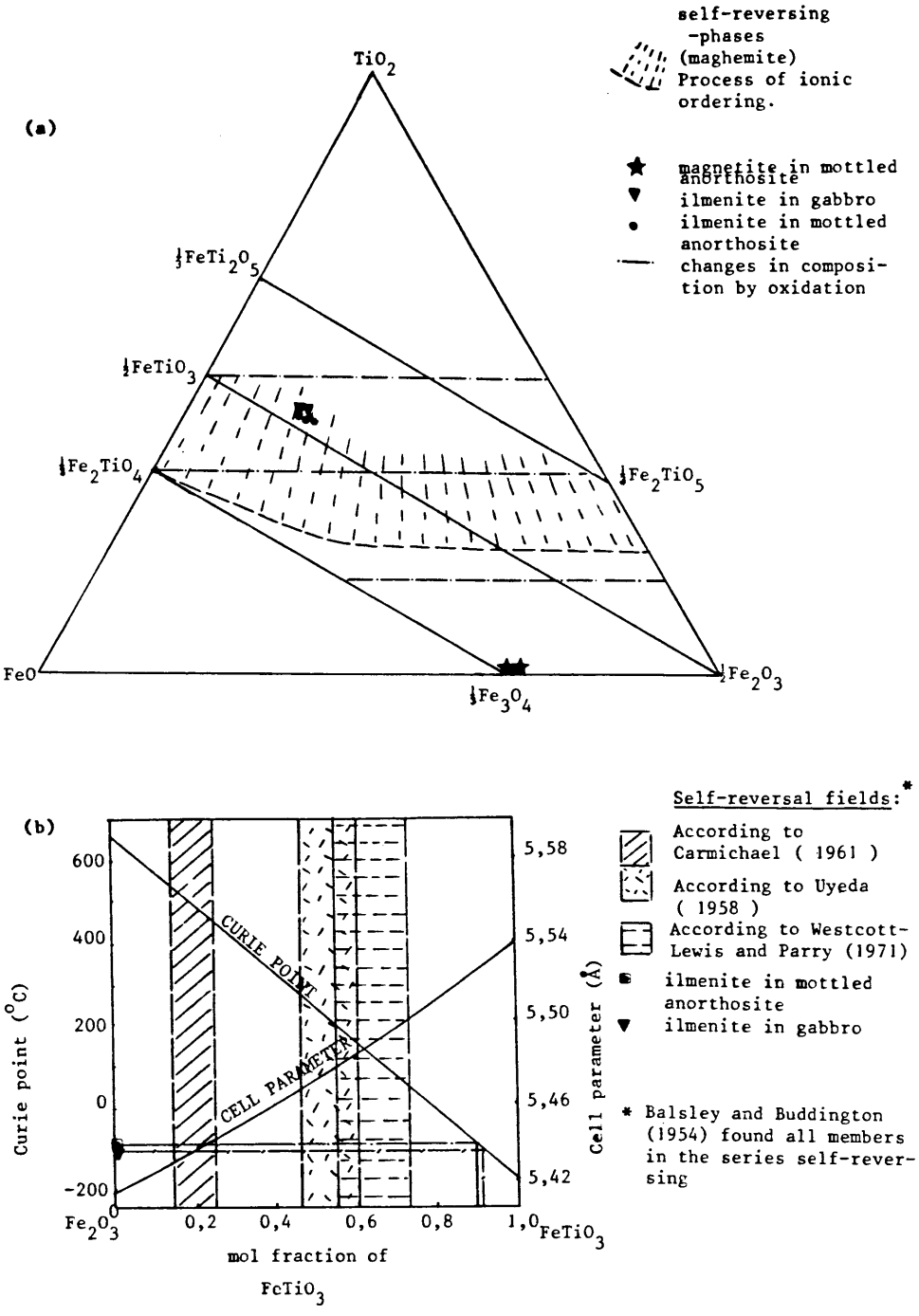

Figure 18(a): Compositional diagram for the system (FeO-TiO_2-$\frac{1}{2}Fe_2O_3$)(after Gorter, 1957).

(b): Variation of Curie temperature and unit cell parameter for the hematite-ilmenite series (after McElhinny, 1973).

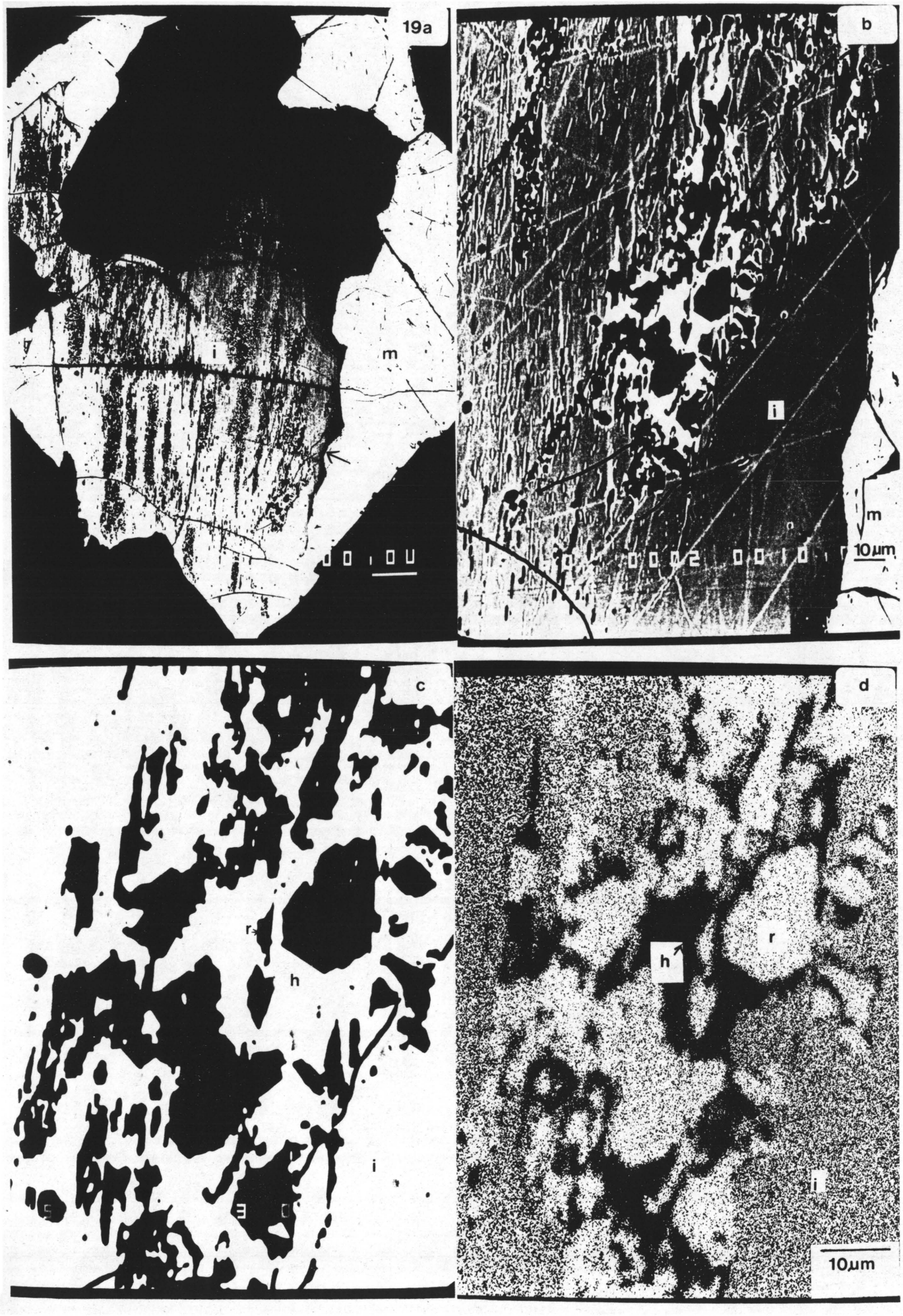

develop by slow diffusion in deep seated intrusive bodies thus representing primary precipitates from the melt.

Tiny orientated rod-like exsolutions characterized by high Ti, Al and Fe-contents are found along {100} in the magnetite. They presumably represent the spinel hercynite ($FeAl_2O_4$) which occurs as exsolutions at the border of minute ilmenite lamellae. These spinel plates or laths were exsolved at high temperatures on the {100} plane of magnetite (Molyneux, 1970). Butcher (1985) described similar exsolutions of pleonaste or spinel in the cores of Bushveld Complex magnetites. Indistinct mottling of the ilmenite-titanomagnetite intergrowth is the first sign of post-exsolution oxidation (Haggerty, 1976b). As defined by the latter author, the C4 stage mottling is due to the formation of minute exsolved transparent spinels in the titanomagnetite and the development of ferri-rutile in the ilmenite (metailmenite). Although the spinel rods were found by probe investigations during the present study, mottling was not observed in these areas. At saturation point for exsolution of ilmenite from magnetite, spinel is exsolved and titanomagnetite is oxidized to titanohematite (Haggerty, 1976b). The larger magnetite grains are not oxidized to hematite indicating that the spinel exsolution represents the onset of post exsolution-oxidation. Hematite is however present as the scattered remnants of the larger ore grains. Maghemite was not identified and this is in accordance with Molyneux (1970) who found that grains of Bushveld ore of nearly pure magnetite alter directly to martite (hematite pseudomorphs after magnetite). This finding is supported by Haggerty (1976a) who suggests that oxidation to maghemite is associated with titaniferous magnetite solid solutions, whereas Ti-poor magnetite solid solutions oxidize more readily to hematite. Furthermore, during the formation of maghemite (which is a low-temperature event) no additional high-temperature oxidation phases such as rutile develop. It is thus evident that the magnetite in this rock represents an intermediate stage of high temperature oxidation and that post-exsolution oxidation did not alter the high-temperature assemblage significantly. Fine grained remnants of the original grains are however generally oxidized to hematite.

Exsolution of hematite from ilmenite is indicative of slow cooling at relatively great depths and the exsolution of the hematite is along the {0001} plane of the host ilmenite (Figure 19). The distribution of the fine lamellae of hematite results in a synneusis texture as described by Haggerty (1976a).

The sub-solidus oxidation and replacement textures of the ores in Figures 15 and 19 indicate that the ilmenite has undergone a more advanced stage of oxidation than the magnetite. The lenses of patchy alteration in the ilmenite are along {0001} and consist of rutile and hematite (Figures 19 (b)-(d)). The ilmenite represents an intermediate stage of high temperature oxidation (stage R4, Haggerty , 1976b), being characterised by a finely disseminated assemblage of rutile and titanohematite in the oxidation zones. The lenses of oxidation are orientated parallel to the hematite exsolutions and rutile replaces the hematite exsolutions randomly. The lamellar lenses are characterized by a higher reflectivity and anisotropy than the host. It appears that the original hematite exsolutions provided sites for subsolidus oxidation. Cracks in the host acted as channelways along which deuteric fluids preferentially migrated. The resulting assemblage of rutile and hematite is thus leucoxene (Fe_2O_3. TiO_2). Sphene ($CaTiSiO_5$) was identified in some lenses but is usually absent. Sphene formation represents magmatic metasomatism; a reaction involving residual liquids and early formed Fe-Ti oxides (Haggerty, 1976a). Rutile is regarded as a pseudomorphic alteration (oxidation) product which develops above 600°C (Haggerty, 1976b). The ilmenite assemblage apparently resembles a more advanced sub-solidus oxidation product than what the magnetite does, but presumably the replacement took place at temperatures above 600°C. According to Cahn (1967) discontinuous exsolution results from the metastable existence of homogeneous compositions below the solvus in the ilmenite-hematite system, until homogeneous nucleation or spinodal decomposition occurs. Furthermore, he infers that this process could occur several times during the cooling history of an ilmenite-hematite assemblage. Thorpe et al. (1977) found the presence of minute magnetite volumes in homogeneous hematite blebs which were exsolved from ilmenite. The existence of such magnetite blebs in hematite from the present investigation cannot be discounted. Additional opaque minerals in the

form of scattered blebs of sulphides, pyrite, chalcopyrite and minor amounts of pentlandite, were identified in some thin sections.

The second type of ore in the mottled anorthosite was found to be much more abundant on investigation at high magnifications. The ore occurs as orientated laths in the plagioclase and pyroxene, and such ore laths were reported by Hattingh (1983) amongst others as needles or lamellae. These laths are often found at the tips of biotite / chlorite platelets (Figures 20 and 21) and they consist of magnetite, ilmenite as well as a variety of sulphides which apparently represent replacements of the original Fe-Ti-oxide assemblages. They were only analyzed qualitatively due to their small size and the Fe:Ti ratios of the Fe-Ti oxides vary from roughly 2:1 to 1:1 to 1:2, indicating that they represent either magnetite, ilmenite or ilmeno-rutile ($FeTi_2O_5$) respectively. In general spot analyses of these areas indicated that they contained either Fe or Ti in abundance, with minor amounts of Al, Si, Ca, and traces of Mn. Al, Si, and Ca suggest alteration of the ore to sphene, whilst the Mn traces can easily be accomodated by the ore assemblage. The implications are that the laths represent discrete magnetite or ilmenite that crystallized separately from the melt. Subsequently high temperature oxidation partially altered these minerals to ilmeno-rutile and sphene. Electron microscopic investigations (SEM) confirmed that these areas containing the laths are characterised by the presence of K, but that they are not always associated with biotite/chlorite flakes. In cases where biotite/chlorite flakes are absent, the K-content is attributed to sub-microscopic exsolutions of K-feldspar in the plagioclase host. According to Gallagher et al. (1968), particles of magnetite smaller than 0,3 micron readily alter to maghemite (at low temperatures). The state of oxidation of the laths could not be determined accurately, but their reflectivity was lower than that of hematite or maghemite and they lacked the bluish tints of the latter two minerals. The Fe-rich laths are thus interpreted as magnetite.

In the plagioclase the laths are orientated in at least three crystallographic directions, one of which is always parallel to the twin lamellae. Groeneveld (1968) reported that magnetite grains were orientated along three crystallographic directions of the plagioclase.

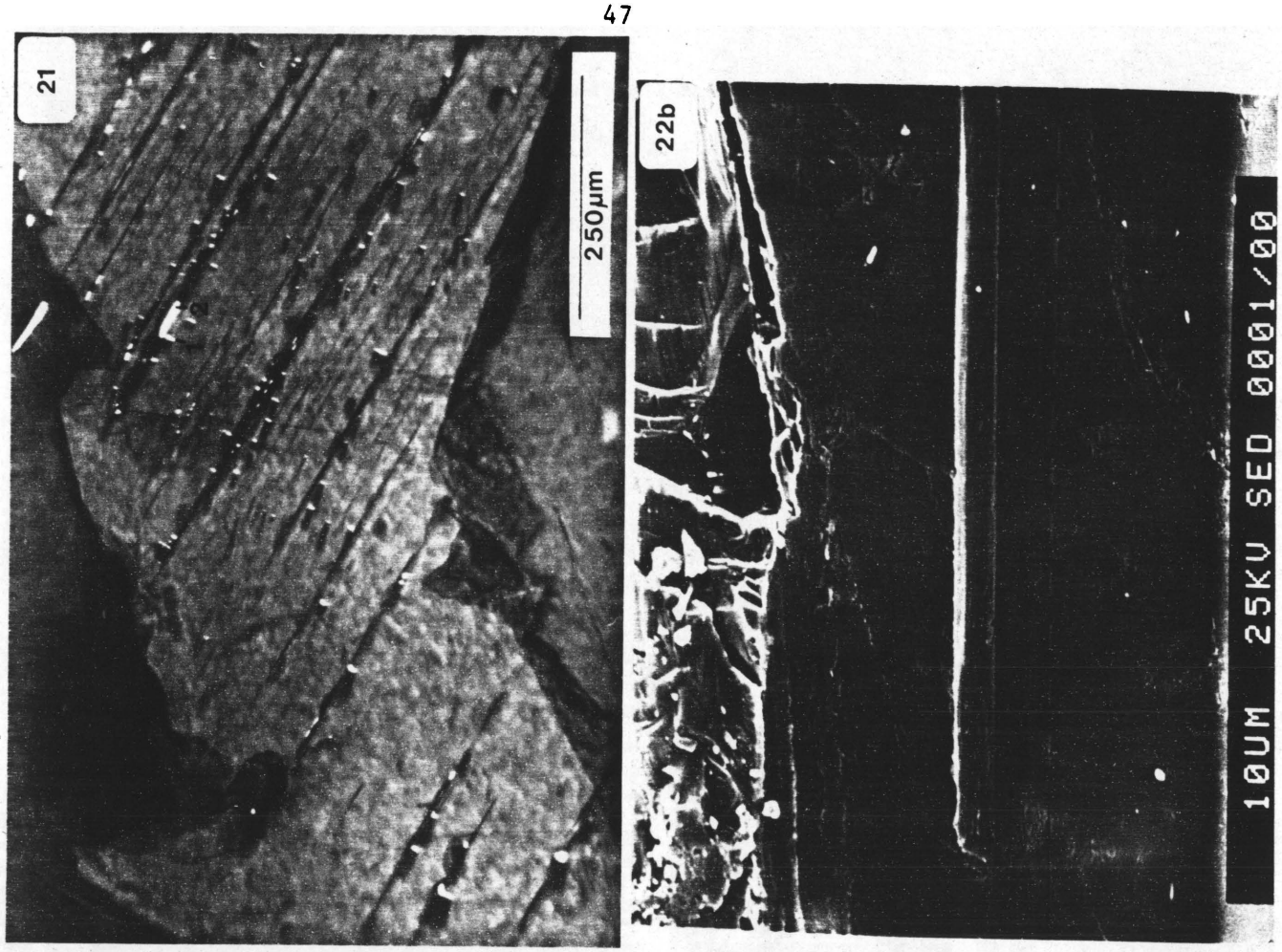

These orientated laths are 10-350 micron in length and 5-20 micron in width. Although microprobe investigations suggested that these laths were in the order of 1 micron in width, SEM investigations revealed the three dimensional structure of these laths (Figure 22). During the SEM investigation no evidence of these thin laths (needles) could be found, and they were all found to be wider than 10 micron. It is nevertheless a possibility that smaller laths do exist, but they are apparently not plentiful.

Two types of orientated ore laths are found in the clinopyroxene grains (Figure 21), namely those that cross-cut the cleavage traces, and those orientated parallel to the cleavage traces. The first type occurs along parting planes, and consists of laths which are orientated parallel to one another, and cross-cut the cleavage traces (Figure 23). Groeneveld (1968, p. 70) found that small crystals of magnetite are haphazardly orientated in the clinopyroxene. Fleet et al. (1980) suggested that, due to the monoclinic symmetry of clinopyroxenes, magnetite inclusions were arranged in irrational directions in the plane containing the X and Z axes. These laths appear to be associated with the alteration of the clinopyroxene and are 50-80 micron in length and 20-50 micron in width. The more common type of lath is found parallel to the cleavage traces, often on the tips of biotite / chlorite flakes (Figure 23(b)). These range from 30-50 micron in length to 5-40 micron in width, and often terminate in rounded or subrounded blebs of ore, normally at the edge of a clinopyroxene grain (Figure 23(c)). Their terminations at the edges of grains suggest that they were exsolved out of the pyroxene. It was illustrated by Fleet et al. (1980) that the magnetite inclusions in pyroxenes developed after crystallization of the primary silicate minerals. In the orthopyroxene grains ore laths are seldom seen, but when they do occur they are parallel to the c-axis and are also associated with biotite and chlorite. Their average size is 30 micron in length and 5 micron in width. Moore (1968) reported rutile exsolutions in orthopyroxenes.

It is thus evident that some of the magnetic minerals which occur in this rock are commonly associated with biotite / chlorite flakes. The composition and structural formulae of the unaltered biotite and

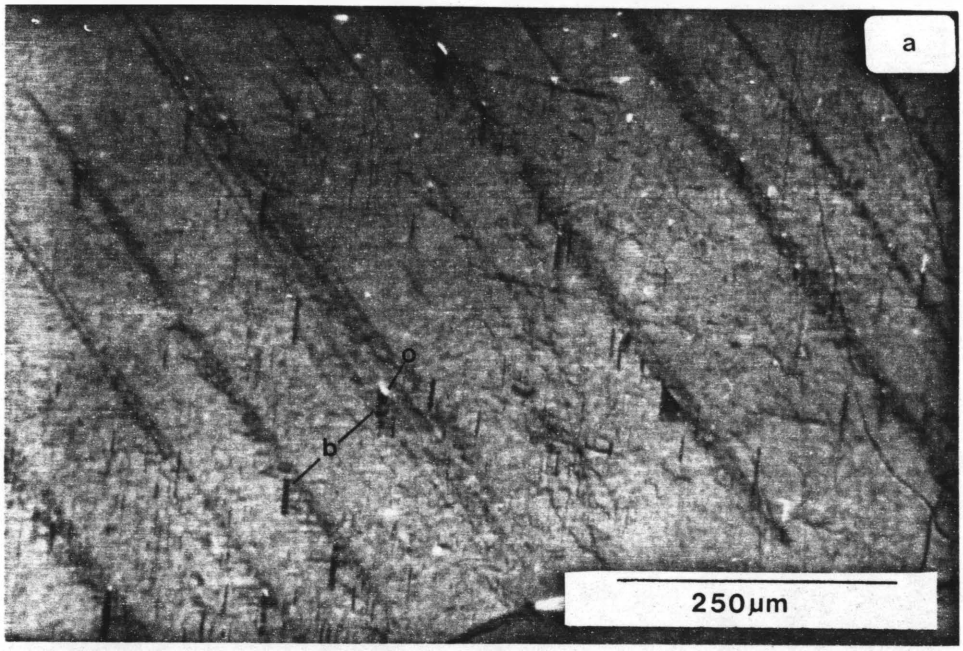

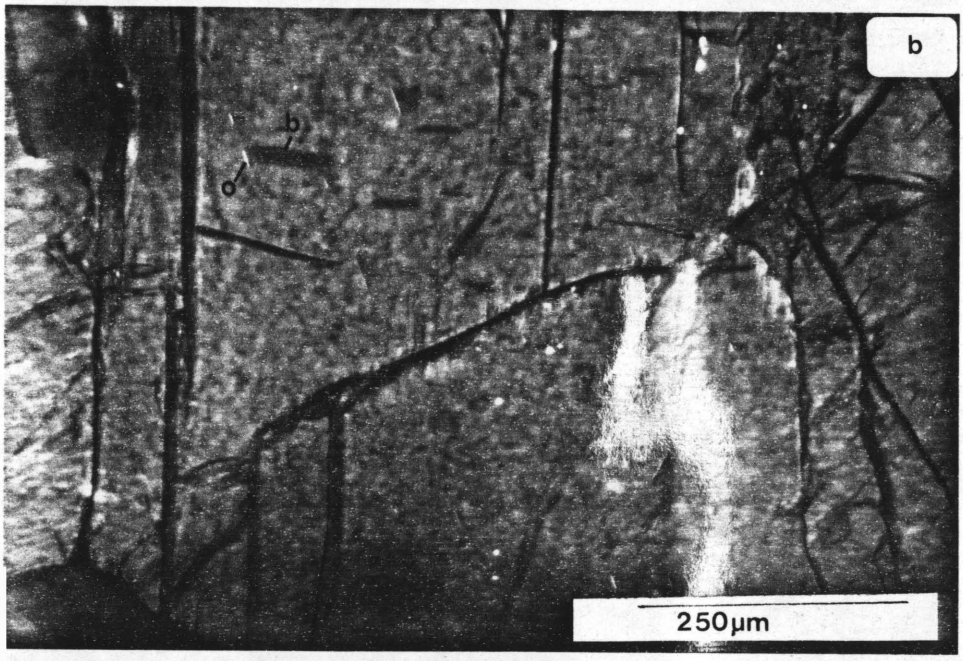

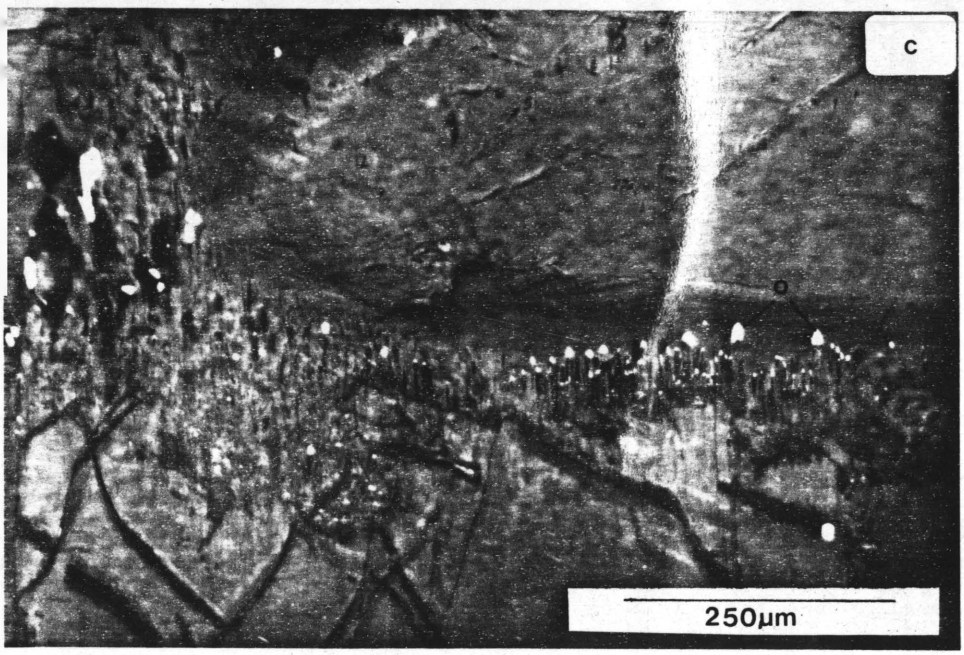

chlorite are given in Table V and VI respectively. Previous workers have found that the needles in the plagioclase are probably inclusions of magnetite (Groeneveld, 1968; Molyneux, 1970; von Gruenewaldt, 1971). This investigation has shown, with the aid of SEM studies, qualitative electron microprobe investigations (X-ray and BEI) and calculations based on plagioclase, chlorite and biotite analyses that these "needles" are laths of either magnetite, ilmenite or ilmeno-rutile.

Table V consists of a calculation in which use was made of a plagioclase analysis which was high in Fe-content. It can be seen that, if it is assumed that the Fe is attributable to the presence of biotite, there is still an excess of Fe. This abundance can be calculated as iron oxide and indicates that the plagioclase contains 0,80% iron oxide which is presumably magnetite. Furthermore, the association of the magnetite with biotite and/or chlorite in some cases implies either a magmatic link such as inclusion or exsolution between the magnetite and silicate or that the magnetite is associated with alteration (possibly deuteric) or replacement. This in turn implies that these may be either primary inclusions or exsolutions of magnetite, or secondary exsolutions of magnetite. They would thus carry either a TRM or a CRM respectively.

Haggerty (1976a) suggests that during autometasomatism (deuteric alteration) and the subsequent formation of sphene, the late-stage phyllosilicates such as biotite are capable of accomodating fairly large proportions of Fe. It seems that ore mineral exsolutions from pyroxenes which terminate in blebs are definitely associated with the decomposition of biotite and chlorite to magnetite. Haggerty (1976a) suggests that this type of magnetite is usually very close in composition to stoichiometric Fe_3O_4 such as that found in the present investigation. According to von Gruenewaldt (1971, p. 105) biotite is often present as tiny flakes embedded in cleavage planes of the plagioclase, and the biotite is not considered to be an original inclusion. He infers that it probably crystallized at a later stage owing to exsolution of some K^+ from the plagioclase at decreasing temperatures.

Table V: Electron microprobe analysis and structural formula of biotite in the mottled anorthosite.

SiO_2	37,61
Al_2O_3	14,46
MgO	16,49
CaO	0,02
K_2O	8,15
TiO_2	2,81
FeO	14,56
MnO	0,11
Cr_2O_3	----
Total	94,21
H_2O	5,79 (assumed)

Number of ions on the basis of 24(O)

Si	5,44
Al	2,42
	7,86
Mg	3,56
Ca	---
Ti	0,30
Fe	1,76
Mn	0,01
	5,63
K	1,50
OH^-	5,59

CALCULATION:*

100% biotite contains 16,49% MgO + 14,56% FeO + 8,15% K_2O (from above analysis).

A plagioclase analysis contained 0,03% MgO and 0,77% FeO. If it assumed that the plagioclase contains biotite, as is often found, then the following holds:

0,03% MgO would require 0,03% FeO + 0,02% K_2O and would yield 0,18% biotite.

Thus there is an excess of (0,77-0,03)% FeO which can be attributed to magnetite. The excess K_2O can form orthoclase.

Thus:

0,74% FeO is available for magnetite in plagioclase, and

$FeO.Fe_2O_3 \longrightarrow$ mol of Fe in FeO: 1/3 x 0,74 = 0,25

remainder = 0,49 in $2FeO + O \longrightarrow Fe_2O_3$

therefore $\frac{Fe_2O_3}{2FeO} = \frac{\text{molmass } 159,69}{\text{molmass} \times 2 = 143,69} = 1,11$

remainder = 0,49 x 1,11 = 0,55.

Therefore,

total magnetite in plagioclase = 0,25 + 0,55 = 0,80%.

*A calculation based on the biotite composition and the analysis of a very Fe-rich plagioclase grain to illustrate that Fe-rich laths are present in the plagioclase.

Table VI: Electron microprobe analysis and structural formula of chlorite in the mottled anorthosite.

SiO_2	30,34
Al_2O_3	15,26
MgO	14,99
CaO	0,84
Na_2O	0,04
K_2O	1,23
TiO_2	3,54
FeO	22,65
MnO	0,15
Cr_2O_3	----
Total	89,04
H_2O	10,96 (assumed)

Number of ions on the basis of 36(O)

Si	6,33
Al	1,67
	8,00
Al	2,08
Mg	4,66
Ca	0,19
Na	0,02
K	0,33
Ti	0,56
Fe	3,95
Mn	0,03
	11,82
OH^-	15,24

The latter places constraints on the crystallization / exsolution temperature of the ore laths associated with biotite or chlorite if they were in fact exsolved from the biotite. The interstitial accessory biotite, as found in this study surrounding the larger ore grains, is regarded by von Gruenewaldt (1973) to have originated by reaction between the liquid and interstitial ore minerals. This is supported by this study. Molyneux (1970, p. 99) suggested that amphibole, biotite and chlorite, and to a lesser extent sulphides replaced oxide ores during late magmatic processes involving volatiles. The latter seems to be an acceptable process to account for the close association between the biotite/chlorite and larger magnetite-ilmenite grains, and probably also explains the association between the ore laths and the hydrated minerals.

The modes of occurence of the Fe-Ti oxides in the mottled anorthosite can be summarized as follows in terms of decreasing relative abundance from (i) to (v):
(i) Microscopic to sub-microscopic Fe-Ti oxide laths in plagioclase.
(ii) Microscopic to sub-microscopic Fe-Ti oxide laths in clinopyroxene.
(iii) Microscopic euhedral to subhedral magnetite and ilmenite grains, where the ilmenite contains hematite exsolutions.
(iv) Sub-microscopic magnetite-hematite blebs.
(v) Microscopic to sub-microscopic Fe-Ti oxide laths in orthopyroxene.

If the Fe-Ti oxide mineral occurences are considered in terms of their volume percentages, then the following subdivision can be made in terms of decreasing abundance from (i) to (iii):
(i) Microscopic interstitial Fe-Ti oxides.
(ii) Microscopic to submicroscopic Fe-Ti oxide laths in plagioclase, clino- and orthopyroxene.
(iii) Submicroscopic magnetite-hematite blebs.

3.4 **Discussion of results:**

It has been illustrated that there is a soft component of magnetization in the mottled anorthosite specimens which is removed at low AF strengths and low temperatures. The direction of this component

corresponds with NRM directions. The removal of this component is accompanied by a sudden initial drop in intensity of magnetization, especially during AF demagnetization, indicating that this is an unstable secondary remanent component. Although this component is probably a VRM, it may also be an IRM (isothermal remanent magnetization) or a CRM (chemical remanent magnetization). These secondary magnetizations may be acquired in the following ways: a VRM is a time-dependent remanence which is normally acquired at a constant temperature in a weak applied field, an IRM may be acquired in a high applied field at low temperatures, whilst a CRM is acquired when a crystallite of a magnetic mineral grows in the presence of an applied magnetic field. Both a VRM and an IRM would characteristically be less resistent to AF cleaning than a TRM. The coercivity of a CRM, which would be acquired during the growth of a crystallite through its critical blocking volume, would depend on the rate of growth, the temperature at which the chemical growth took place and the composition of the crystallite (Tarling, 1983). The acquisition of this secondary magnetization component is probably related to the multidomain magnetite in the specimens.

AF- and thermal demagnetization of the specimens from the mottled anorthosite indicates that a low to intermediate component of magnetization is present in these specimens. This component has an intermediate coercivity and blocking temperature, and has an antipodal direction to the hard magnetization component. This direction does however not correspond with the present day magnetic field direction. It is possible that this magnetization component represents a VRM carried by hematite, although magnetite laths which exsolved from the pyroxene may also carry this component. The latter are larger than single domain grains, and they must have formed at temperatures below that of the primary magnetite, thus they could be associated with this magnetization component, rather than with the consistent hard component.

Both AF- and thermal demagnetization indicated that a consistent mid-point is reached at high AF strengths and at temperatures approaching the Curie point of magnetite. This component thus has a high blocking temperature and represents a stable primary component acquired during

the cooling of the rock. Since this component is destroyed at about 578°C, it represents a TRM acquired by magnetite. This primary component of magnetization corresponds with the primary magnetization direction which was isolated by Hattingh (1983) as the representative direction of the central and upper portions of the main zone of the Bushveld Complex. It is envisaged that the magnetite laths included in plagioclase are responsible for the hardness of this magnetization component.

The submicroscopic hematite blebs which are present in this rock, probably do not contribute to the remanence, since Hedley (1968) found that submicroscopic hematite (smaller than 0,2 micron) is virtually non-magnetic. Although magnetite in this range may be single-domain, and would thus be associated with a high coercivity (Tucker and O'Reilly, 1980a), no evidence for the existence of such a hard remanence associated with secondary magnetite, was found. The submicroscopic magnetite is probably sub-single-domain, and thus superparamagnetic.

Two specimens from the mottled anorthosite showed the ability to spontaneously reverse their magnetization directions while in storage over an 18 month period. This feature strongly suggests that these specimens have an ability to acquire a VRM which has a reversed magnetization direction to the primary direction of magnetization which these specimens carry. It may be that this ability is somehow linked to hematite. Hematite in this rock occurs as exsolutions in ilmenite and as submicroscopic magnetite-hematite. A relevant observation at this stage is that these specimens had been cleaned magnetically at high AF strengths prior to this reversal in magnetization direction. The latter thus indicates that a large component of the magnetization of the specimens had already been removed. The spurious behaviour of specimen H4 during thermal cleaning at temperatures above 600°C serves as an indication that the magnetic component carried by hematite may be significant during cleaning at high temperatures.

The main palaeomagnetic characteristics of the mottled anorthosite can thus be summarized as follows:

(i) The mean intensity of magnetization is extremely high (4 434 x $10^{-3}A.m^{-1}$).

(ii) The rock has a high mean magnetic susceptibility of 6,5 x 10^{-3}SI, but the magnitude of anisotropy (0,27) is low.

(iii) A consistent primary magnetization direction (TRM) was identified from both alternating field and thermal demagnetization as a component (D = 17,33°, I = 67,75°) carried by primary magnetite; the laths included in plagioclase are probably responsible for the high coercivity of this component.

(iv) A soft secondary component of magnetization which is probably associated with multidomain magnetite, is present in some specimens.

(v) A magnetization which has a low to intermediate coercivity and an intermediate blocking temperature, was identified. This component is roughly antipodal to the primary TRM, and is carried by hematite and/or secondary magnetite laths in pyroxene.

(vi) Two specimens displayed the ability to spontaneously reverse their magnetization directions after a storage period of 18 months. This behaviour is probably linked to a type of magnetic interaction between hematite exsolutions in ilmenite, and one or more of the other magnetic minerals in these specimens.

4. THE TWO-PYROXENE GABBRO:

4.1 Introduction:

The two-pyroxene gabbro unit is at most 1 m thick and displays lateral impersistence, pinching in and out between the upper and lower-lying units. The gabbro is however always present on the contact between the fine-grained norite and the mottled anorthosite, and grades into a spotted anorthosite and a pegmatoidal feldspathic rock at the norite contact (Figure 5(a)). The two-pyroxene gabbro is characterised by an undulating upper contact with "fingers" of anorthosite protruding downwards into the gabbro (Figure 4(b)), and slithers of anorthositic material near the upper contact. Igneous lamination of the tabular plagioclase crystals is common in the gabbro. The pegmatoidal rock which is intrusive into the norite is anorthositic, and contains lesser pyroxene blebs near the contact. This gives the rock a spotted appearance. Two apparent xenoliths, similar to the pegmatoidal body, occur in the underlying norite. These coarse-grained xenolithic bodies, which contain plagioclase crystals of up to 2 cm in length, appear to represent similar pegmatoidal bodies which are orientated roughly parallel to the strike of the layered units (Figures 5(b) and 5(c)).

Three specimens for palaeomagnetic purposes (M5A, M5B and M5C) were obtained from the pegmatoidal intrusive during drilling. An additional six specimens (B1-B5 and H2) from the two-pyroxene gabbro near the contact with the mottled anorthosite were also used in this study. The average intensity of magnetization of these specimens is 611×10^{-3} $A.m^{-1}$ (standard deviation = 103×10^{-3}, minimum intensity = 475×10^{-3}, maximum intensity = 765×10^{-3}), which is considerably lower than that of the mottled anorthosite.

4.2 Palaeomagnetic results:

(a) Natural remanent magnetization:

Natural remanent magnetization directions of the two-pyroxene gabbro are characteristically scattered. The distribution of NRM directions is indicated in Figure 24 and listed in Table VII. No significant grouping of directions can be made. It is evident that there are both positively and negatively magnetized NRM components in these specimens, suggesting that secondary magnetization components must be superimposed on the original TRM. The mean magnetic susceptibilty of the gabbro is 1,6 x 10^{-3}SI (standard deviation = 0;7 x 10^{-3}), whilst the magnitude of anisotropy of 0,15 is negligible (standard deviation = 0,05).

Table VII: NRM results from the two-pyroxene gabbro.

Specimen	D^o	I^o
B1	280,00	-14,99
B2	271,96	-25,58
B3	316,62	28,83
B4	306,48	22,34
B5	260,99	-32,71
H2	277,04	68,33
M5A	15,39	8,66
M5B	171,13	-65,86
M5C	28,00	34,95
	mean 287,25	mean - 3,73

with α_{95} = 56,79, k = 2, R_o = 4,76.

(b) Alternating field demagnetization:

Five specimens were subjected to stepwise AF demagnetization. The normalized intensity response curve for specimen B2 (Figure 25(b))

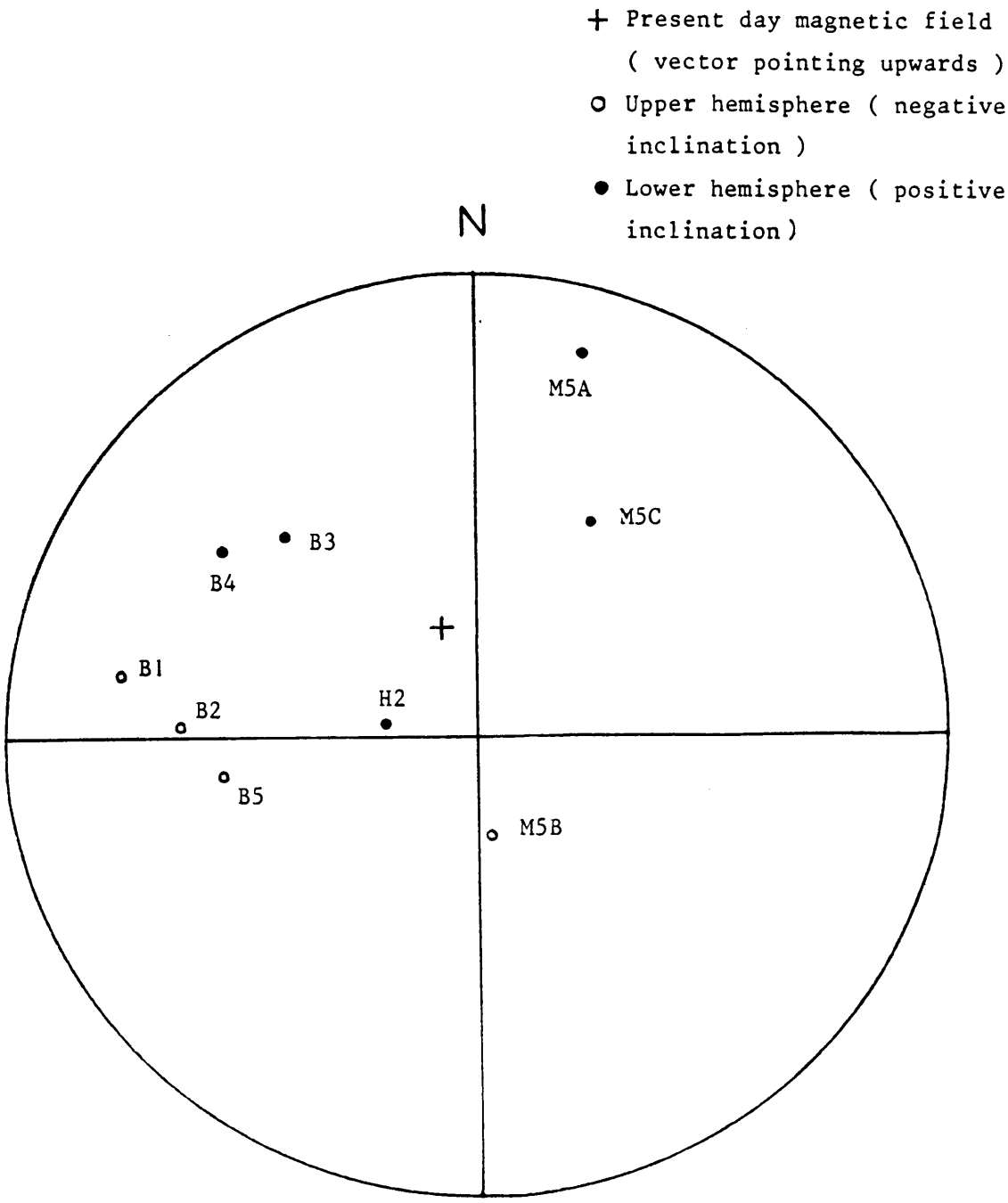

Figure 24: Stereographic projection of NRM directions of specimens from the two-pyroxene gabbro.

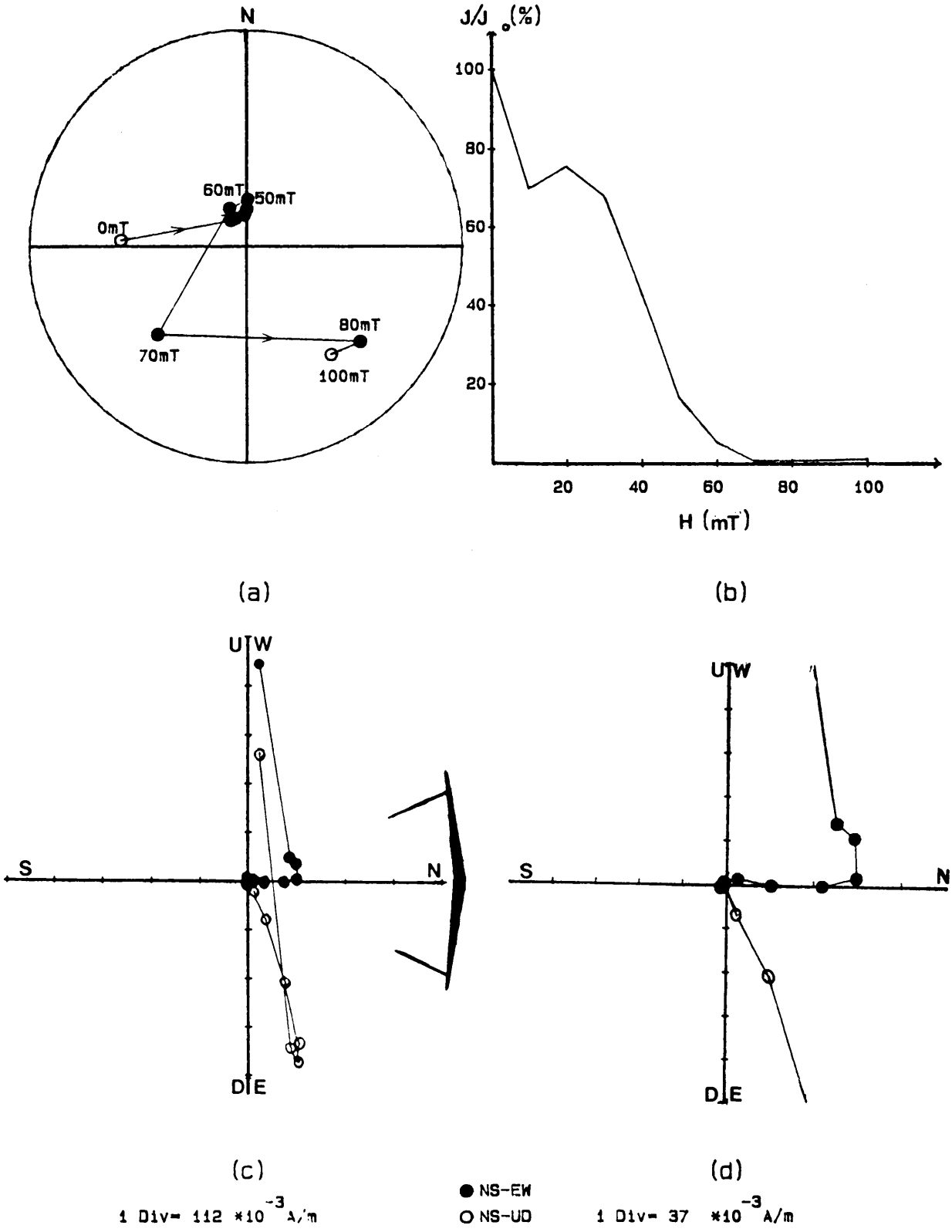

Figure 25: Stepwise AF demagnetization of specimen B2.

(a) Resultant vectors (plotting convention as in Fig.6).

(b) Normalized intensity response curve.

(c) Zijderveld stability diagram.

(d) Magnification of Zijderveld diagram (c).

indicates that a soft, low coercivity magnetization component is removed at low alternating fields. This is probably a VRM. At low to intermediate alternating fields an antipodal component of magnetization is removed. This is indicated by the large increase in intensity at these fields (Figure 26(b)). The intensity response curves indicate overlapping coercivity spectra at intermediate to high AF strengths (Figure 25(b) and 26(b)).

AF resultant vectors for specimens B2 and B3 (Figure 25(a) and 26(a)) display vector movement towards the consistent mid-point which was identified in the anorthosite, at high peak fields. The resultant and difference vectors converge at these field strengths, indicating that only one component of magnetization is being removed here (Figure 27). The consistent magnetization direction which was determined for the gabbro from AF data, has a declination of $9,34^{o}$ and an inclination of $58,70^{o}$.
The statistics for this determined direction are
$N = 5, \alpha_{95} = 5,31^{o}$; $k = 160$, where N = number of specimens.
The pegmatoidal two-pyroxene gabbro contains the same consistent magnetization component.

Zijderveld stability diagrams indicate that a low coercivity component of magnetization is removed initially (Figure 26(c)). A magnetization component is also indicated at intermediate field strengths. The Zijderveld stability diagram for specimen B2 (Figure 25(c)) indicates this component at low to intermediate fields. However, rounding of the vector path indicates overlapping coercivity spectra of magnetization components in this region (Figure 25 (c)).

A progressive breaking down of a high coercivity component is indicated at intermediate to high alternating fields, and the estimated direction from Zijderveld diagrams ($D = 20,5^{o}$, $I = 65,5^{o}$) corresponds with the consistent mid-point identified in the mottled anorthosite.

During AF cleaning three specimens reversed their inclinations between repeated magnetic measurements. In the case of all three specimens, their intensities of magnetization were well above $0,05 \times 10^{-3} A.m^{-1}$.

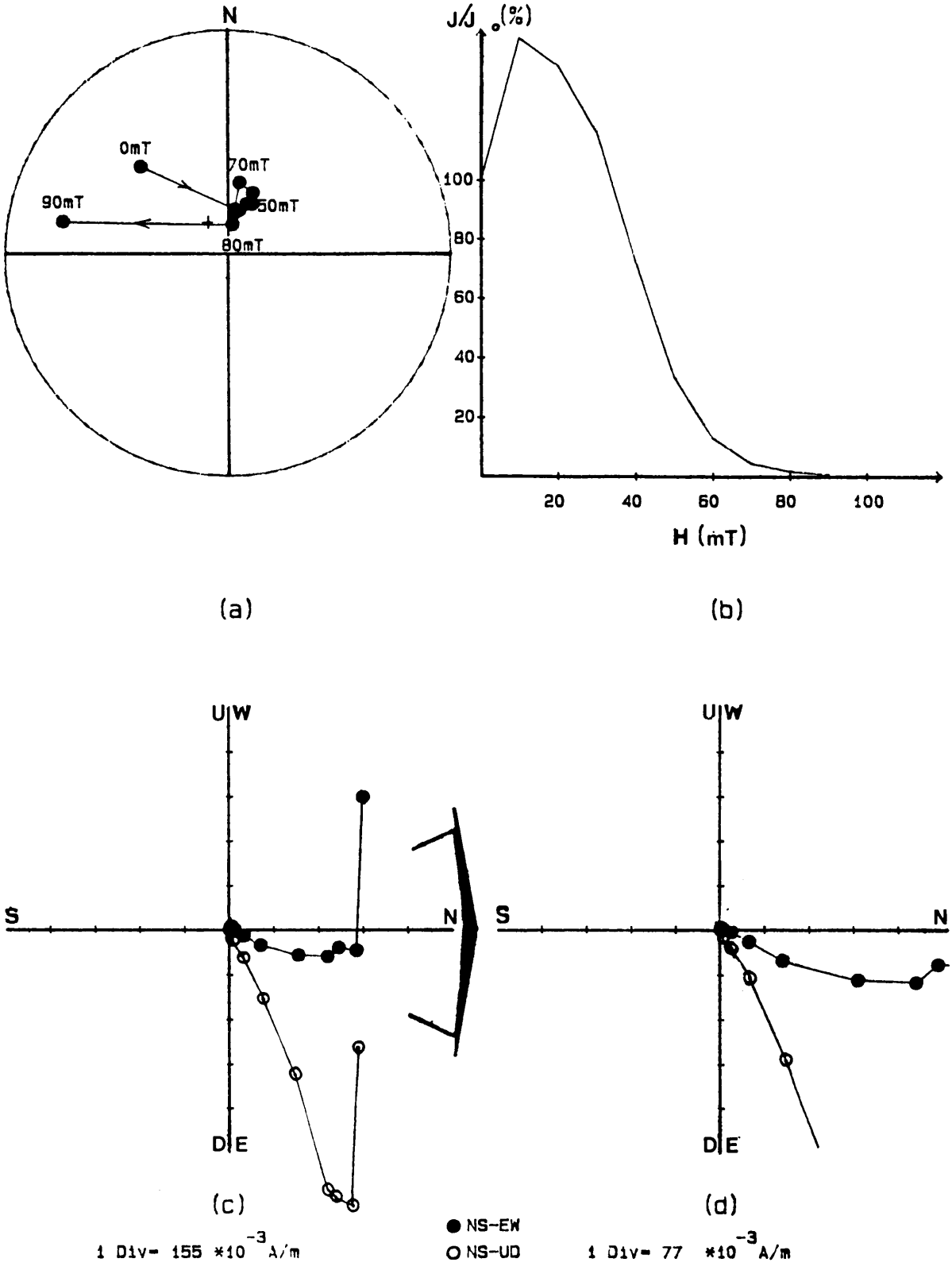

Figure 26: Stepwise AF demagnetization of specimen B3.

(a) Resultant vectors (plotting convention as in Fig.6).

(b) Normalized intensity response curve.

(c) Zijderveld stability diagram.

(d) Magnification of Zijderveld diagram (c).

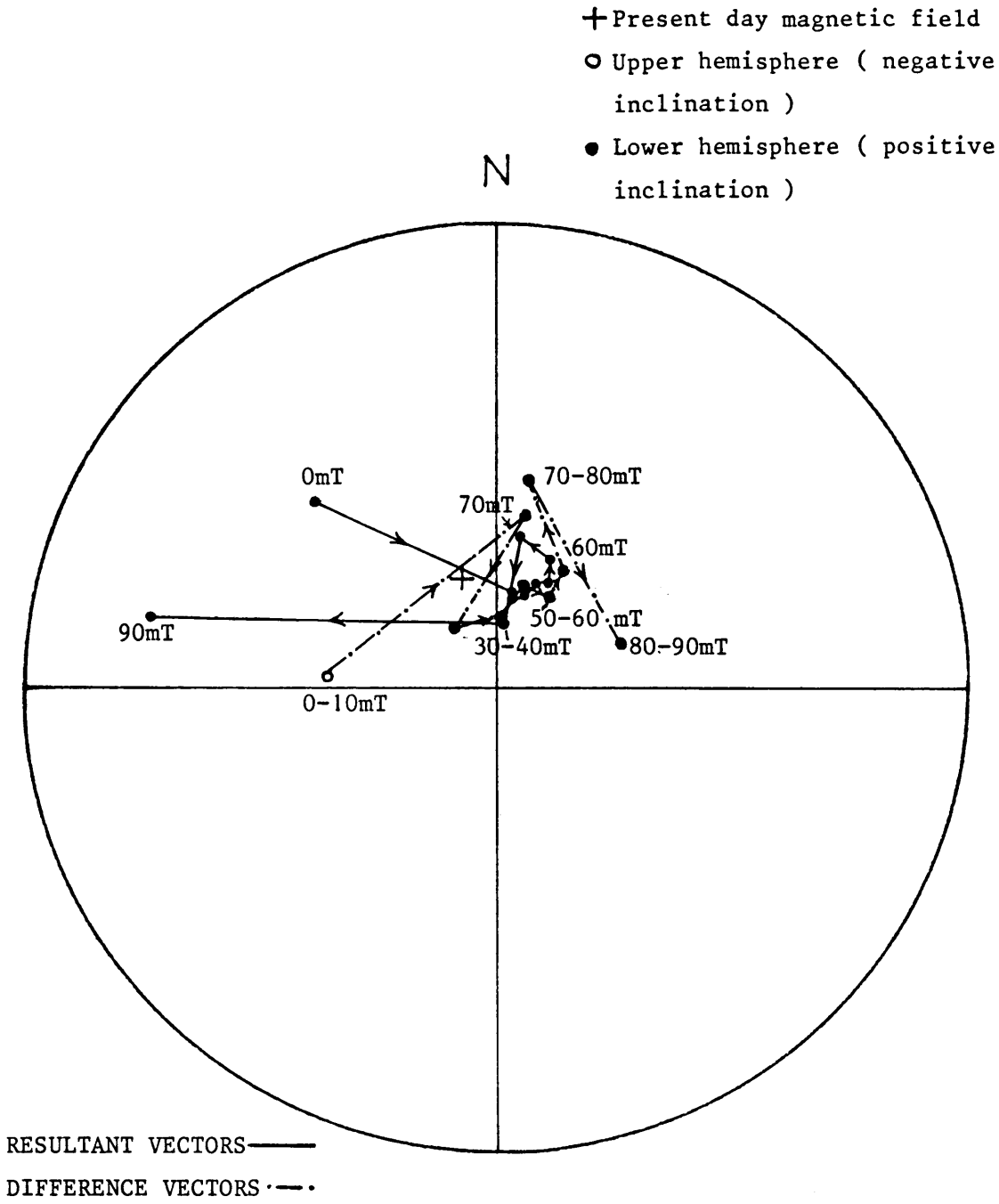

Figure 27: Resultant and difference vectors of specimen B3 during AF demagnetization.

Specimen B2: The specimen was cleaned magnetically at 115 mT, and its intensity and direction of magnetization was measured. The specimen was then left in the laboratory overnight. The following day magnetic measurements were made again. The inclination of the specimen had reversed and the intensity of magnetization had dropped. The specimen was then cleaned again at 115 mT. However, this redemagnetization did not change the magnetization direction, and the direction of the reversed inclination remained remarkably consistent during repeated measurements of magnetization. Although this behaviour could be attributed to the acquisition by the specimen of a VRM, it is unusual in that the inclination became reversed.

Specimen B3: This specimen was cleaned magnetically at 90 mT and magnetic measurements were made. This whole procedure was then repeated, and magnetization measurements indicated that the inclination had reversed in sign. Following this reversal, repeated magnetic measurements indicated no change in the magnetization direction. This behaviour could be attributed to a laboratory-induced magnetization such as RRM (rotational remanent magnetization). However, the consistency of the acquired direction is unusual.

Specimen B4: The specimen was subjected to an alternating field of 105 mT, and measurements of magnetization were made. A repeated magnetic measurement directly after the previous measurement, indicated that a reversed inclination had been acquired by the specimen, although the declination remained unchanged. The specimen was subjected to an alternating field of 105 mT once more, and measurements of magnetization showed that the inclination had reversed back to its original sign. In this case a laboratory-induced magnetization could be inferred to account for the reversed inclinations.

To explain the unusual behaviour of the above specimens, their mineralogy must be taken into account. If it is a laboratory-induced magnetization that these specimens acquired, the reversal in sign of their inclinations reflects an unusual ability which these specimens have.

(c) Thermal demagnetization:

(i) Continuous thermal demagnetization:

Continuous thermal cleaning was done on three specimens of the two-pyroxene gabbro. The normalized intensity response curves to thermal demagnetization for specimens from the gabbro display a distributed blocking temperature range (Figures 28 (b), 29(b) and 30(b)). At low temperatures a magnetization component with a low blocking temperature may be present (Figure 29(b)). The intensity of magnetization of specimens B1 and B5 (Figure 28(b) and 30(b)) increases at intermediate temperatures. This intensity increase suggests the presence of an antipodal magnetization component with an intermediate blocking temperature. The intensity response curves for all three specimens indicate decay of a magnetization component at temperatures of c. 578°C (Figure 30(b)). The increase in intensity at temperatures greater than 580°C (Figure 29(b)) suggests that a magnetization component with a high blocking temperature (greater than 578°C) may be present in these specimens.

Figure 31 shows that a single magnetization component is removed at low to intermediate temperatures in this specimen. The corresponding Zijderveld stability diagram for specimen B5 (Figure 30(c)) displays a linear decay of magnetization up to intermediate temperatures, whereafter an increase in the intensity of magnetization takes place. The latter confirms the presence of an antipodal magnetization component at higher temperatures.

Thermal demagnetization resultant vectors (Figure 29(a) and 30(a)) indicate vector movement towards the consistent magnetization direction (D = 9,34°, I = 58,70°) at temperatures approaching the Curie temperature of magnetite.

Zijderveld stability diagrams for specimens B1 and H2 (Figure 28(c) and 29(c)) indicate a magnetization component with an intermediate blocking temperature, and one with a high blocking temperature. The latter two components have overlapping blocking temperature spectra. Furthermore, stabilization of the vector at high temperatures is

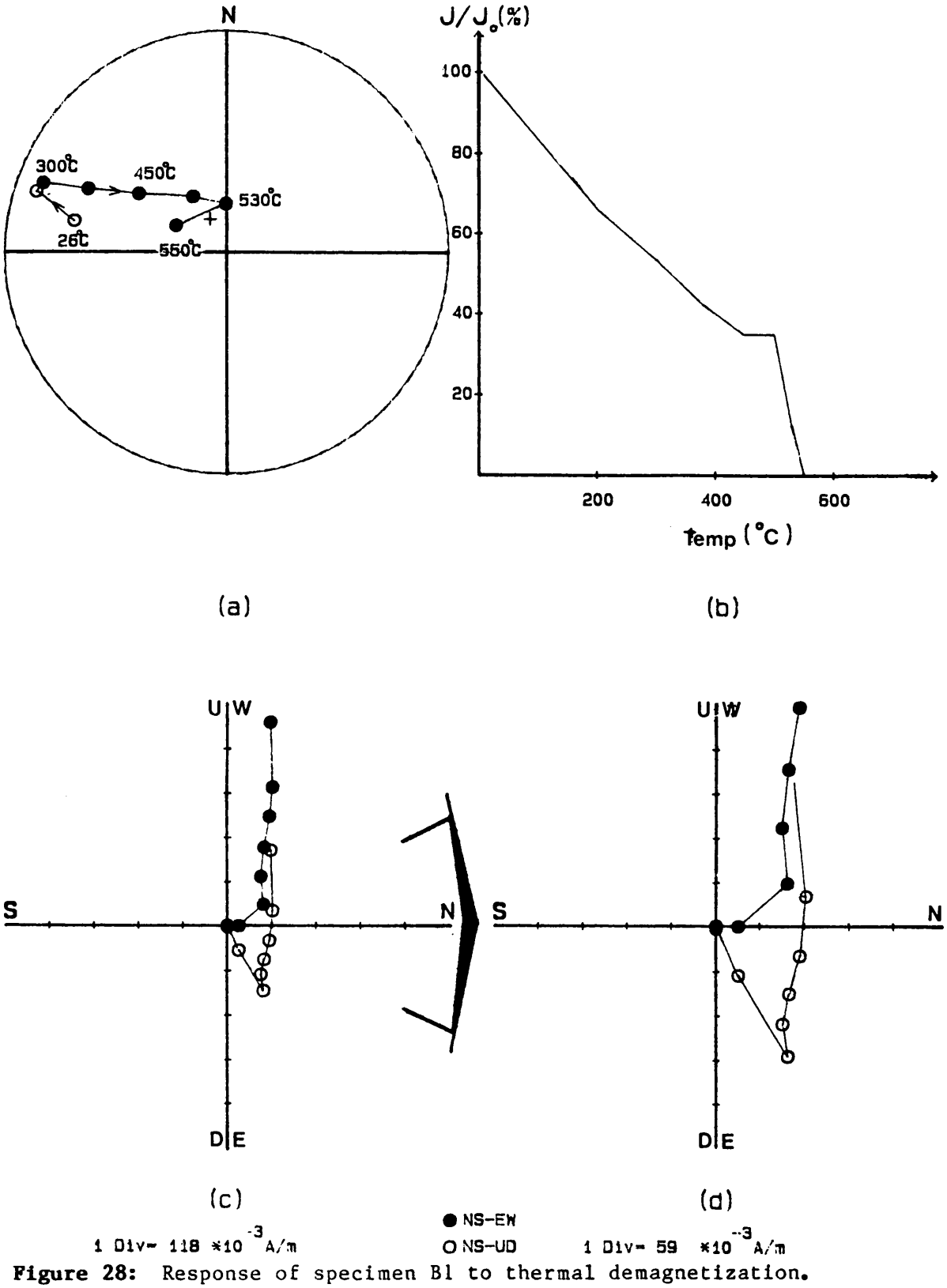

Figure 28: Response of specimen B1 to thermal demagnetization.

(a) Resultant vectors (plotting convention as in Fig.6).

(b) Normalized intensity response curve.

(c) Zijderveld stability diagram.

(d) Magnification of Zijderveld diagram (c).

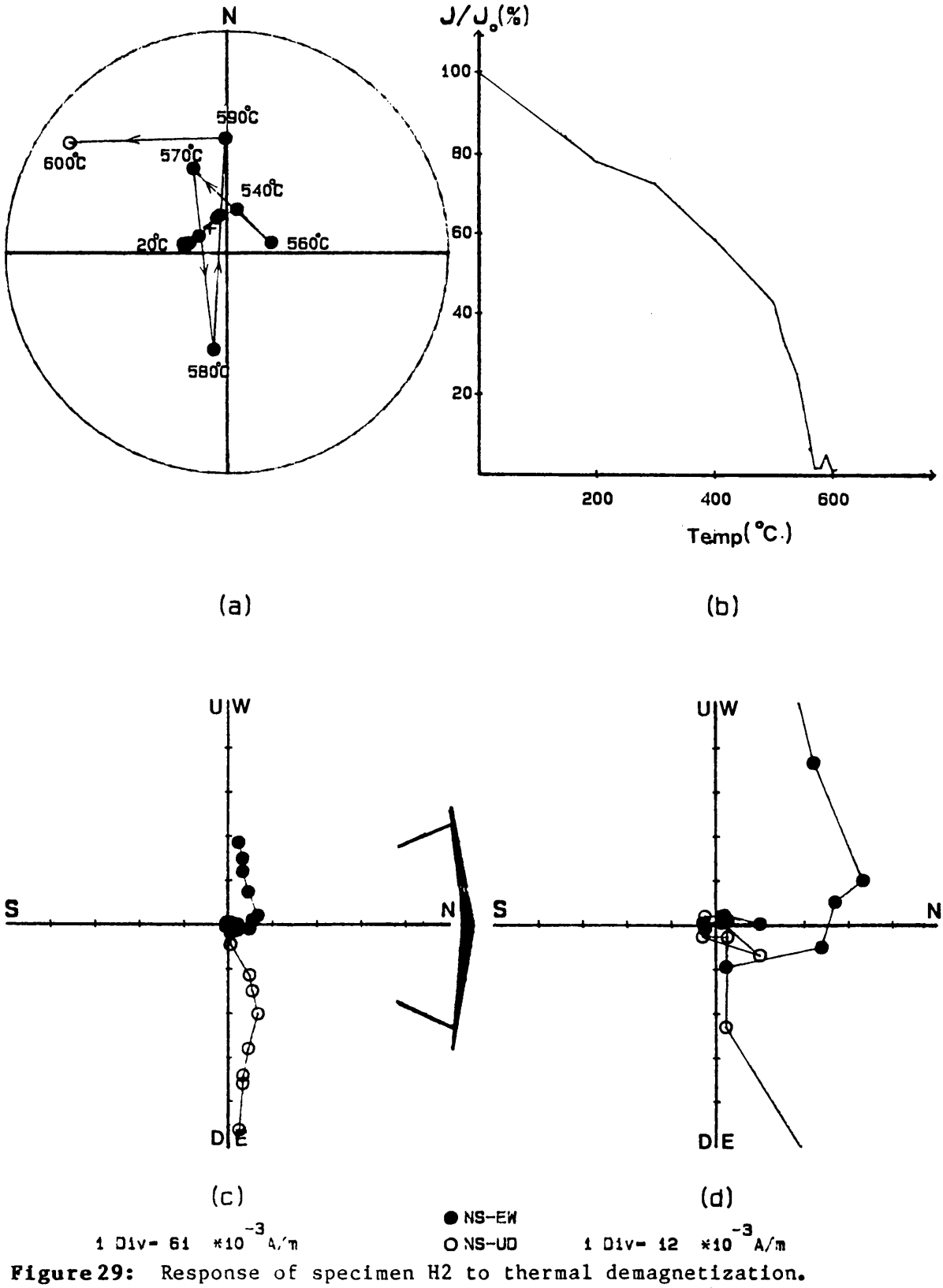

Figure 29: Response of specimen H2 to thermal demagnetization.

(a) Resultant vectors (plotting convention as in Fig.6).

(b) Normalized intensity response curve.

(c) Zijderveld stability diagram.

(d) Magnification of Zijderveld diagram (c).

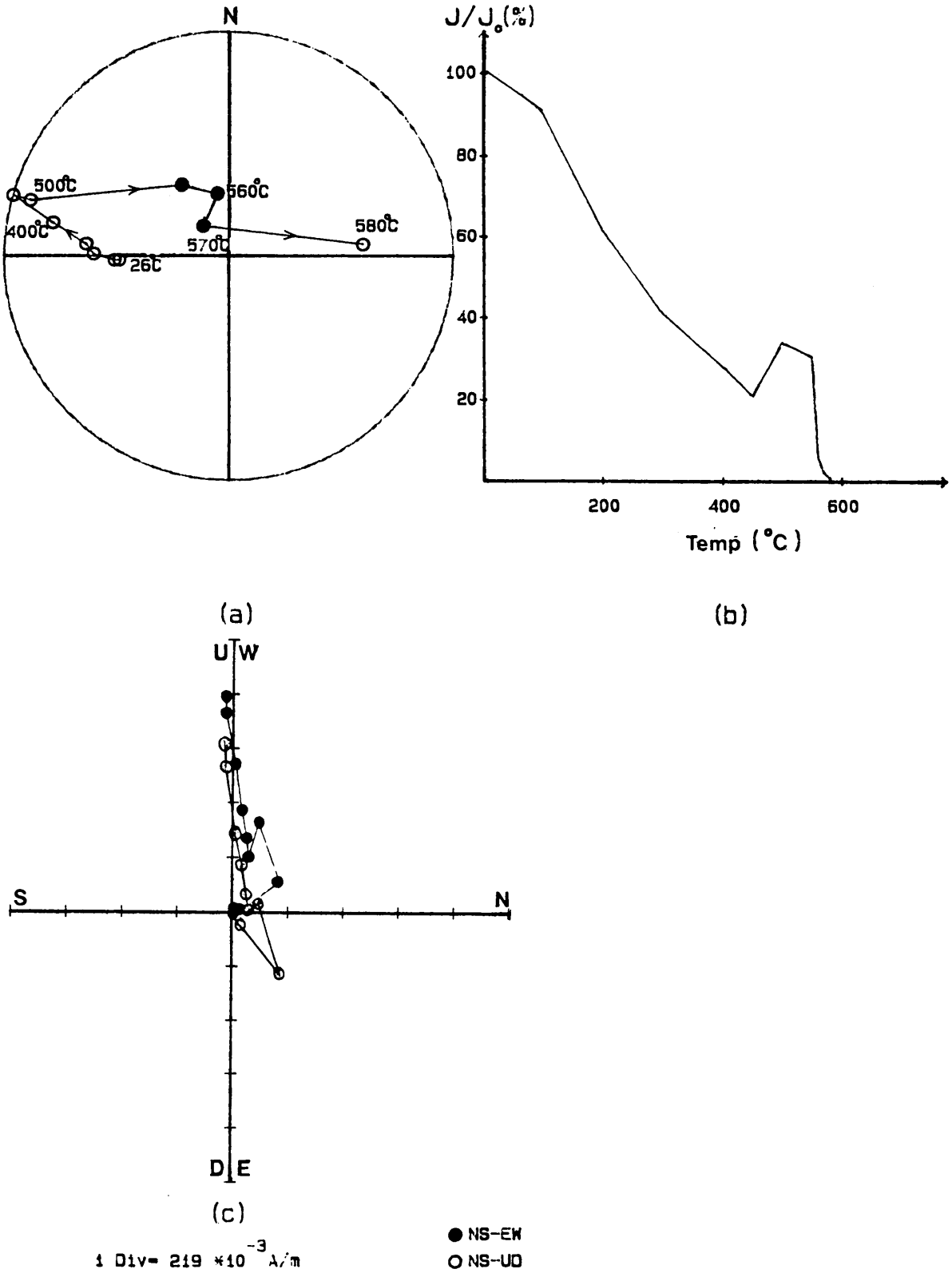

Figure 30: Response of specimen B5 to thermal demagnetization.
(a) Resultant vectors (plotting convention as in Fig.6).
(b) Normalized intensity response curve.
(c) Zijderveld stability diagram.

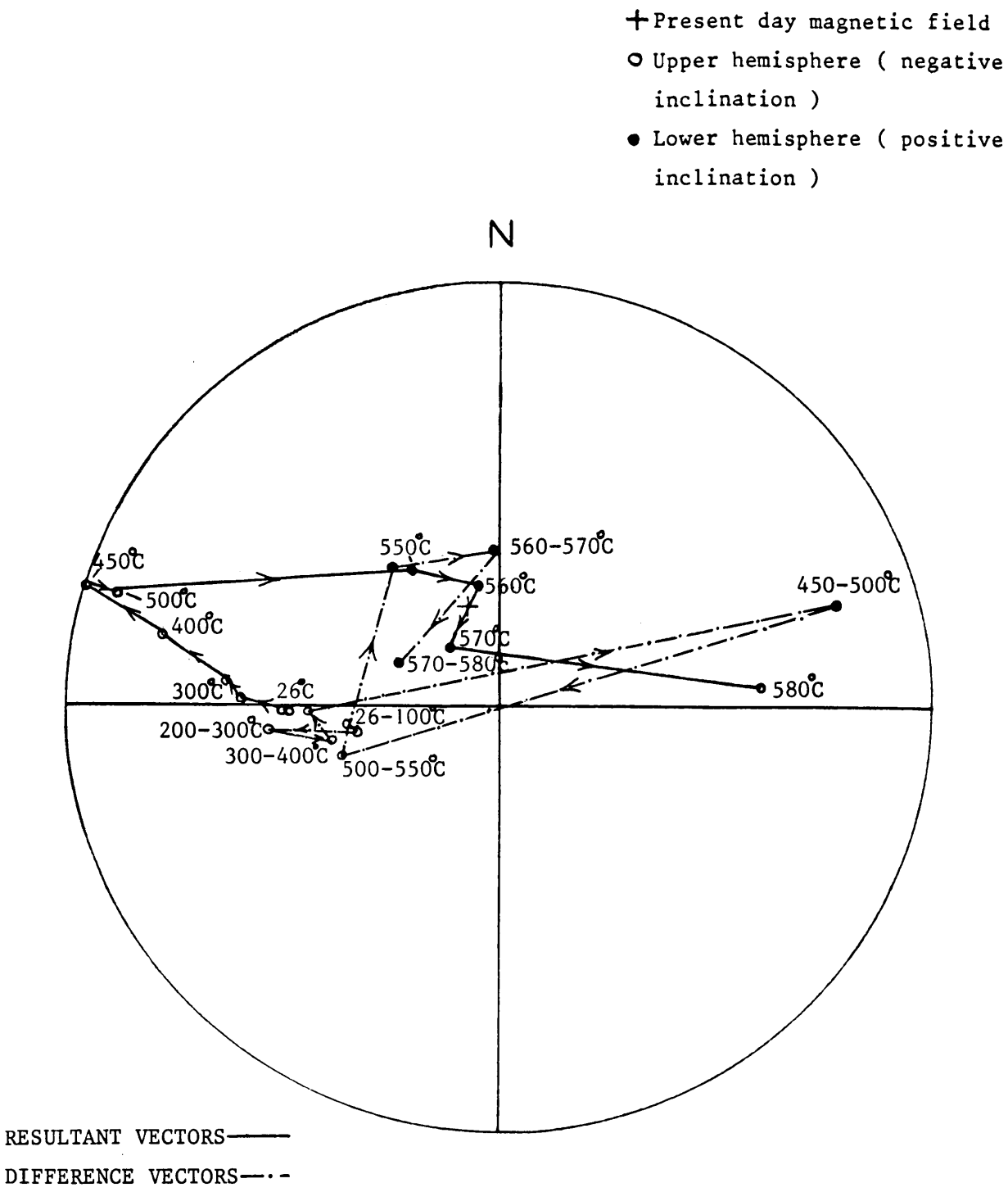

Figure 31: Resultant and difference vectors of specimen B5 during thermal demagnetization.

evidently not achieved during thermal cleaning of specimen H2 (Figure 29(d)).

(ii) Stepwise thermal demagnetization:

After continuous thermal demagnetization was done up to 580°C on specimen B5, stepwise thermal demagnetization was carried out on this specimen. The experiment was undertaken to gain more information about the nature of the carriers of magnetization which are present in the gabbro. This specimen was chosen because of its repeatability of magnetic measurements during continuous thermal demagnetization, even at low intensities of magnetization.

The procedure which was followed is described in Table VIII. It involved heating the specimen to the desired temperature in a high temperature spinner magnetometer and cooling the specimen in a field-free space. The specimen was cooled to room temperature (25°C) or to -6°C. The direction and intensity of magnetization was measured after transferring the specimen to a cryogenic magnetometer, after each successive step. Use of the cryogenic magnetometer was made necessary because of the low intensities of magnetization which were involved. Changes in intensity and direction of magnetization are described in Table VIII.

The results of this experiment indicate that the carriers of magnetization in this specimen are somehow responsible for the acquisition of a magnetization by the specimen, in a field-free space. This behaviour is probably connected with the unusual behaviour of specimens during AF cleaning.

4.3 Petrographical and mineralogical results:

(a) Petrography:

The two-pyroxene gabbro consists of orientated cumulus plagioclase laths with rounded intercumulus orthopyroxene grains and larger ophitic clinopyroxene. Up to 2 volume percent interstitial quartz is present.

Table VIII : Stepwise thermal demagnetization of Specimen B5.

Treatment of specimen	Intensity of magnetization (x 10^{-3} A/m)	Direction of magnetization	
		significant observations	unorientated D and I
1. Continuous thermal demagnetization until 580° C was reached			
2. Specimen cooled to room temperature in a field-free space	Decrease in intensity (8)	no significant change	D = 333 I = +9
3. Specimen left in a field-free space at room temperature for 14 hours	Increase in intensity (16)	direction changed	D = 297 I = +63
4. Specimen heated to 590° C and cooled to room temperature in a field-free space	No change (16)		D = 12 I = -36
5. Specimen cooled to -6° C for 15 minutes in a field-free space	No change (16)		D = 14 I = -34
6. Specimen heated to 600° C and cooled to room temperature in a field-free space	No change (16)		D = 248 I = -62
7. Specimen left in a field-free space for 14 hours at room temperature NB specimen was not moved after measurements following step 6.	No change (16)	D remained constant, I reversed in sign	D = 240 I = +28
8. Specimen heated to 610° C and cooled to room temperature in a field-free space	No change (16)		D = 66 I = +11
9. Specimen heated to 650° C and cooled to room temperature in a field-free space	No change (16)	I reversed in sign	D = 88 I = -11
10. Specimen left for 48 hours in a field-free space at -6° C	No change (15)		D = 88 I = -3
11. Specimen placed in a controlled low induced field for 5 hours	No change (17)	D remained constant, I reversed in sign	D = 83 I = +31

The plagioclase crystals are twinned and are often bent where they interpenetrate other crystals. The laths are 3 mm to 15 mm in length and tend to be orientated parallel to the upper contact. Normal zoning is developed and the cores of crystals were analysed for the determination of the composition which was found to be An_{67} (Table IX). The plagioclase is fairly unaltered and mirmekitic textures are developed on the contacts of some crystals. There is no difference between the composition the cores of plagioclase crystals included in pyroxene, and the larger euhedral to subhedral plagioclase crystals. The included plagioclase crystals, which are normally euhedral to subhedral, are however not zoned.

The clinopyroxene, which has a composition of $Wo_{44}En_{42}Fs_{14}$ (Table X), exhibits an interesting texture. Orthopyroxene evidently replaced the earlier formed plagioclase and the clinopyroxene in turn reacted with the earlier mineral assemblage. Several included plagioclase grains in the clinopyroxene are severely corroded and display irregular and rounded shapes. Orthopyroxene remnants rim these plagioclase inclusions, and orthopyroxene remnants are also orientated along parting planes of the clinopyroxene (Figure 32). The intercumulus orthopyroxene has a composition of Fs_{32} (Table X), which is considerably lower than that of the orthopyroxene in the anorthosite. The Mg/(Mg + Fe) values for coexisting Ca-poor and Ca-rich pyroxenes of 0,67 and 0,74 respectively, indicate that these pyroxenes are in equilibrium. This is illustrated graphically in Figure 17(a).

(b) Ore mineralogy:

The two-pyroxene gabbro is characterized by the absence of euhedral or subhedral magnetite grains. Ilmenite is the most abundant interstitial opaque phase in this rock and is invariably accompanied by various sulphides.

The ilmenite occurs as partially resorbed subhedral to anhedral crystals, up to 600 micron in length (Figure 33). Ilmenite is commonly associated with interstitial clinopyroxene. Table XI gives the composition of ilmenite, and indicates an unusually high Mn-content. The composition of the ilmenite is plotted on Figure 18(a), which

Table IX: Electron microprobe analyses, structural formulae and molecular percentages of plagioclase in the two-pyroxene gabbro.

Sample #	2PL1	2PL2	2PL3	2PL4	2PL5
SiO_2	52,14	52,17	51,89	52,45	51,97
Al_2O_3	30,64	30,14	30,90	30,23	30,47
FeO	0,36	0,40	0,29	0,32	0,34
MgO	0,01	0,01	0,02	----	----
CaO	13,05	13,29	13,55	13,22	13,57
Na_2O	3,34	3,60	3,27	3,41	3,60
K_2O	0,23	0,21	0,25	0,23	0,22
Total	99,77	99,82	100,17	99,86	100,17

Number of cations on the basis of 32(O)

Si	9,48	9,49	9,41	9,53	9,44
Al	6,56	6,46	6,60	6,47	6,52
	16,04	15,95	16,01	16,00	15,96
Fe	0,05	0,06	0,04	0,05	0,05
Mg	----	----	0,01	----	----
Ca	2,54	2,59	2,63	2,57	2,64
Na	1,18	1,28	1,16	1,20	1,26
K	0,06	0,04	0,06	0,06	0,06
	3,83	3,97	3,90	3,88	4,01

mol%	An	67,2	66,3	68,3	67,1	66,7
	Ab	31,2	32,7	30,1	31,3	31,8
	Or	1,6	1,0	1,6	1,6	1,5

Table X: Electron microprobe analyses, structural formulae and Mg/(Mg+Fe) values for coexisting ortho- and clinopyroxenes in the two-pyroxene gabbro.

	ORTHOPYROXENE					CLINOPYROXENE				
Sample #	2OPX1	2OPX2	2OPX3	2OPX4	2OPX5	2CPX1	2CPX2	2CPX3	2CPX4	2CPX5
SiO_2	53,79	53,42	53,69	53,58	53,95	51,83	52,33	52,18	52,62	52,86
TiO_2	0,25	0,30	0,20	0,23	0,24	0,45	0,48	0,41	0,36	0,50
Al_2O_3	0,67	0,67	0,66	0,72	0,76	1,58	1,64	1,40	1,41	1,17
FeO_T	20,79	19,98	20,47	20,78	20,64	9,16	8,80	8,75	8,52	8,93
MnO	0,43	0,42	0,39	0,41	0,42	0,24	0,23	0,26	0,24	0,22
MgO	23,81	23,53	23,63	23,75	23,73	14,52	14,28	14,47	14,20	14,54
CaO	1,00	1,06	1,15	1,07	1,16	21,17	21,16	21,69	20,81	21,44
Na_2O	----	----	----	----	----	0,20	0,24	0,48	0,20	0,16
K_2O	----	----	0,01	----	0,01	0,02	0,01	0,06	----	----
Cr_2O_3	0,07	0,09	0,07	0,07	0,08	0,19	0,17	0,20	0,21	0,13
Total	100,81	99,47	100,27	100,61	100,99	99,36	99,34	99,90	98,57	99,95
Number of cations on the basis of 6(O)										
Si	1,97	1,99	1,98	1,97	1,97	1,95	1,96	1,95	1,98	1,97
Al	0,03	0,01	0,02	0,03	0,03	0,05	0,04	0,05	0,02	0,03
	2,00	2,00	2,00	2,00	2,00	2,00	2,00	2,00	2,00	2,00
Al	----	0,02	0,01	----	0,01	0,02	0,03	0,01	0,04	0,02
Ti	0,01	0,01	0,01	0,01	0,01	0,01	0,02	0,01	0,01	0,02
Fe_T	0,64	0,62	0,63	0,64	0,63	0,29	0,28	0,27	0,27	0,28
Mn	0,01	0,01	0,01	0,01	0,01	0,01	0,01	0,01	0,01	0,01
Mg	1,30	1,30	1,30	1,30	1,29	0,81	0,80	0,81	0,80	0,81
Ca	0,04	0,04	0,05	0,04	0,05	0,85	0,85	0,87	0,84	0,86
Na	----	----	----	----	----	0,01	0,02	0,03	0,01	0,02
K	----	----	----	----	----	----	----	----	----	----
Cr	----	----	----	----	----	0,01	----	0,01	0,01	0,01
	2,00	2,00	2,01	2,00	2,00	2,01	2,01	2,02	1,99	2,03
$Mg/(Mg+Fe^{2+})$	0,67	0,68	0,67	0,67	0,67	0,74	0,74	0,75	0,75	0,74
Mol % Wo	2,0	2,0	2,5	2,0	2,5	43,6	44,0	44,6	42,0	44,1
Mol % En	65,7	66,3	65,7	65,7	65,5	41,5	41,5	41,6	44,0	41,5
Mol % Fs	32,3	31,7	31,8	32,3	32,0	14,9	14,5	13,8	14,0	14,4

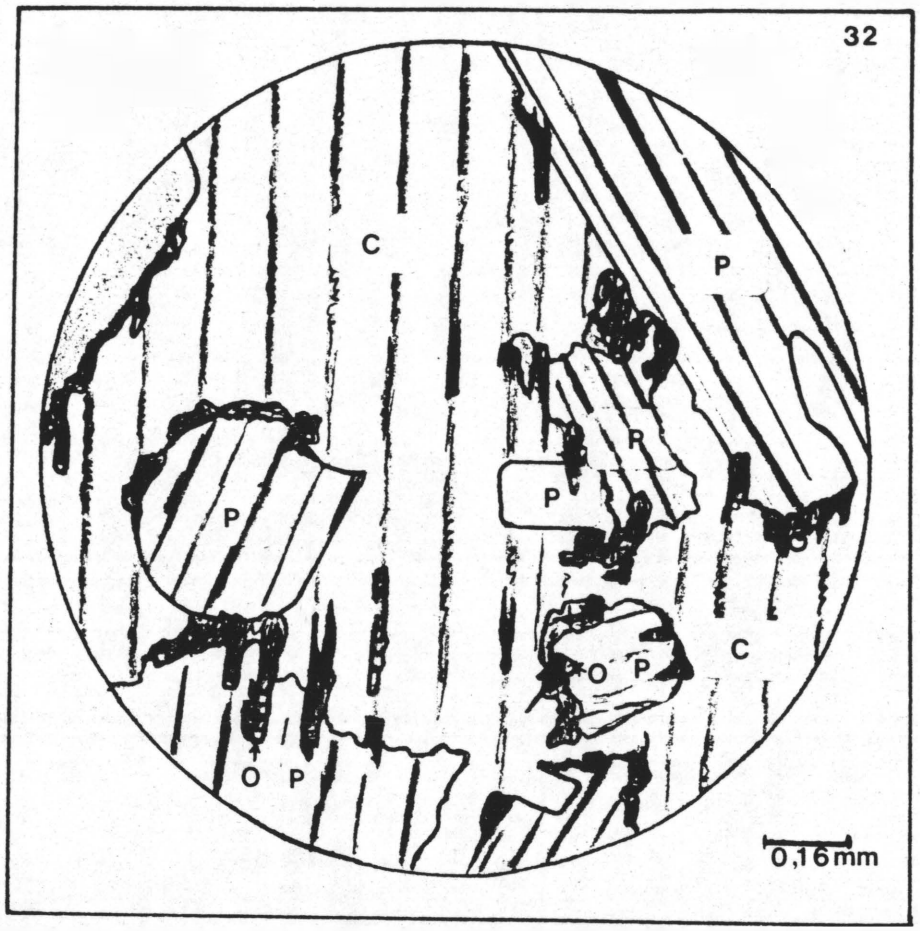

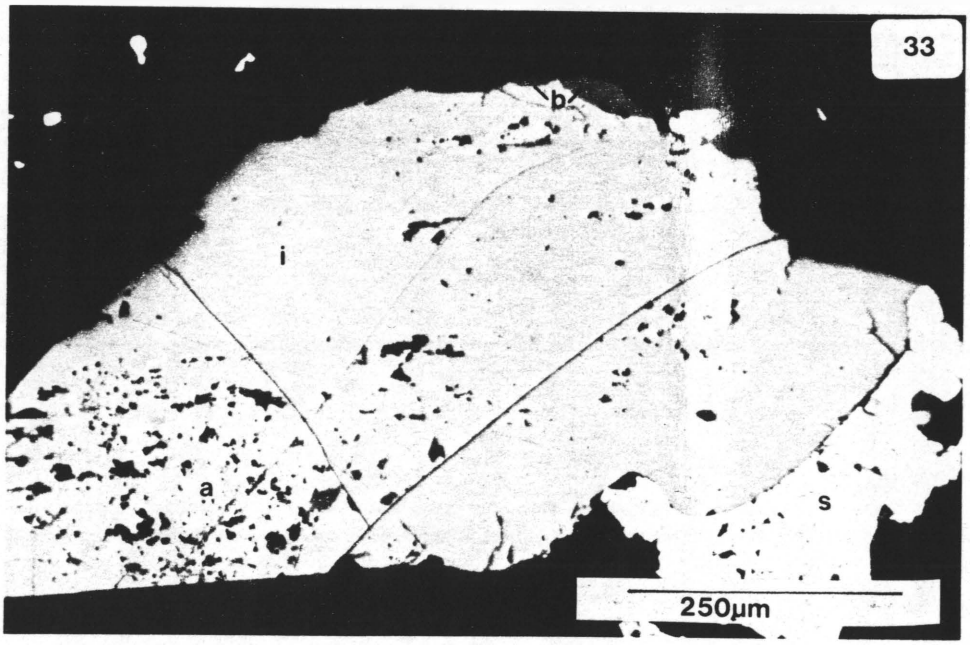

Table XI: Electron microprobe analyses of ilmenite in the two-pyroxene gabbro.

Sample #	MC1A	MC1B	MC1C	MC1D
SiO_2	0,01	0,03	0,01	0,02
TiO_2	47,26	46,44	47,38	47,87
Al_2O_3	0,01	----	0,01	----
Fe_2O_3	10,02	10,22	10,01	9,35
FeO	38,85	38,26	38,89	39,36
MnO	3,42	3,28	3,46	3,41
MgO	0,11	0,12	0,13	0,14
Cr_2O_3	0,30	0,31	0,30	0,29
V_2O_3	0,36	0,34	0,33	0,36
Total	100,34	99,00	100,52	100,80
Number of ions on the basis of 3(O)				
Si	----	----	----	----
Ti	0,90	0,89	0,90	0,90
Al	----	----	----	----
Fe^{3+}	0,19	0,20	0,19	0,18
Cr	0,01	0,01	0,01	0,01
V	0,01	0,01	0,01	0,01
	1,11	1,11	1,11	1,10
Fe^{2+}	0,82	0,82	0,82	0,83
Mn	0,07	0,07	0,07	0,07
Mg	----	----	----	0,01
	0,89	0,89	0,89	0,91

Table XII: Comparison of the chemical composition of ilmenite associated with baddeleyite from the Basistoppen sill in Greenland with the ilmenite from the gabbro in the present investigation.

Sample	#208-5	#208-13	MC1A	MC1D
SiO_2	----	----	0,01	0,02
TiO_2	47,65	48,84	47,26	47,87
Al_2O_3	0,18	0,12	0,01	----
Fe_2O_3	8,11	7,54	10,02	9,35
FeO	40,11	40,93	38,85	39,36
MnO	1,57	1,46	3,42	3,41
MgO	0,67	0,87	0,11	0,14
Cr_2O_3	0,68	0,74	0,30	0,29
V_2O_3	0,19	----	0,36	0,36
Total	99,15	100,50	100,34	100,80

\# ilmenite from the Basistoppen sill (from Naslund, 1987)

indicates that the ilmenite does not contain the Fe_2TiO_4 component as it falls in the triangle $FeTiO_3$-Fe_3O_4-TiO_2.

Mottled alteration areas are always present in the ilmenite and these are related to submicroscopic hematite exsolutions parallel to the {0001} plane of the host (Figure 34). The alteration is patchy and unevenly distributed, but closely resembles the oxidation stage of the ilmenite in the mottled anorthosite. The alteration patches (Figure 34 (b)) consist predominantly of sphene, with lesser rutile and hematite exsolution. As in the case of the mottled anorthosite, the possible presence of minute magnetite grains associated with the exsolved hematite, cannot be excluded. An anomolously high Cr-content was identified qualitatively in the alteration patches. These zones of alteration are anisotropic and display numerous, predominantly white, internal reflections. Replacement of ilmenite by sphene is associated with oxidation-exsolution and is characteristically coarsely crystalline, as observed by Haggerty (1976a). The abundance of ilmenite as the opaque mineral in this rock would explain the higher sphene concentration, as sphene occurs preferentially as a replacement of ilmenite rather than magnetite (Haggerty, 1976a).

Sulphides are always present in close proximity to the ilmenite. Chalcopyrite and pyrite are the most abundant, with lesser violarite [(Ni,Fe,Co)(Co,Ni)$_2S_4$] and millerite (NiS). Violarite and pyrite are regarded as alteration products of pentlandite and pyrrhotite respectively (von Gruenewaldt, 1976), whilst millerite is a product of incipient weathering of Ni-rich sulphides (Ramdohr, 1980, p.630).

An unusual occurence of baddeleyite (ZrO_2) was found during a qualitative microprobe investigation. The baddeleyite occurs in two adjacent patches which form a cuspate contact with the adjoining ilmenite grain (Figure 33). Chemically the baddeleyite is nearly pure ZrO_2. The length of the two grains is 90 micron in total. Baddeleyite is a rare constituent of subalkaline terrestrial gabbros and basalts, but has been reported as a primary late stage magmatic mineral in two gabbros from the Canadian Arctic Archipelago (Keil and Fricker, 1974) and in ultramafic cumulates from the Rhum Complex (Williams, 1978).

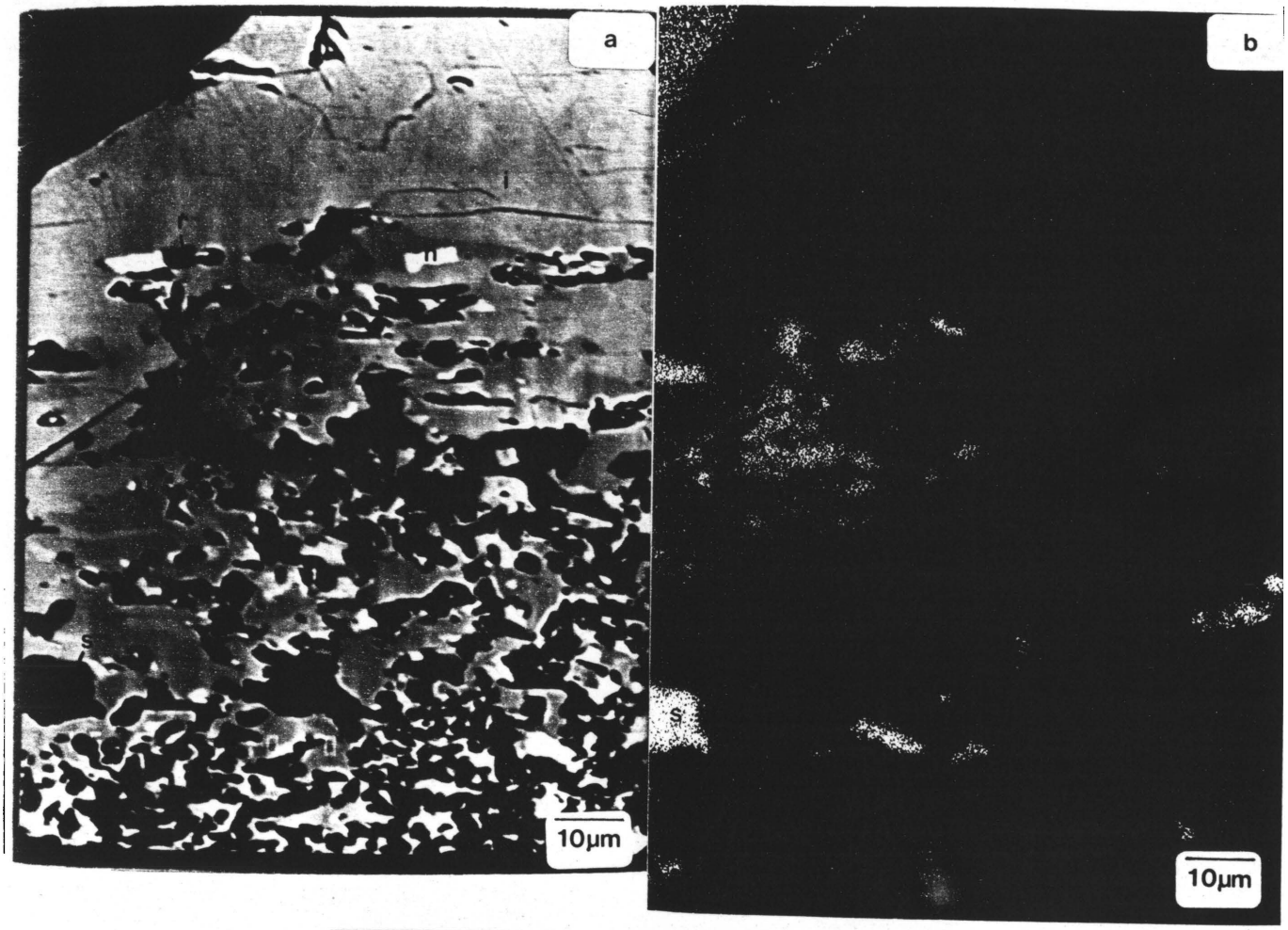

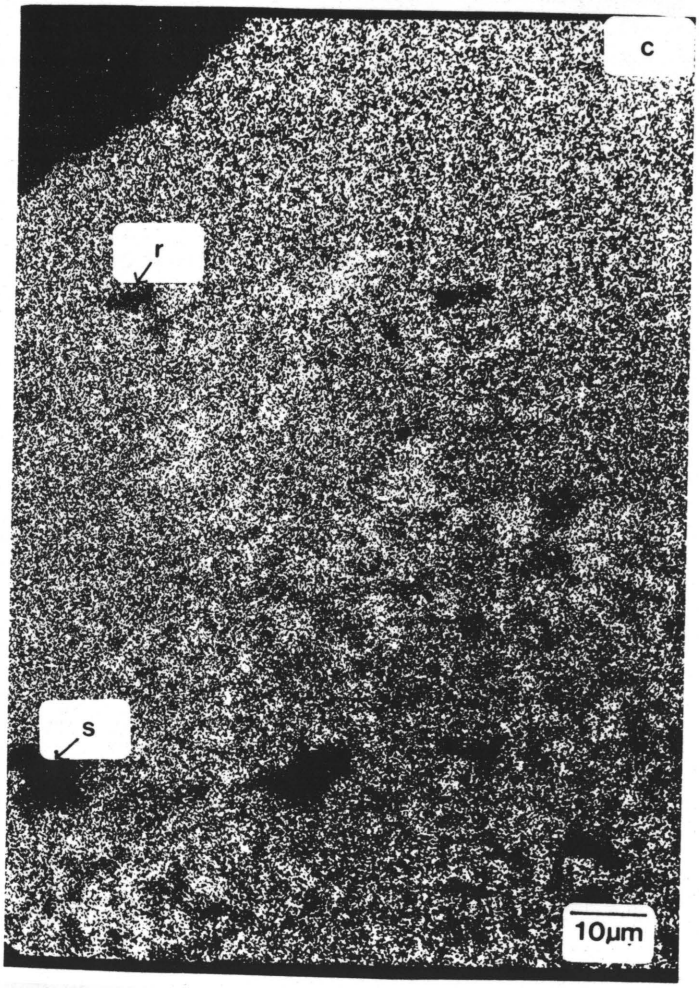

Exsolution of baddeleyite and Fe-Cr-spinel in ilmenite has been reported in East Greenland (Naslund, 1987). Here it occurs in a gabbro picrite zone and it is related to reduction during subsolidus re-equilibration. The baddeleyite grains found in this investigation are very much larger than those previously reported, which ranged from 0,01 to 20 micron in length. According to Naslund (1987), the Fe-Cr-spinel exsolved due to exceeding the solubility limit of Cr in ilmenite, and the baddeleyite exsolution possibly compensated for the reduction of the ilmenite. It is not clear, however, how this mechanism is proposed to operate. As the alteration zones in the ilmenite from the two-pyroxene gabbro are rich in Cr, a similar mechanism could have allowed the crystallization or exsolution of the baddeleyite. A second possibility is that direct oxidation of the ilmenite resulted in the exsolution of the baddeleyite. Table XII illustrates a comparison between the composition of the ilmenite from the gabbro picrite in East Greenland, and the ilmenite from the two-pyroxene gabbro in the present investigation.

The second type of ore mineral in the two-pyroxene gabbro is stubby ilmenite laths (Figure 35(a)) which are associated with clinopyroxene and are normally orientated parallel to the cleavage traces. These laths are on average 20 X 15 micron and are presumably exsolution products due to oxidation of the clinopyroxene as they are invariably present on the borders of the clinopyroxene grains. Laths, 10-15 micron in length and c. 5 micron wide, are found along cleavage traces of ortho- and clinopyroxene grains, and these are associated with biotite (Figure 35(b)). These laths are predominantly ilmenite, but magnetite laths are present in small quantities. Much shorter laths with a length : width ratio of 3:1 also occur along cleavage traces of orthopyroxene. The latter needles are associated with rounded or irregularly shaped blebs (10 - 20 micron in diameter) and indicate that oxidation-exsolution of the pyroxene took place (Haggerty, 1976a).

Laths of magnetite in the plagioclase do occur, but are rare in this rock. Furthermore, areas of magnetite-hematite dust are found associated with the larger laths and grains of ore minerals.

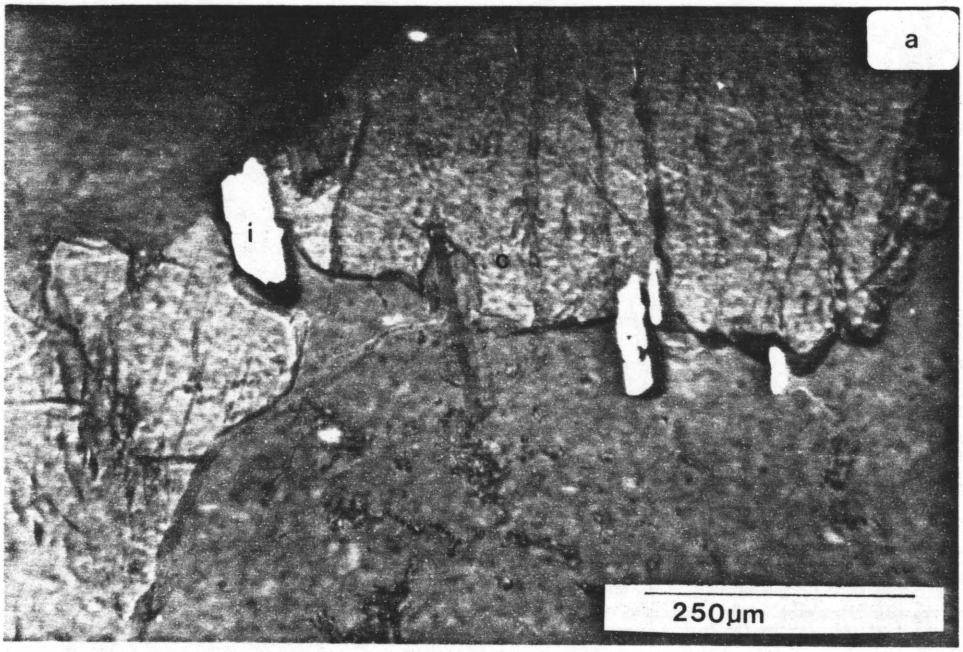

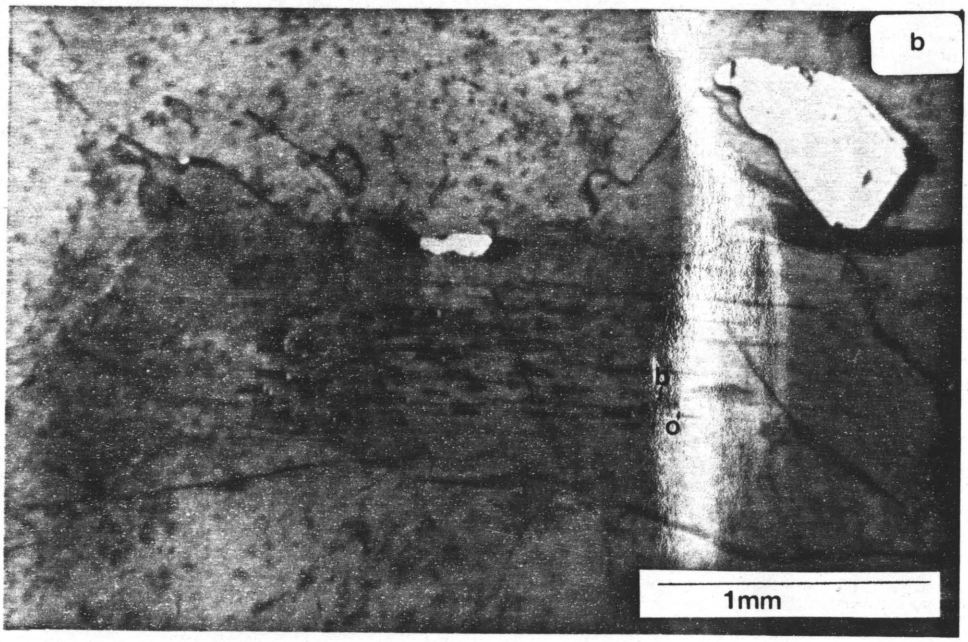

4.4 Discussion of results:

Alternating field demagnetization results indicate that a low coercivity component of magnetization is present in the gabbro. This component corresponds with NRM directions, and probably represents a VRM which was acquired by the rock after its formation. The carrier of this soft component is presumably multidomain magnetite, which is present as larger magnetite blebs in pyroxene.

Thermal and AF demagnetization tests also indicated the presence of two further magnetization components; an intermediate component and a high coercivity component with a high blocking temperature. These two components have overlapping coercivity and blocking temperature ranges. The similarity in magnetic minerals and magnetization directions between the gabbro and anorthosite suggests similar magnetic carriers for the various magnetization components. Thus, although secondary magnetite in pyroxene may be the carrier of this intermediate magnetization component in the gabbro, the antipodal nature of this component with respect to the primary magnetization direction suggests that it could also be carried by hematite.

As in the case of the anorthosite, magnetite laths in plagioclase must be the primary carriers of a TRM which is destroyed at temperatures of about 578^{o}C. These laths are thus responsible for the high coercivity magnetization component in the gabbro. The low mean magnetic susceptibility of the gabbro can be attributed directly to the small quantity of laths which are present in the plagioclase of this rock.

A characteristic feature of the two-pyroxene gabbro during thermal cleaning is that stabilization of the vector does not always occur. This behaviour could be attributed to the presence of a carrier of magnetization with a high blocking temperature. In comparison with the mottled anorthosite, the gabbro contains less magnetite and more ilmenite (with exsolved hematite). It thus seems that the effect of hematite at high temperatures, when the magnetization of the magnetite has been partially or completely destroyed, is more pronounced in the gabbro. Spurious behaviour of three specimens which had been cleaned magnetically at high alternating fields, may also be attributable to

the effect of high coercivity ilmeno-hematite. The latter effect could thus be pronounced in these circumstances because the decay of the magnetization carried by magnetite had already taken place.

The reversal in inclination of specimen B5 which was subjected to stepwise thermal demagnetization, indicates a unique behaviour which must be directly associated with the specific mineralogy of the rock. Since the specimen was cooled down or stored in a field-free space, a laboratory-induced VRM could not have been acquired by it to explain the reversal in inclination between steps 6 and 7 (Table VIII). At temperatures above 580°C it can be assumed that the magnetic component carried by magnetite has been destroyed. Furthermore, the ilmeno-hematite presumably carries a hard magnetic component and has a high blocking temperature. Thus the magnetization of the specimen after thermal cleaning at high temperatures is probably attributable to the hematite. It seems that the contribution of hematite to the remanence of the specimen only becomes obvious at high temperatures, once the dominating magnetizations carried by magnetite, have been destroyed. The reversal in magnetization may be time-dependent, suggesting some form of VRM acquisition. A TRM carried by hematite may however also be involved. The mechanism which would enable a magnetic carrier to acquire a reversed VRM in a field-free space, could involve an antiparallel, possibly magnetostatic, interaction between two magnetic carriers. Since no euhedral magnetite grains are present in the gabbro, this antiparallel coupling could involve either magnetite laths, or minute (undetected) magnetite grains associated with ilmeno-hematite, and hematite exsolutions. Minute magnetite exsolutions in ilmeno-hematite would be a favourable explanation for a magnetostatic interaction involving two closely intergrown magnetic minerals with different Curie points. Magnetite grains could thus acquire an antiparallel magnetization direction in the presence of a weak magnetic field of hematite, at a stage when the magnetization of the magnetite has been destroyed. Balsley and Buddington (1958) and Merrill and Grommè (1969) reported cases of self-reversal which were apparently linked to hematite.

The main palaeomagnetic characteristics of the two-pyroxene gabbro can be summarized as follows:

(i) The rock has an intermediate intensity of magnetization (611 x 10^{-3} $A.m^{-1}$).

(ii) The mean magnetic susceptibility is 1,6 x 10^{-3}SI, and the magnitude of anisotropy is negligible (0,15).

(iii) A consistent primary magnetization direction, with D = 9,34° and I = 58,70°, was isolated for the gabbro. This magnetization is associated with a Curie point of 578°, implying that it is carried by primary magnetite. The hardness of this component suggests that the magnetic carrier is magnetite laths in plagioclase.

(iv) A soft, low coercivity component is present in the specimens, and this component of magnetization is probably carried by multidomain magnetite blebs in pyroxene.

(v) An intermediate component of magnetization , which is possibly a VRM, was identified in the gabbro. This component and the primary magnetization component have overlapping blocking temperature spectra, and indications are that they have antipodal magnetization directions. The magnetic carrier of this intermediate component is probably ilmeno-hematite, although magnetite blebs and laths which exsolved from pyroxene could also contribute to this magnetization component.

(vi) Three specimens underwent reversals in inclination after being cleaned at high alternating fields. Furthermore, one specimen displayed the ability to undergo a reversal in inclination whilst in storage in a field-free space. This behaviour is linked to ilmeno-hematite. A magnetostatic exchange reaction, or another unknown mechanism, is somehow responsible for antiparallel coupling between magnetic phases in this rock.

5. THE FINE-GRAINED NORITE:

5.1 Introduction:

The fine-grained norite underlies the mottled anorthosite- two-pyroxene gabbro unit and is intruded by the pegmatoidal two-pyroxene gabbro. In the field it has the appearance of a chilled rock with rather unusual blebs, up to 10 cm in diameter, of pyroxene and amphibole, as well as pyroxenite stringers (Figure 5(d)). The blebs and stringers are only present within a 5 m radius from the pegmatoidal two-pyroxene gabbro. It was found during field investigations that numerous feldspathic veins are present in this rock. The pyroxenite stringers and blebs appear to be related to the feldspathic veining, as the blebs and stringers are always rimmed by anorthositic material (Figure 36). The norite cannot be followed in outcrop on strike as it wedges out against coarsely recrystallized quartzite. At first it was thought that the quartzite is xenolithic, but on further inspection it became apparent that it represents floor rock of the layered suite.

Twenty eight specimens were obtained from the norite for palaeomagnetic investigations. Palaeomagnetically the rock is characterized by an extremely low intensity of magnetization of 16 x $10^{-3}A.m^{-1}$ (standard deviation = 12 x 10^{-3}, minimum intensity = 2 x 10^{-3}, maximum intensity = 38 x 10^{-3}), and this hampered palaeomagnetic tests. As a result of this low intensity, extensive AF demagnetization in particular was carried out on specimens of the norite to assist in identifying a stable vector direction of magnetization.

5.2 Palaeomagnetic results:

(a) Natural remanent magnetization:

The NRM directions of the specimens which are shown in Figure 37 indicate three negatively inclined NRM groups, named A, B and C. Magnetization directions of the specimens are given in Table XIII. Group B corresponds roughly with that identified by Hattingh (1983) as Bcz3AF, which he determined from multiple sites.

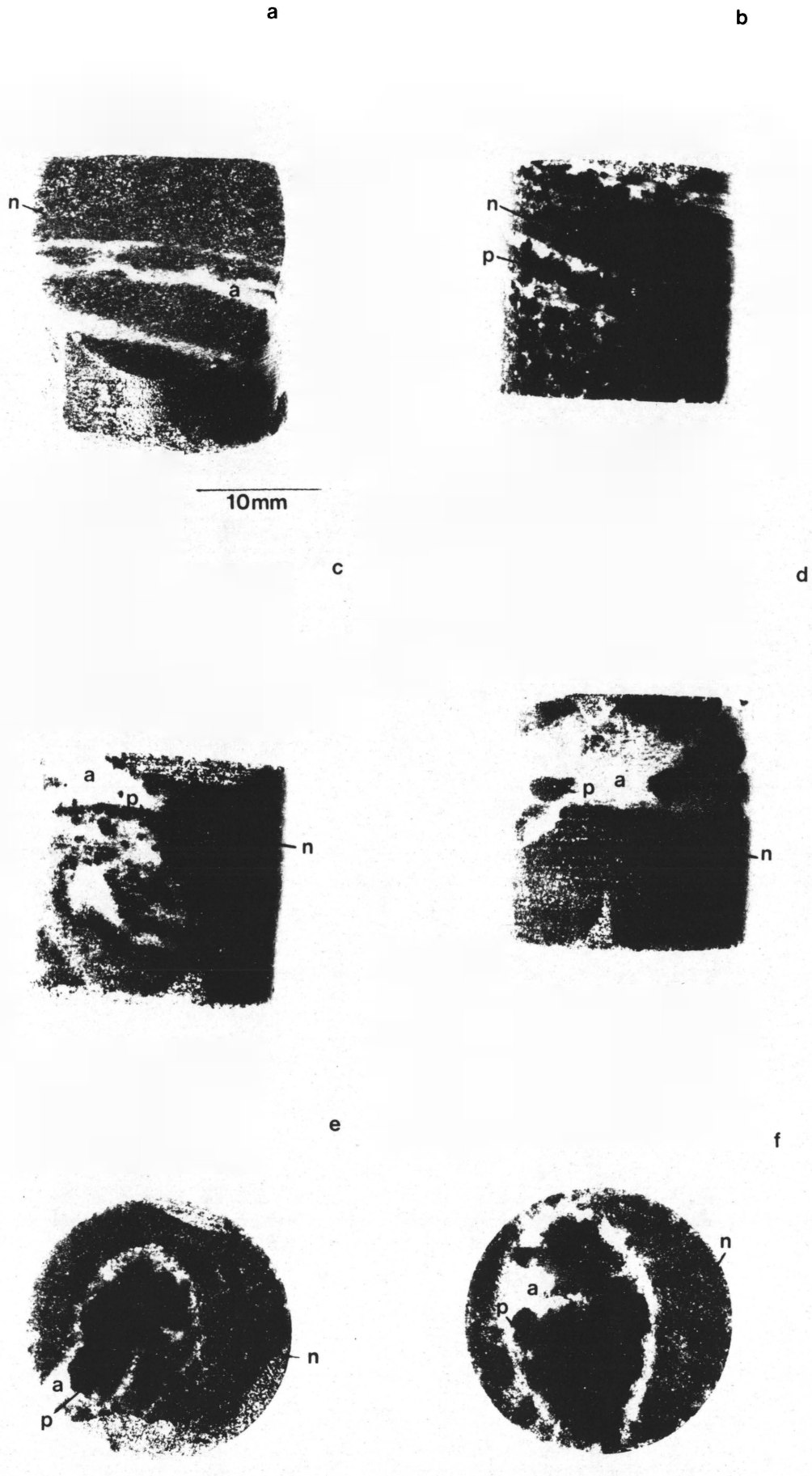

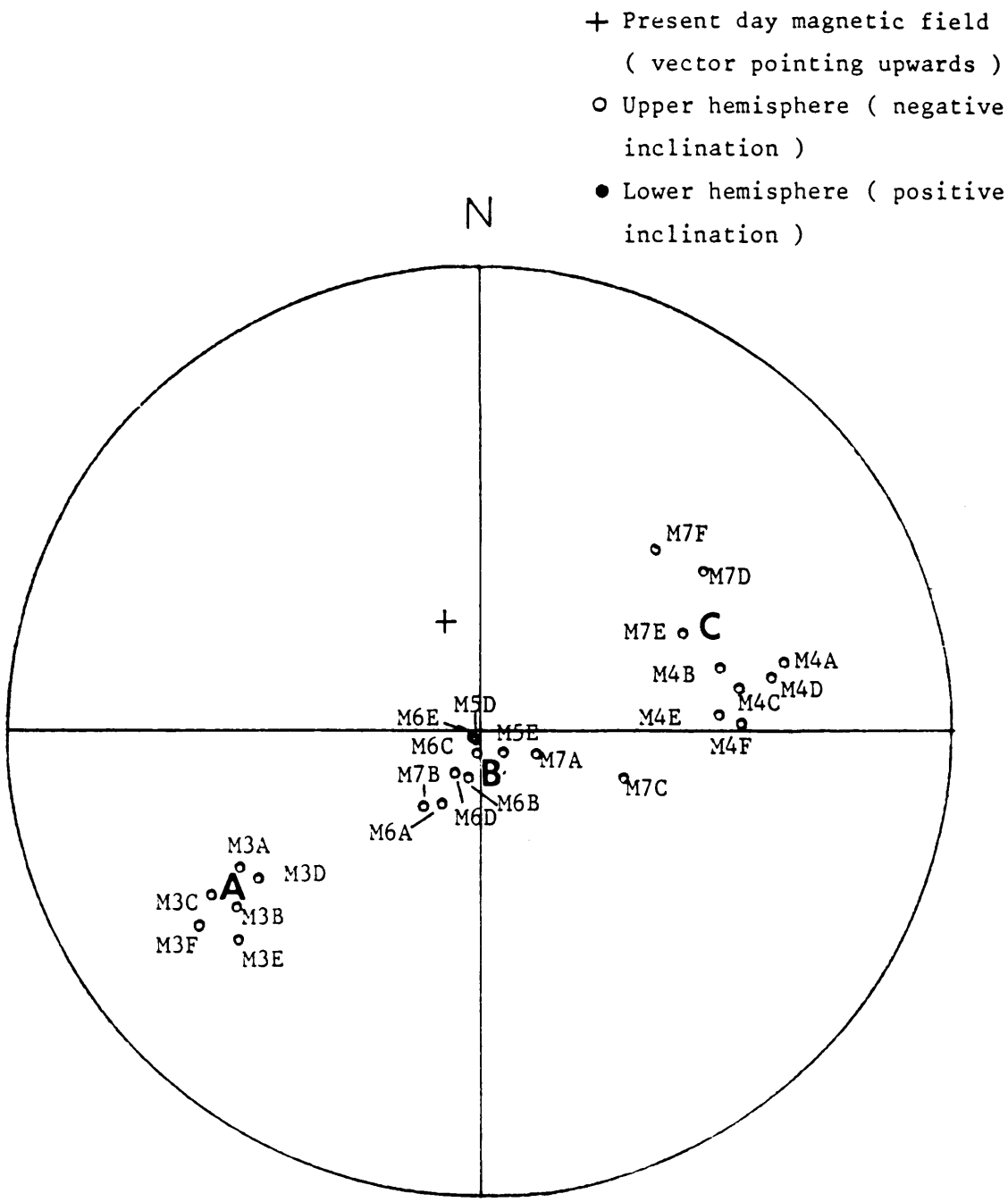

Figure 37: Stereographic projection of NRM directions of specimens from the fine-grained norite. NRM groups A, B and C are indicated.

During NRM measurements, two specimens exhibited an unusual behaviour. Between repeated measurements of NRM directions, both specimens underwent a reversal in their inclinations, whilst their intensities of magnetization remained the same. It appears that these specimens acquired a laboratory-induced remanence, but the reversal in sign of this induced remanence is unusual.

Table XIII: NRM results from the norite.

GROUP A		
Specimen	D^o	I^o
M3A	240,01	-29,06
M3B	234,85	-18,02
M3C	236,00	-30,91
M3D	238,21	-22,38
M3E	228,72	-21,54
M3F	233,73	-24,80
mean	235,19	mean -24,49

$\alpha_{95} = 4,99^o$, k = 181, $R_o = 3,85$

GROUP B

Specimen	D^o	I^o
M6A	216,39	-66,86
M6B	194,62	-77,79
M6C	189,07	-84,07
M6D	210,55	-77,56
M6E	229,24	-87,30
M7A	113,94	-75,27
M7B	207,51	-69,71
M7C	109,09	-54,49
M5D	208,00	-87,19
M5E	135,89	-82,18
mean	171,20	mean -80,52

$\alpha_{95} = 8,84^o$, k = 31, R_o = 5,03

GROUP C

Specimen	D^o	I^o
M4A	77,43	-23,12
M4B	75,41	-34,64
M4C	80,95	-31,85
M4D	79,77	-25,83
M4E	86,47	-36,34
M4F	88,66	-32,08
M7D	54,32	-29,44
M7E	64,45	-39,13
M7F	44,34	-34,45
mean	72,66	mean -32,66

$\alpha_{95} = 8,72^o$, k = 36, R_o = 4,76

GROUPS A, B AND C:

D = 131,18°, I = -77,35° where

N = 25, α_{95} = 19,99, k = 3,08 and R_o = 8,02.

Together with a very low intensity of magnetization, the norite has a low mean susceptibilty of 0,3 x 10^{-3}SI (standard deviation = 0,07),

and as in the case of the two-pyroxene gabbro, the magnitude of anisotropy is negligible at 0,14 (standard deviation = 0,02).

(b) Alternating field demagnetization:

Eighteen norite specimens were subjected to AF demagnetization. High AF values were not always reached during AF demagnetization, because of the very low intensities of magnetization of specimens, which did not allow repeatability of results.

The AF demagnetization results of specimens from the norite revealed complex coercivity spectra for the magnetization components. The normalized intensity response curves to AF demagnetization for specimen M7F (Figure 38(b)) displays irregular increases and decreases in magnetization intensity. Although the intensity of magnetization at this stage was low, it reflects the magnetic carriers' ability to readily acquire either a VRM or an RRM during subjection of this specimen to alternating fields. Furthermore, this effect made it extremely difficult to isolate magnetization components.

A sharp initial decrease in intensity of magnetization (Figure 39 (b)) indicates that a soft magnetization component is removed at low peak fields. In the case of this specimen, an NRM direction corresponding with group B, is removed at these low fields. However, AF cleaning of specimen M3A (Figure 40), indicates that the removal of a magnetization component, which corresponds with NRM group A, is responsible for this intensity drop.

The resultant vectors for the specimens during AF demagnetization indicate that vectors associated with both groups B and C can be identified during magnetic cleaning. The AF resultant vectors for specimen M6C (Figure 39(a)) illustrate the progressive removal of component C at intermediate fields. Component B is apparently gradually removed at AF strengths greater than 60 mT, as the direction of the vector changes along an arc of a great circle towards direction B. Both the resultant and the difference vectors indicate that the vector returns, without stabilizing, to direction B (Figure 41). The vector does not stabilize at either of these two main

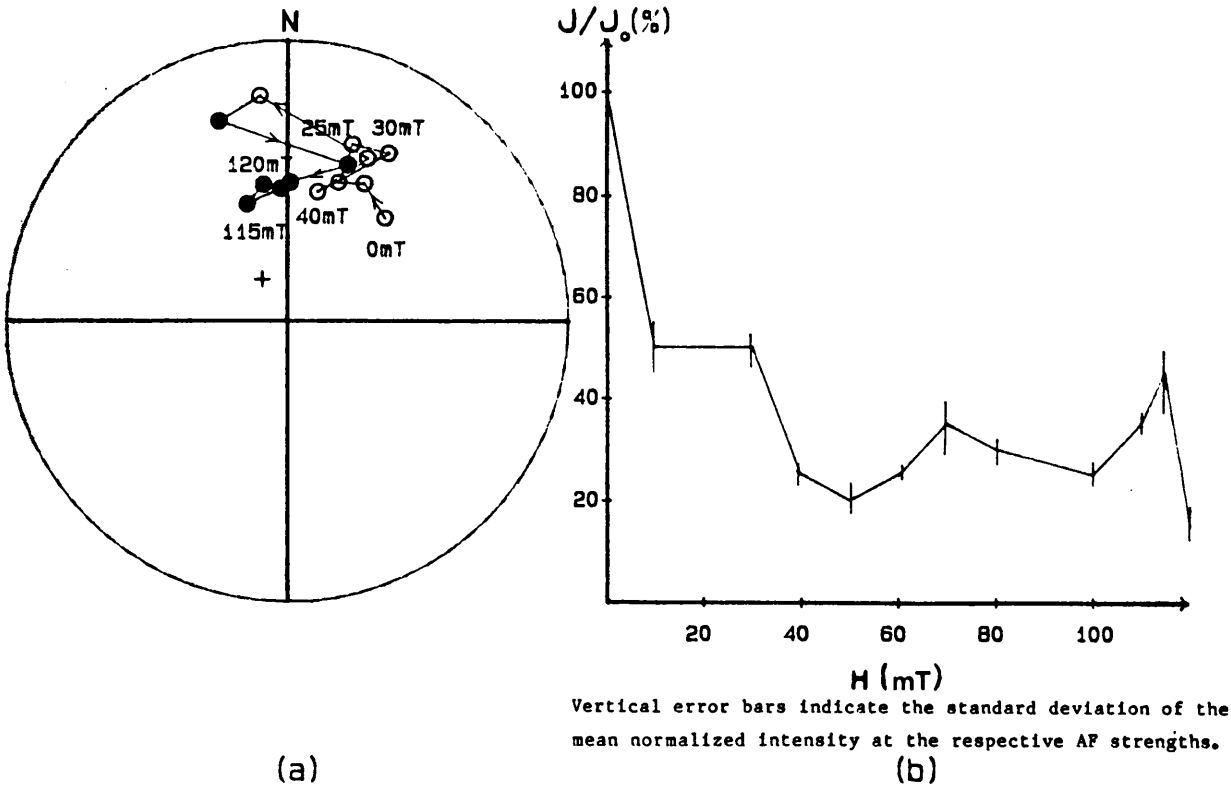

Vertical error bars indicate the standard deviation of the mean normalized intensity at the respective AF strengths.

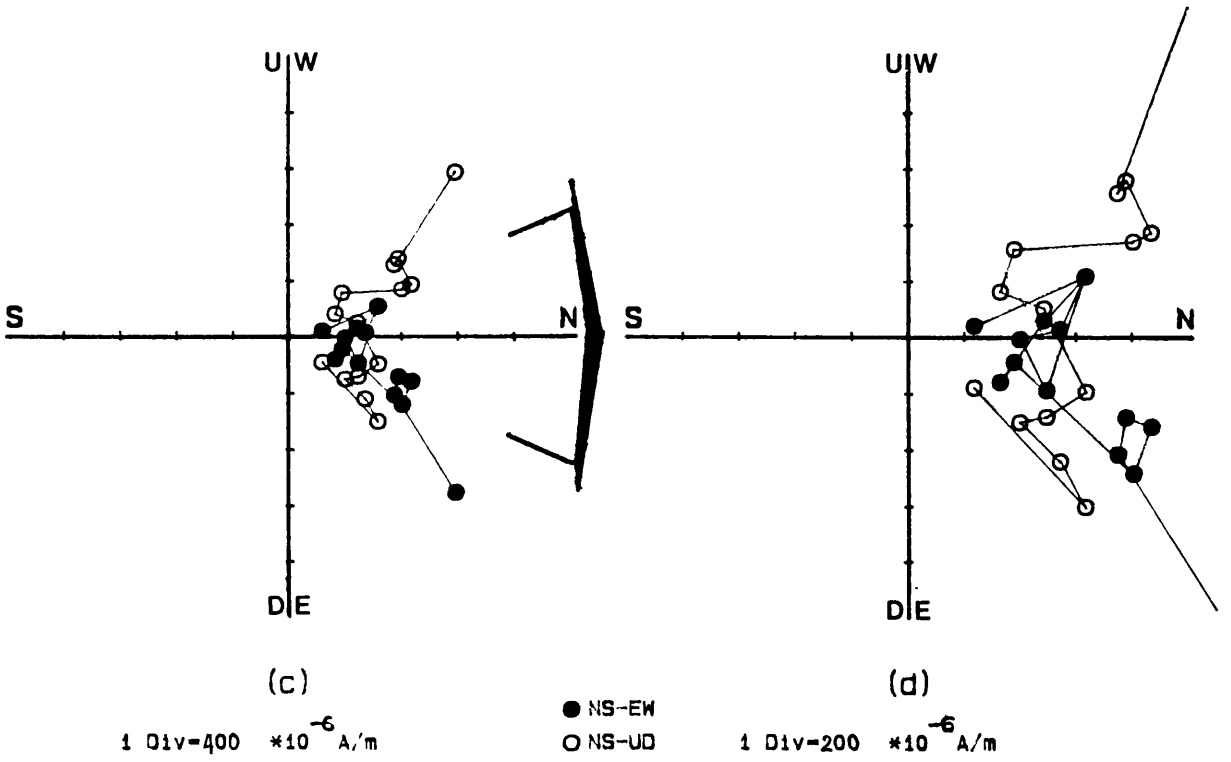

Figure 38: Stepwise AF demagnetization of specimen M7F.

(a) Resultant vectors (plotting convention as in Fig.6).

(b) Normalized intensity response curve.

(c) Zijderveld stability diagram.

(d) Magnification of Zijderveld diagram (c).

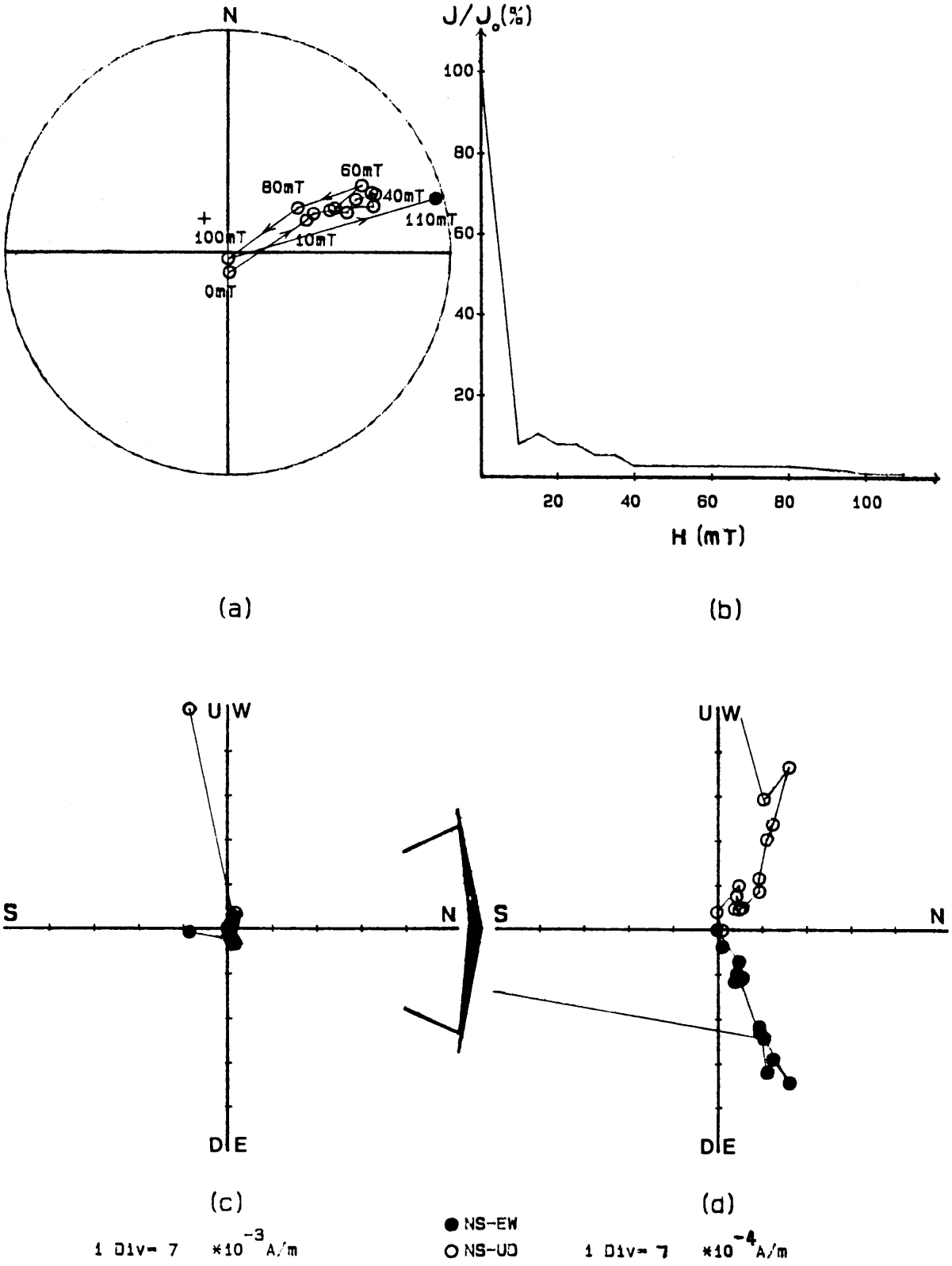

Figure 39: Stepwise AF demagnetization of specimen M6C.

(a) Resultant vectors (plotting convention as in Fig.6).

(b) Normalized intensity response curve.

(c) Zijderveld stability diagram.

(d) Magnification of Zijderveld diagram (c).

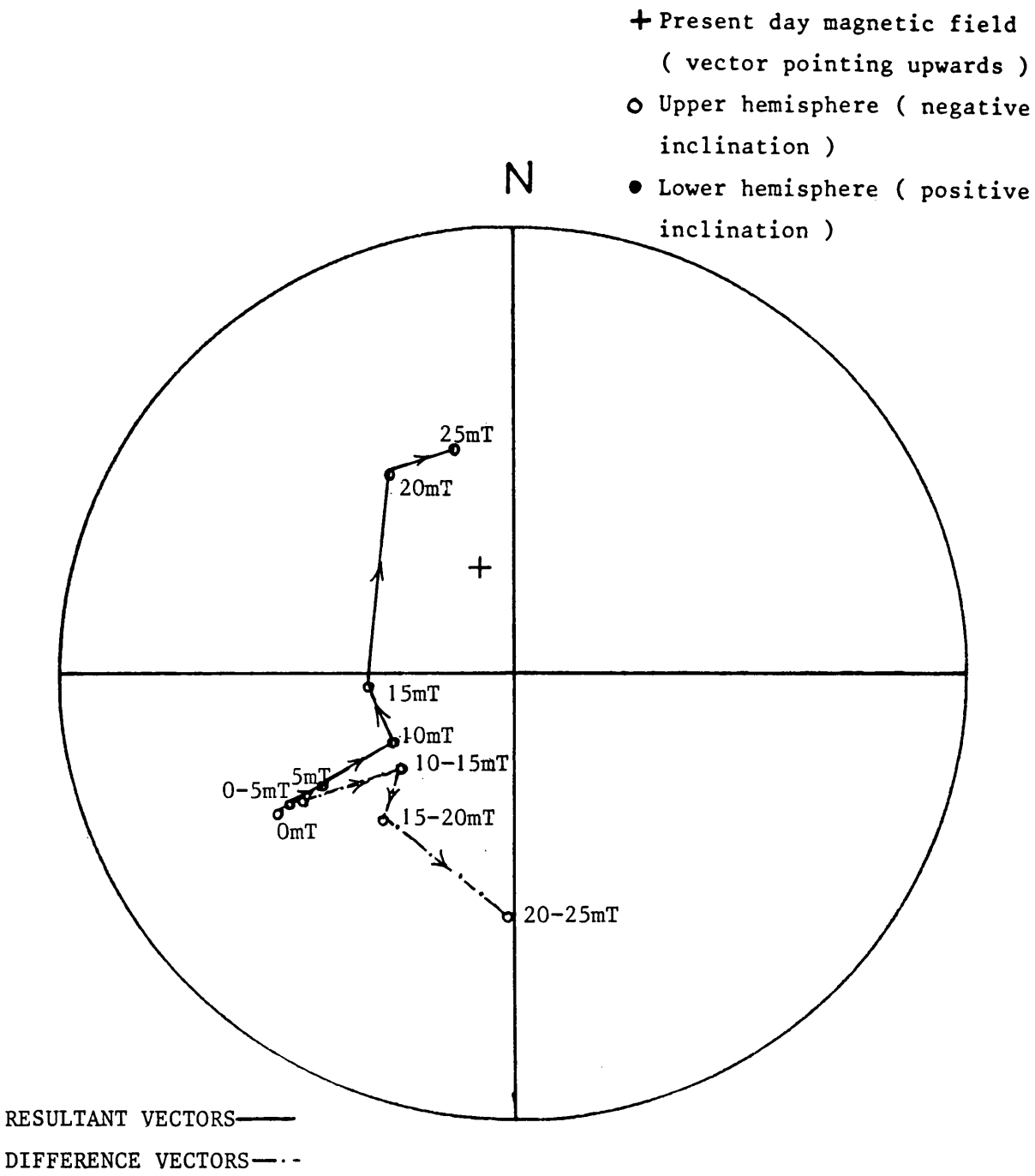

Figure 40: Response of specimen M3A to AF demagnetization.

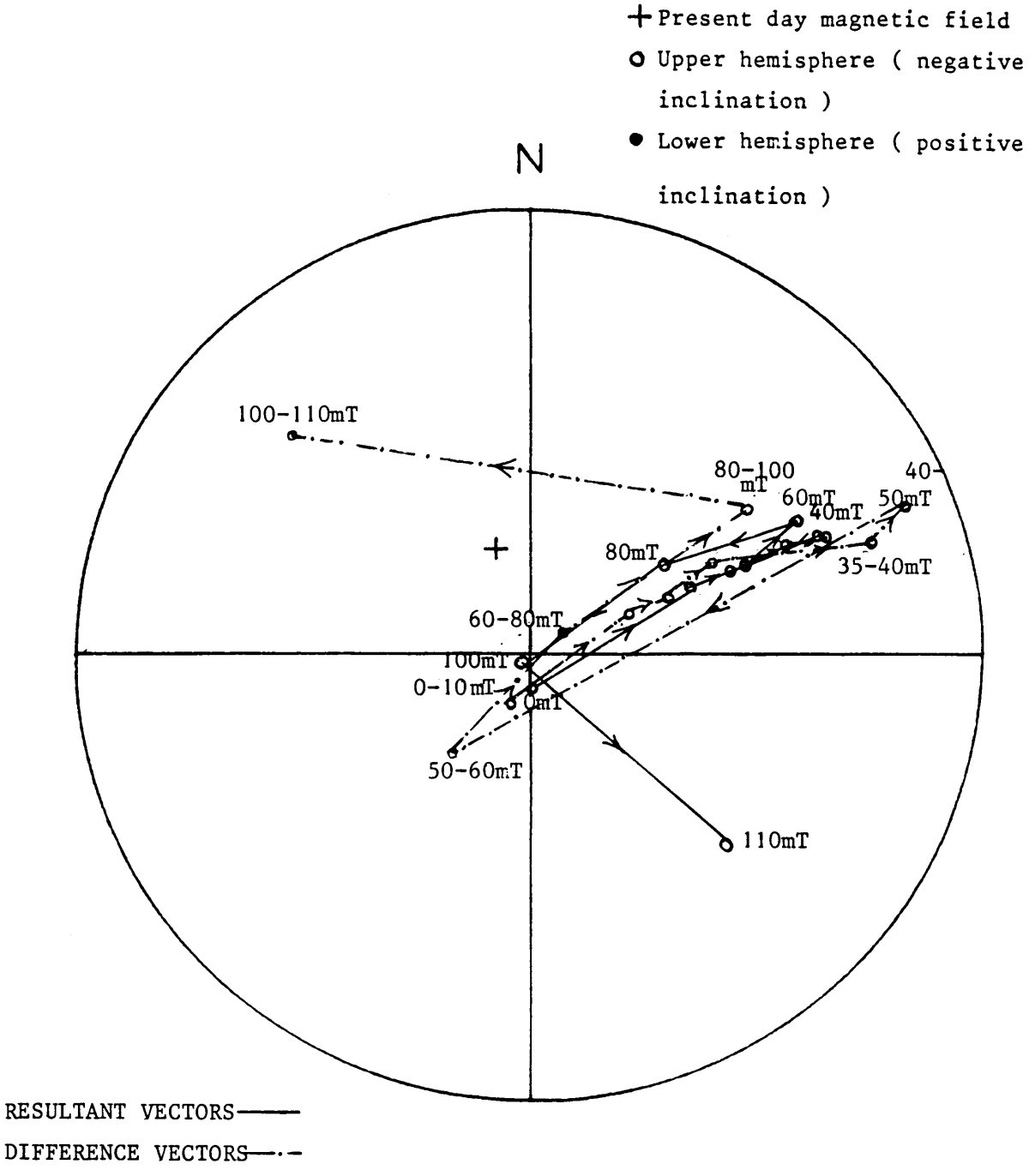

Figure 41: Resultant and difference vectors of specimen M6C during AF demagnetization.

magnetization directions, and the smearing of the vector path may be due to overlapping coercivity spectra. Isolation of components with the use of intersecting great circles followed by difference vectors (Hoffman and Day, 1978) was unsuccessful. However, the use of the corresponding Zijderveld stability diagrams (Figure 39(d)) enabled an estimated magnetization direction, with D = 65,5^{o} and I = -67,0^{o}, to be identified. This direction thus corresponds with NRM group C. The apparent absence of group B at high fields is probably attributable to the lack of data at fields greater than 100 mT. The latter could not be obtained due to the low intensity of magnetization of specimens at these fields.

Although the typical RRM acquisition of specimens from the norite during AF demagnetization (Figure 38(b)) makes vector analysis extremely difficult, the change in sign of the vector in Figure 38(a) at high alternating fields is interesting. The vector changes towards a direction which corresponds broadly with that identified as a consistent primary direction in both the gabbro and the anorthosite. Thus, it seems that the primary magnetization component which is present in the gabbro and mottled anorthosite, may also present in the norite. Analysis of corresponding Zijderveld stability diagrams (Figure 38(c),(d)) proved unsuccessful due to the effect of RRM.

(c) Continuous thermal demagnetization:

Three specimens were subjected to continuous thermal demagnetization. The typical normalized intensity response curve for the norite specimens (Figure 42(b)) displays distributed blocking temperature ranges. In the vicinity of 500^{o}C a magnetization component is completely destroyed. At temperatures of c. 580^{o}C, the typical intensity response curve to thermal demagnetization (Figure 42(b)) indicates irregular increases and decreases in magnetization intensity. This is an RRM-like effect. Although the intensity of magnetization was extremely low, the fact that the magnetization of the specimen was not destroyed at temperatures above 580^{o}C, indicates that hematite must be responsible for this magnetization. The latter magnetization could involve VRM-acquisition of the magnetic carriers at temperatures greater than 580^{o}C.

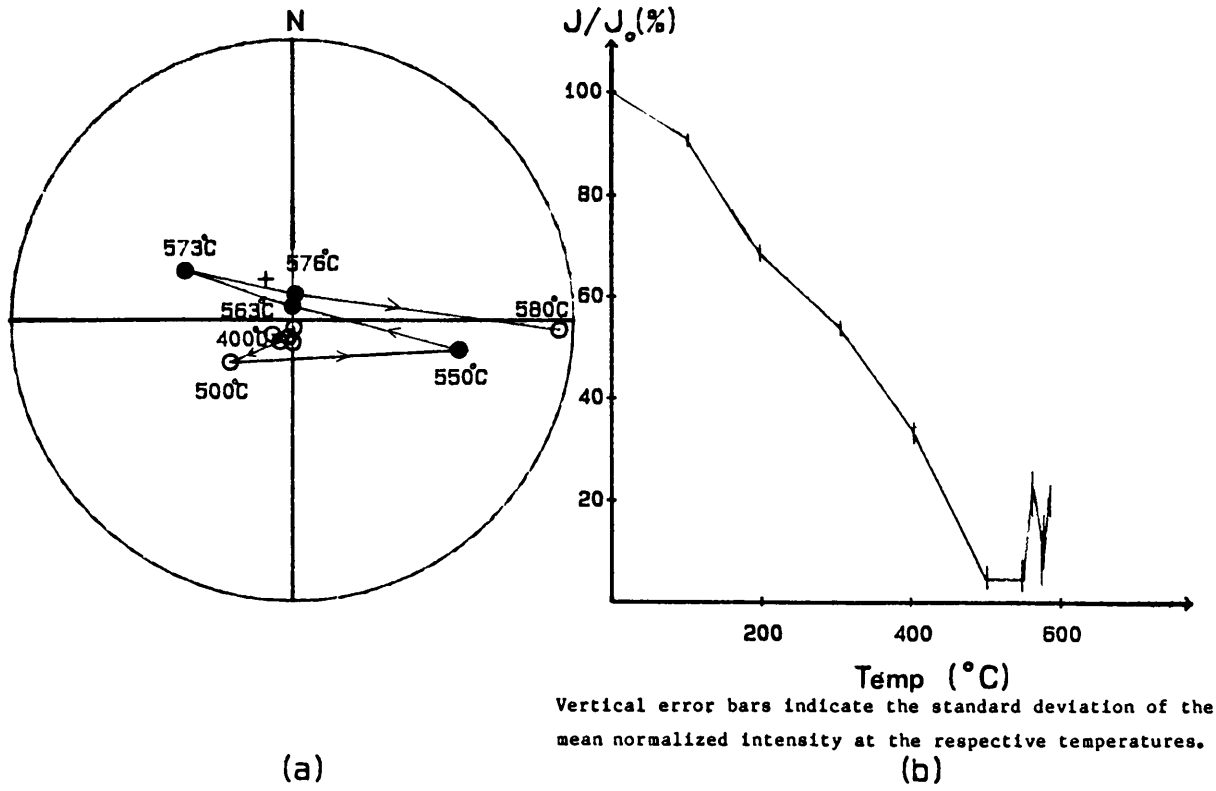

Vertical error bars indicate the standard deviation of the mean normalized intensity at the respective temperatures.

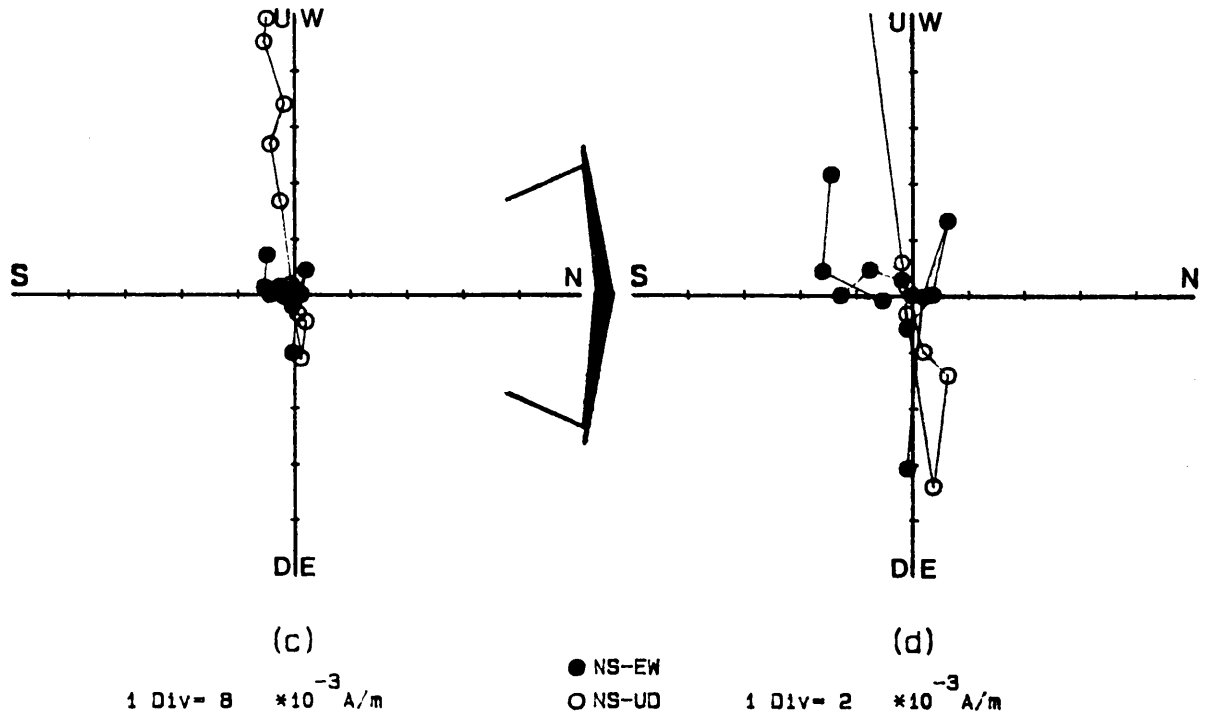

1 Div= 8 $*10^{-3}$ A/m

1 Div= 2 $*10^{-3}$ A/m

Figure 42: Response of specimen M6E to thermal demagnetization.

(a) Resultant vectors (plotting convention as in Fig.6).

(b) Normalized intensity response curve.

(c) Zijderveld stability diagram.

(d) Magnification of Zijderveld diagram (c).

An interesting feature of the thermal demagnetization is that the magnetization direction which is indicated by the resultant vectors in Figure 42(a) corresponds with NRM direction B at temperatures up to c. 500°C. This indicates that this component has a high blocking temperature and that B represents a main secondary magnetization direction. Furthermore, this direction, with
D = 171,20° and I = -80,52°, is antipodal to the consistent primary direction which was isolated in the mottled anorthosite and gabbro. Although no stabilization of vectors occurs at temperatures of c. 580°C, and the resolution at this stage was low, vectors in Figure 42(a) apparently move towards the primary magnetization direction at these temperatures. The change in polarity towards that of the antipodal positively inclined direction, at temperatures above 500°C, may be significant.

5.3 **Petrographical and mineralogical results:**

(a) Petrography:

The rock is fine grained, consisting of tiny stubby cumulus plagioclase crystals, 0,2-0,4 mm in length, and intercumulus orthopyroxene (Figure 43(a)). A small amount of intercumulus clinopyroxene mantles the orthopyroxene, or occurs as large intercumulus patches which are altered to amphibole.

The plagioclase crystals are twinned and have a composition of An_{68} (Table XIV). They are pristine and exhibit a polygonal-granoblastic texture, with well-developed triple junctions.

Two textural types of orthopyroxene occur. Orthopyroxene occurs primarily as large optically homogeneous areas, up to 10 mm in diameter (Figure 43(b)), which contain coarse exsolutions of clinopyroxene that are particularly well developed in one crystallographic direction (Figure 43(a)). Blebs and irregularly shaped exsolutions of clinopyroxene are however also present in the orthopyroxene. Large (c. 2 mm in diameter) rounded orthopyroxene grains, which enclose numerous globular or rounded plagioclase grains, are also found. The latter grains exhibit a poikilitic texture and do

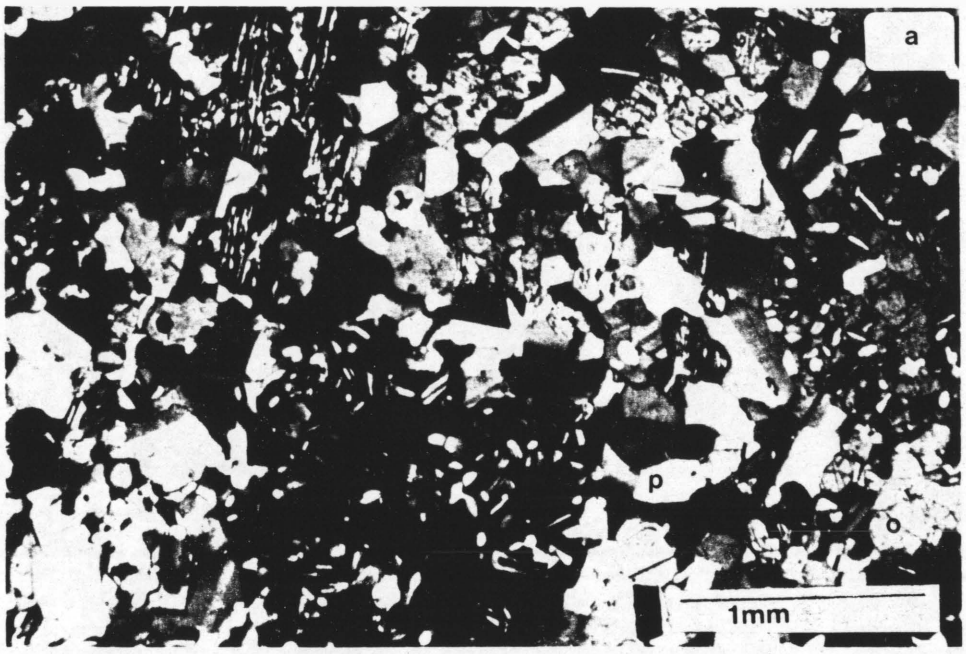

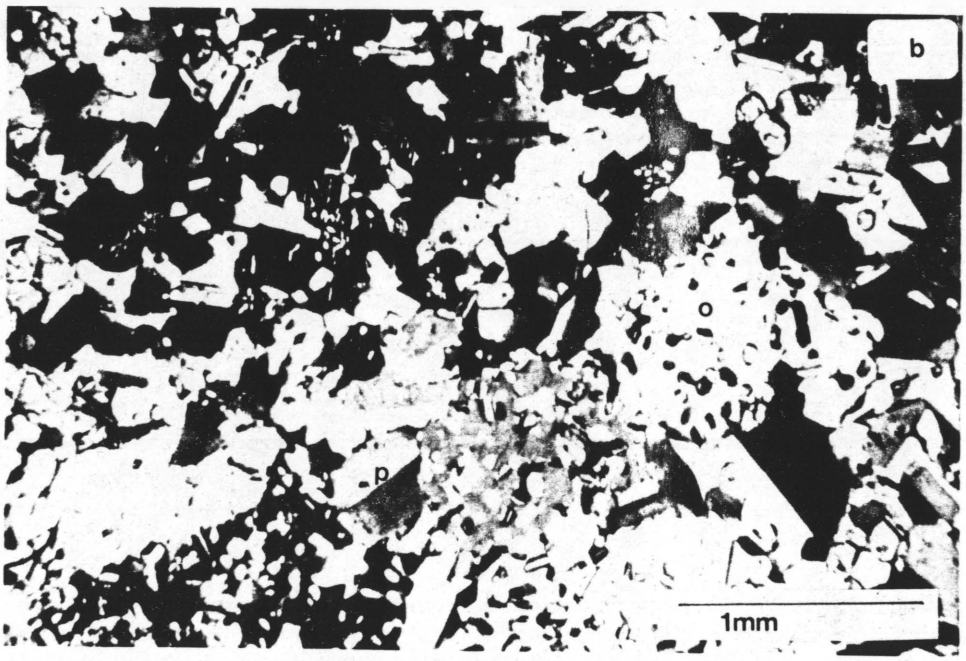

Table XIV: Electron microprobe analyses, structural formulae and molecular percentages of plagioclase in the norite.

Sample #	3PL1	3PL2	3PL3	3PL4	3PL5
SiO_2	51,59	51,33	51,19	51,20	51,56
Al_2O_3	30,35	30,61	30,91	30,24	30,72
FeO	0,26	0,16	0,24	0,17	0,33
MgO	0,01	0,01	0,02	----	0,02
CaO	13,71	13,84	13,94	13,83	14,00
Na_2O	3,46	3,50	3,37	3,46	3,33
K_2O	0,23	0,23	0,21	0,21	0,14
Total	99,61	99,68	99,88	99,11	100,10

Number of cations on the basis of 32(O)

Si	9,42	9,37	9,33	9,40	9,37
Al	6,53	6,59	6,64	6,54	6,57
	15,95	15,96	15,97	15,94	15,94
Fe	0,04	0,02	0,04	0,03	0,08
Mg	----	----	0,01	----	0,01
Ca	2,68	2,71	2,72	2,72	2,72
Na	1,22	1,24	1,20	1,24	1,18
K	0,06	0,06	0,04	0,04	0,04
	4,00	4,03	4,01	4,03	4,03

	An	67,7	67,6	68,7	68,0	69,0
mol%	Ab	30,8	30,9	30,3	31,0	30,0
	Or	1,5	1,5	1,0	1,0	1,0

not contain coarse exsolutions of clinopyroxene like the former type, but do contain fibrous Ca-rich exsolutions. The optically continuous areas of orthopyroxene have been reported by many previous workers including Lombaard (1934, p. 26) and Raal (1965, p. 16), and according to von Gruenewaldt (1970) they can be up to 30,5 cm in diameter. These areas are described as "chains" or "groups of chains with similar orientation" by von Gruenewaldt (1970; 1971, p. 71), but in this case (Figure 44(a)), they are probably more accurately described as large rounded orthopyroxene grains which enclose plagioclase laths poikilitically. The term "ophitic" is not appropriate here seeing that the plagioclase inclusions are randomly orientated in the host. Von Gruenewaldt (1971) considers this texture to be the result of post-cumulus processes. There is no difference in composition between the two types of orthopyroxene grains, and the average composition is Fs_{28} (Table XV), which is much lower than the Fs-compostion of the orthopyroxene in the other two rocks at this locality. Figure 17(b) indicates this relationship.

A small amount of clinopyroxene, which has a composition of $Wo_{45}En_{43}Fs_{12}$ (Table XV), occurs as interstitial material. However, in the vicinity of the pegmatoidal body, the clinopyroxene occurs chiefly as large grains which enclose clusters of tiny plagioclase grains as well as rounded orthopyroxene grains ophitically to subophitically (Figure 44(b)). The clinopyroxene exhibits parting parallel to {001}, but it is virtually completely altered to amphibole. Figure 17(a) illustrates that equilibrium between the coexisting pyroxenes does not exist at this stage. Clusters of rounded orthopyroxene grains enclose these hydrated areas, and muscovite and talc are also present surrounding these patches (Figure 44(c)).

(b) Ore mineralogy:

The rock contains minute quantities of opaque minerals. A very interesting feature is the occurrence of chromite in the norite. It occurs as euhedral to subhedral grains which are poikilitically enclosed by orthopyroxene (Figure 45), and the chromite grains are on average 20 micron in diameter. The texture suggests that the chromite crystallized before the orthopyroxene. A characteristic feature of the

Table XV: Electron microprobe analyses, structural formulae and Mg/(Mg+Fe) values for coexisting ortho- and clinopyroxenes in the norite.

	ORTHOPYROXENE					CLINOPYROXENE	
Sample#	30PX1	30PX2	30PX3	30PX4	30PX5	3CPX1	3CPX2
SiO_2	54,58	54,09	54,37	54,33	53,99	52,83	53,12
TiO_2	0,22	0,19	0,20	0,19	0,20	0,26	0,29
Al_2O_3	0,71	0,73	0,66	0,69	0,75	1,14	1,26
FeO_T	17,83	17,88	17,88	17,75	17,86	7,43	7,06
MnO	0,32	0,39	0,36	0,32	0,28	0,19	0,15
MgO	25,28	25,87	25,97	25,25	25,67	15,31	15,03
CaO	0,94	1,05	0,98	0,97	1,02	22,03	22,57
Na_2O	----	----	----	0,01	0,03	0,19	0,19
K_2O	----	----	----	0,01	0,01	----	----
Cr_2O_3	0,11	0,10	0,13	0,12	0,15	0,19	0,17
Total	99,99	100,30	100,55	99,64	99,96	99,57	99,84
Number of cations on the basis of 6(O)							
Si	1,99	1,97	1,98	1,99	1,97	1,96	1,97
Al	0,01	0,03	0,02	0,01	0,03	0,04	0,03
	2,00	2,00	2,00	2,00	2,00	2,00	2,00
Al	0,02	----	0,01	0,02	----	0,01	0,02
Ti	0,01	0,01	0,01	0,01	0,01	0,01	0,01
Fe_T	0,54	0,55	0,54	0,54	0,55	0,23	0,22
Mn	0,01	0,01	0,01	0,01	0,01	0,01	----
Mg	1,37	1,41	1,40	1,38	1,40	0,85	0,83
Ca	0,04	0,04	0,04	0,04	0,04	0,88	0,90
Na	----	----	----	----	----	0,02	0,02
K	----	----	----	----	----	----	----
Cr	----	----	0,01	----	----	0,01	0,01
	1,99	2,02	2,02	2,00	2,01	2,02	2,01
$Mg/(Mg+Fe^{2+})$	0,72	0,72	0,72	0,72	0,72	0,79	0,79
Wo	2,0	2,0	2,0	2,0	2,0	44,4	45,9
Mol% En	70,4	70,3	70,7	70,4	70,0	43,4	42,9
Fs	27,6	27,7	27,3	27,6	28,0	12,2	11,2

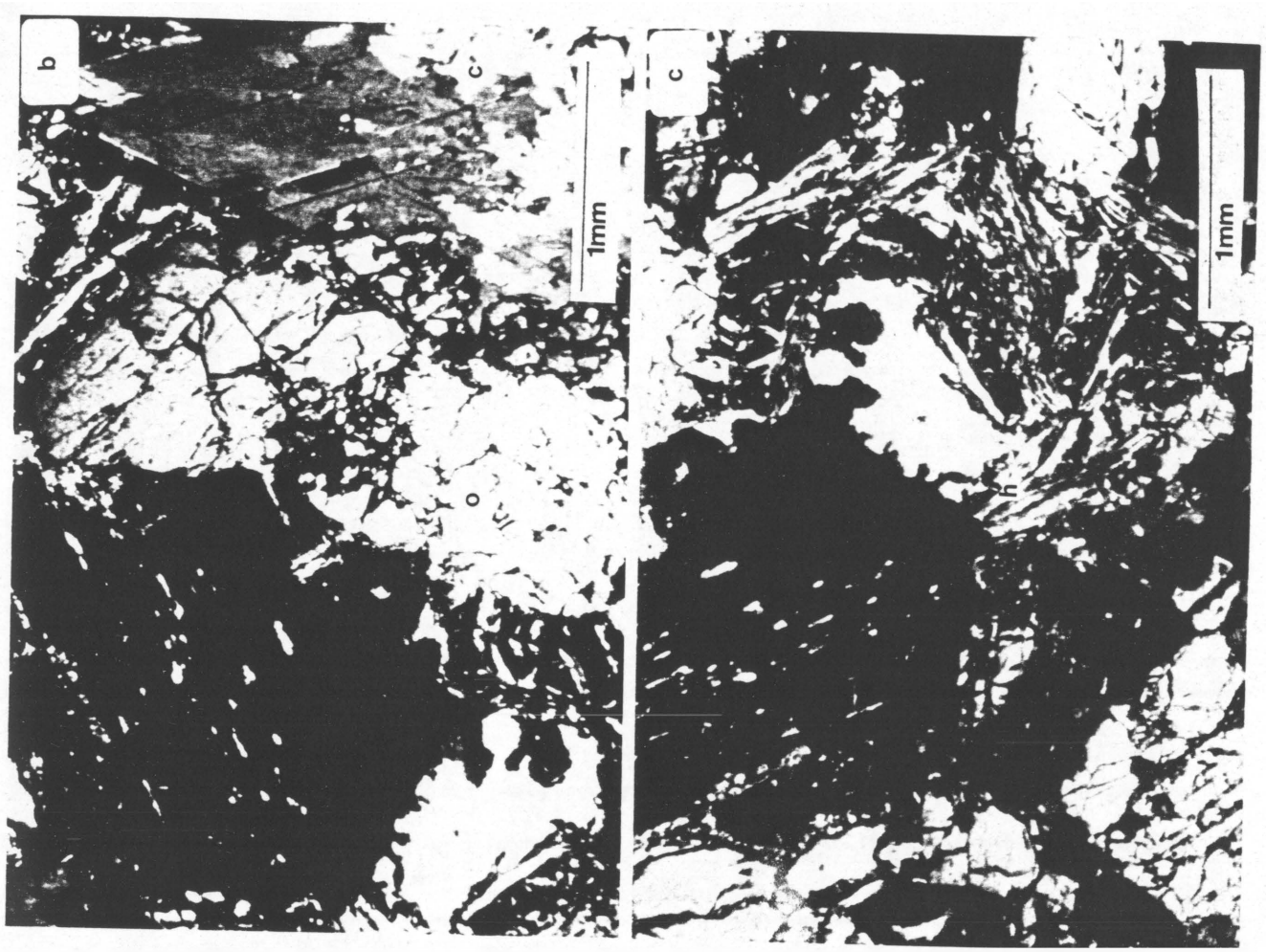

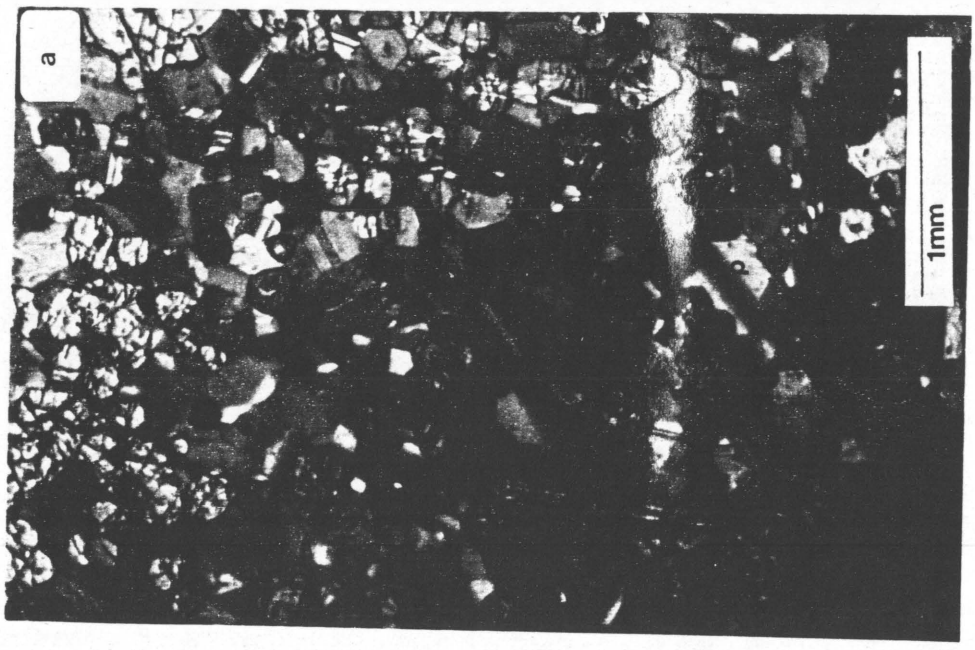

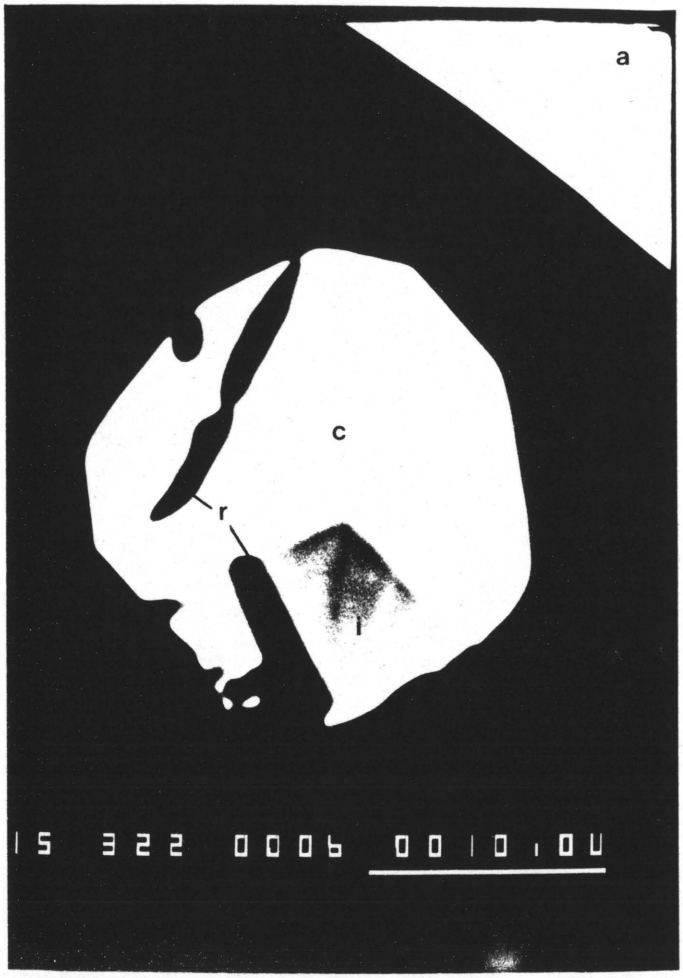

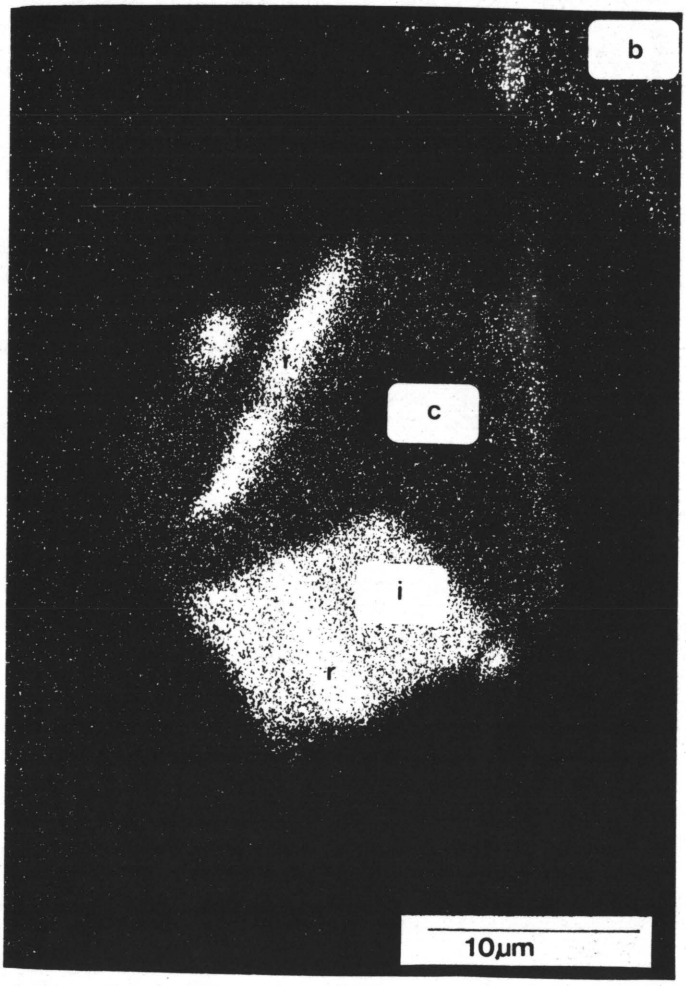

chromite is that it is unevenly distributed in the rock. The chromite illustrates wedge-shaped zonation, as is illustrated by the Ti-distribution in Figure 45(b). In Figure 45(a) the black patches are rutile, whilst the grey area is relatively rich in Ti and poor in Fe, indicating that it could be either ilmenite or ilmeno-rutile. Interestingly, the titanium-rich phase apparently represents an exsolution feature. The possibility of the exsolution of ilmenite from chromite was suggested by Van Zyl (1970) for certain horizons in the Merensky Reef. The exsolution of Ti-chromites from ilmenite has also been reported in kimberlite by Danchin and d'Orey (1972). According to Ramdohr (1980 , p. 922) high temperature chromites can unmix, and he reported exsolution bodies of ilmenite in very Fe-rich chromites from the Bushveld Complex (p. 948 ,op. cit.). Furthermore, the possible presence of minute quantities of exsolved hematite in the ilmenite, which is associated with the chromite, cannot be ruled out. The composition of the chromite in this investigation (Table XVI) indicates that the chromite is Fe-rich, suggesting late-stage crystallization in the chromite crystallization sequence.

Regarding the contribution of chromite to the remanence of the norite, Banerjee (1972) found that although pure chromite is antiferromagnetic, it can become ferrimagnetic when Ti is present as substitution for Cr. Furthermore, according to Schmidtbauer (1971), Ti-bearing chromites can have a Curie point at between -150°C and 400°C. If hematite is present as ilmeno-hematite in the chromite, then a high coercivity-high blocking temperature component could be predicted for this assemblage.

Ore laths in the plagioclase and pyroxene were not found, but may be present, and tiny anhedral exsolutions of magnetite, roughly 20 micron in diameter, occur in the orthopyroxene in small quantities.

5.3 **Discussion of results:**

AF demagnetization indicated that a soft magnetization component is present in some norite specimens, and in specimens from sample M3, this component corresponds with NRM group A (D = 235,19°, I = -24,49°). It thus appears that NRM group A is probably a soft VRM.

Table XVI: Electron microprobe analyses of chromite in the norite.

Sample #	MD1	MD2	MD3	MD4
SiO_2	0,08	0,03	0,07	0,07
TiO_2	2,68	3,73	2,89	2,83
Al_2O_3	4,09	4,34	3,95	3,96
Fe_2O_3	32,42	28,72	32,72	32,56
FeO	31,94	32,68	32,07	31,88
MnO	0,40	0,40	0,37	0,39
MgO	1,58	1,75	1,53	1,55
Cr_2O_3	26,23	27,77	25,44	25,50
V_2O_3	0,71	0,69	0,75	0,76
Total	100,13	100,11	99,79	99,50
Number of ions on the basis of 4(O)				
Si	----	----	----	----
Ti	0,07	0,10	0,08	0,08
Al	0,18	0,19	0,17	0,17
Fe^{3+}	0,89	0,79	0,90	0,90
Cr	0,76	0,80	0,74	0,74
V	0,02	0,02	0,02	0,02
	1,92	1,90	1,91	1,91
Fe^{2+}	0,98	1,00	0,98	0,98
Mn	0,01	0,01	0,01	0,01
Mg	0,09	0,09	0,08	0,08
	1,08	1,10	1,07	1,07

Magnetization directions corresponding with NRM direction C (D = 72,66°, I = -32,66°) were removed at intermediate fields during AF demagnetization. It is possible that these fairly soft secondary magnetization directions may have the same magnetic carrier.

Thermal demagnetization indicated that direction B is a major secondary magnetization direction which has a blocking temperature in the vicinity of 500°C. It is interesting that direction B is antipodal to the primary magnetization direction which was isolated in the anorthosite (D = 17,33°, I = 67,75°) and gabbro. Furthermore, removal of component B is normally associated with a change in polarity, suggesting that another magnetic component is destroyed at temperatures greater than c. 500°C. This observation would be in accordance with mineralogical evidence, which indicates that magnetite is present in this rock. Thus, magnetite could be the magnetic carrier which is destroyed at temperatures approaching 580°C. It is possible that magnetite in the norite may be the carrier of a primary magnetization component which corresponds with the primary magnetization direction in the anorthosite and gabbro. Since magnetite laths were not found in the norite, anhedral magnetite in pyroxene may be the carrier. However, the role of chromite in this regard cannot be determined, due to lack of experimental data. Chromite may thus also contribute to a primary magnetization component in the norite. It seems possible that ilmeno-hematite (in chromite) may be the carrier of magnetization component B. When this magnetization component is removed, and the temperatures exceed that that of the Curie temperature of magnetite, hematite is probably responsible for the magnetization of the specimens.

An important observation regarding the spurious behaviour of norite specimens, is the reversal in inclination of two specimens between repeated NRM measurements. This suggests that a carrier of magnetization in the norite is able to acquire a VRM before its magnetization components are partially or completely broken down. Furthermore, the ability to undergo a polarity reversal during VRM acquisition, is unusual.

In summary the main palaeomagnetic characteristics of the norite are as follows:

(i) The rock has an extremely low intensity of magnetization of 16 x $10^{-3}A.m^{-1}$, a very low mean magnetic susceptibility of 0,3 x $10^{-3}SI$ and the magnitude of anisotropy is 0,14.

(ii) A soft component of magnetization is present in some specimens.

(iii) Directions of magnetization corresponding with NRM group C are removed at intermediate alternating fields.

(iv) A major secondary magnetization component corresponding with NRM group B (D = 171,20°, I = -80,52°) is present. The blocking temperature of this component is in the vicinity of 500°C. It seems as if this component may be carried by ilmeno-hematite. This direction is antipodal to the primary magnetization direction which was identified in both the anorthosite and gabbro.

(v) A magnetization direction corresponding with that identified as the primary magnetization direction in the previous rock-types, may be present in the norite. The carrier of this component of magnetization may be magnetite blebs in pyroxene, although magnetite laths in plagioclase may be present in small quantities as well.

(vi) Two specimens exhibited the ability to undergo a reversal in inclination between repeated NRM measurements. Furthermore, the typical behaviour of specimens during AF demagnetization indicates an RRM effect, and specimens exhibited an RRM-like behaviour at temperatures above 580°C during thermal demagnetization. This behaviour strongly suggests that, due to a very specific mineralogy, specimens of the norite have the ability to readily acquire secondary magnetizations, possibly VRMs, even at room temperature.

6. DISCUSSION:

6.1 Petrological aspects:

The mottled anorthosite at site M occurs at the correct stratigraphic height, and as already discussed, represents the Upper mottled anorthosite unit. The polarity of this unit is consistent with that of the main zone as isolated by Hattingh (1983). However, with respect to textural and field relations of the three rock-types at this site, it is evident that this succession does not represent the normal stratigraphic sequence.

Folds and fragments which are attached to the floor of the Complex have been reported by Sharpe and Chadwick (1982). Prior to the latter paper, Button (1978) proposed that these domal occurrences in the meta-sedimentary floor rocks are diapirs, but Sharpe and Chadwick in the former paper argued that if this were so, then trunks of diapirs should have been exposed by erosion. These authors also proposed that regional heating during the intrusion of the Bushveld magmas caused buckling of the floor rocks due to increased ductility of the floor. The chilled texture of the norite, and the fact that it is in contact with floor quartzite, suggests that it represents a sill which was emplaced into the Pretoria Group meta-sediments. It appears that updoming of the floor must have taken place prior to the emplacement of the mottled anorthosite, to explain the contact between the noritic sill and the anorthosite. Furthermore, the occurrence of chromite in the norite suggests that it must be a chilled marginal rock associated with the emplacement of the critical zone. A magnetization component with D = 171,20^{o} and I = -80,52^{o} was identified in the norite. There is a broad similarity between this direction and that isolated by Hattingh (1983) as representative of the critical zone. Thus, the textural features and the presence of chromite in the norite, together with the magnetic signature points to this being a critical zone-associated sill.

A problem however arises due to the fact that the Mg/(Mg+Fe) values of the orthopyroxene are not consistent with those presented by Sharpe (1981) as being representative of critical zone-associated sills. He

divides these chilled rocks into an N and a B2 type, the former representing an earlier quenched norite and the latter a border facies of the critical zone. The calculated Mg/(Mg+Fe) value for the orthopyroxenes in these rocks is c. 0,83, whilst a value of 0,72 was found in the present study. The latter value is however consistent with values presented (op.cit.) for upper critical zone rocks in the vicinity of the Merensky Reef. Engelbrecht (1986) found that calculated Mg/(Mg+Fe) values for orthopyroxenes and olivines in the marginal zone of the western Bushveld were unrealistically high in comparison with actual values. His conclusion is that the chilled rocks in the Nietverdiend area do not represent the parent magma of the marginal, lower and critical zones. If, however, the latter does not hold for the eastern compartment, the majority of evidence nevertheless points to this norite representing a sill associated with the border facies of the critical zone, probably the upper critical zone. The discrepancy in the Mg/(Mg+Fe) values could be explained by interpreting the sill as being representative of residuum of the critical zone material which was intruded into the floor along a fractured zone. Either way, there is a relative age difference between the sill and the associated rocks at site M.

The intrusion of the two-pyroxene gabbro represents a later magmatic event. It appears that this intrusion must be related to the intrusion of the magmas that formed the main zone, as the rock carries the characteristic main zone polarity, and its Mg/(Mg+Fe) value for the orthopyroxene of 0,67 is consistent with central main zone values (Sharpe, 1981). The relatively low intensity of magnetization of the gabbro is attributable to the smaller amount of Fe-Ti oxide laths in the plagioclase of the gabbro, in comparison with the anorthosite. The magma which intruded after the formation of the mottled anorthosite to give rise to the gabbro was rich in volatiles, as is evident from the pegmatoidal gabbroic intrusion in the norite. This resulted in the hydration of pyroxenes in the norite, possibly due to chemical gradients which developed, and the subsequent formation of amphibole and talc in the blebs in the norite. The blebs, stringers and veinlets of pyroxene and plagioclase in the norite (Figure 36) thus represent gabbroic material which intruded the norite. The blebs are possibly cross sections of veinlets. Evidence for the relationship between the

intrusive two-pyroxene gabbro and the hydrated minerals also lies in the fact that the pyroxene blebs only occur in close proximity to the pegmatoidal intrusion. The irregular contact between the gabbro and the mottled anorthosite indicates that limited mixing between these two layers took place (Figure 4b). Another interpretation for the intrusive coarse grained plagioclase-rich bodies in the norite (Figures 5(a),(b) and (c)) is that they represent anorthosite flame structures which, according to Lee (1981), are analogous to ball-and-pillow structures in clastic sediments. The latter author describes structures such as these from the Bushveld Complex, below the Merensky Reef at the contact between anorthosite and norite, but such an explanation would not account for the differences in ore mineralogy and magnetic signature between the anorthosite/gabbro unit and the norite.

6.2 **Carriers of magnetization:**

Regarding the differences in intensity of magnetization and magnetic fabric of the different rocks, the following should be noted:

(i) The range in intensity of magnetization of the mottled anorthosite is orders of magnitude greater than that of the other two rocks. The norite has the lowest intensity of magnetization, with the gabbro having intermediate intensities.

(ii) The mean magnetic susceptibility of the mottled anorthosite is higher than that of both the gabbro and the norite. The values of the norite are by far the lowest.

(iii) The anisotropy of susceptibility is higher for the mottled anorthosite than for the other two rock-types. The latter suggests that the primary carrier of magnetization in the anorthosite is partially orientated, probably due to the orientation of plagioclase crystals parallel to the igneous layering.

In the analysis of the contributions of the respective magnetic mineral occurrences to the remanence of the rocks, the origin of the laths should be considered. They are present in both the mottled anorthosite and the gabbro, and probably occur in very small quantities in the norite. Firstly, they need to be subdivided in terms of occurrence, and this has implications for their genesis.

Various authors have referred generally to similar laths as both inclusions and exsolutions. In the case of the plagioclase it seems improbable that they could represent exsolutions. The latter would imply that Fe is dissolved in plagioclase at high temperatures, and this has been suggested by Scharlau (1972) and Davis (1981). Nienaber-Roberts (1986) proposed that these laths must have formed by exsolution, due to the similarity in composition between laths in plagioclase and platelets known to have exsolved from clinopyroxene. This argument is however not convincing, since no quantitative analyses were presented (op. cit.) An alternative origin, where the laths may have originated as a result of epitaxial growth, is also possible. This mechanism would involve the simultaneous crystallization of magnetite and/or ilmenite, and plagioclase. This mechanism infers the orientated growth of ore laths on plagioclase during simultaneous growth of the plagioclase crystal lattice. Magnetite laths would preferentially be lengthened along [111] of magnetite. If it is envisaged that the magnetite crystallized as cubes, as is often the case, then the hard magnetization associated with these laths could readily be explained if they grew by attachment at their corners (Figure 46). Such dendritic growth is illustrated by Phillips (1963, Fig. 302). The [111] direction represents the "easy" direction of magnetite (O'Reilly, 1976) in terms of its magnetization, thus the effect of shape anisotropy will be enhanced by the crystalline anisotropy along the "easy" direction of magnetite. Ilmenite, due to its rhombohedral structure, would readily form laths which are lengthened along {0001} since a tabular habit is common in ilmenite (Ford, 1932, p.486). According to Ramdohr (1980, p. 990) ilmenite grains orientated with {0001} parallel to the fabric of the rock have been observed. He also comments that the {0001} direction can preferentially develop in ilmenite aggregates. This model implies that the ore laths in the plagioclase can be regarded as primary, and are the carriers of a TRM, which they would have acquired during the rock-forming process.

The ore laths in the clino- and orthopyroxene are clearly related to biotite and chlorite, and are orientated along planes where some alteration of the pyroxene has taken place. Since the magnetite and ilmenite laths are found at the tips of biotite or chlorite flakes in

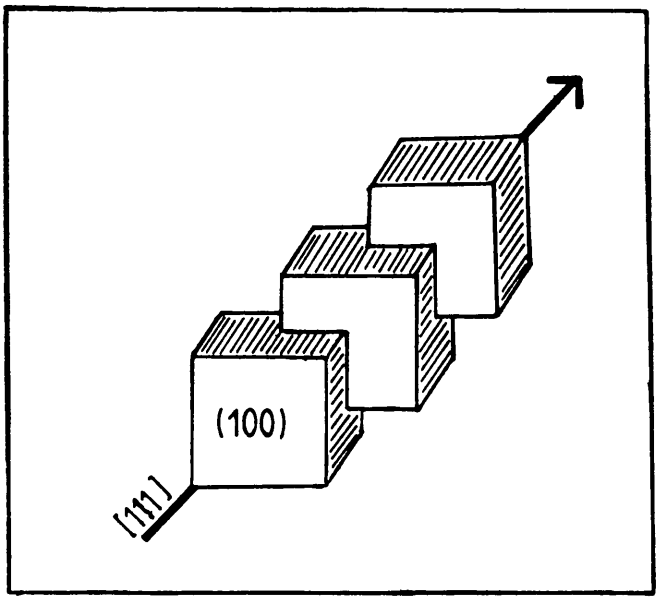

Figure 46: Schematic representation of magnetite cubes lengthened along [111], the "easy" direction of magnetite.

the pyroxenes, they probably represent exsolutions from the biotite. The latter is also obvious as the laths tend to terminate in ore blebs at the borders of grains and is indicative of exsolution (Haggerty, 1976b). The magnetite in the pyroxenes thus represents exsolutions from the late-stage phyllosilicates and could therefore carry a CRM.

In the case of the anhedral magnetite in pyroxene in the norite, no associated biotite or chlorite was found. Thus this may represent primary magnetite, which could carry a TRM.

Finally, in the analysis of the contribution of the magnetite laths to the remanence of the rocks, the consideration of shape anisotropy due to the larger length : width ratios, as well as their domain configuration must be considered. Shape anisotropy, such as in the case of the laths, has been reported by numerous authors such as Evans and McElhinny (1969) to be associated with a high coercivity and stable magnetization. It has however been reported by Moon (1984) that there is a critical ratio after which the coercivity decreases. Single-, pseudo-single or multidomain analysis is a more complex problem. The domain configuration of a magnetic particle depends on the size and shape of the particle (Day, 1977). Furthermore, it is well documented that single-domain particles are characterized by stable remanences and high coercivities, but at a critical minimum size these particles lose their remanence since they become superparamagnetic. It is well known that multidomain particles are generally characterized by low coercivities since domain wall movement can readily take place in these grains. According to Day (1977) this is not necessarily true for small multidomain grains in which few walls are developed. Such particles can act as pseudo single-domain grains and Day (op. cit.) summarizes four mechanisms which have been proposed to facilitate pseudo-single-domain behaviour. It is apparent from the latter mechanisms that the coercivity of TRM varies inversely with grain diameter. Although numerous occurrences of single-domain magnetite needles have already been discussed, the assumption that these "needles" are in the size range for single domains to operate may be at fault. This study has indicated that no evidence for the existence of laths of c.1 micron in width could be found during SEM investigation of the three dimensional structure of these laths.

Pseudo-single-domain behaviour may be more important in this case since Day (1977) regards the transition size for pure magnetite from pseudo-single- to multidomain at 10-20 micron. The latter would imply that measured laths in the plagioclase in this study are pseudo-single-domain. Their great contribution to the remanence is supported by findings of Halgedahl and Fuller (1980). The latter is consistent with findings of Bergh (1970) for remanence associated with single- or pseudo-single-domain magnetite grains in plagioclase from the Stillwater intrusion.

The larger, partially resorbed Fe-Ti oxide assemblages, such as those found in the mottled anorthosite and in the two-pyroxene gabbro are evidently in the multidomain range. The magnetization of these grains has already been partially destroyed due to resorption and alteration of the grains. In the ilmenite grains, which are relatively common in both the anorthosite and the gabbro, the hematite exsolutions are in the single-domain range. Although not observed, it seems probable that the norite contains such exsolutions in ilmenite as well. According to Tarling (1983), hematite in the size range of 1-3 micron falls in the peak coercivity range for hematite. If the exsolution of the hematite took place above the Curie temperature of hematite these exsolutions would carry a TRM. The latter requirement may not be met as exsolution takes place below 600°C according to Ramdohr (1980, p.987). However, investigations such as that of Thorpe et al. (1977) have indicated that such hematite exsolutions (in ilmenite) contain minute magnetite grains. Furthermore, TEM investigations like that of Morgan and Smith (1981) have indicated that more than one scale of ilmenite-hematite lamellae can be present, thus another generation of undetected exsolutions may be present in the ilmenite from the present investigation. Thus, depending on grain size and genesis, the hematite may carry a CRM, VRM or TRM. Another consideration is that hematite exsolutions in ilmenite are along [0001] of ilmenite. Since hematite and ilmenite are both rhombohedral, the crystalline anisotropy of hematite along [0001] (O'Reilly, 1976) may have a significant effect on the remanence.

The contribution of chromite, which is the chief ore mineral in the norite, to the remanence of a rock, has not been investigated in much

detail previously. It has been shown that the chromite in the norite is a ferrous chromite with Ti-rich zones, and this may lead to a complicated TRM spectrum. According to Banerjee (1972), Ti-bearing chromite can become ferrimagnetic. Schmidtbauer (1971) found that the Curie point of Ti-bearing chromites varies between -150 and 400°C.

Finally, the magnetite-hematite dust, as found in the mottled anorthosite and gabbro, needs consideration. It appears that the hematite dust is sub-single-domain (smaller than 0,2 micron), and thus is virtually non-magnetic (Hedley, 1968), whilst the magnetite dust is probably also sub-single-domain, and thus superparamagnetic.

7. SUMMARY AND CONCLUSION:

The study was undertaken at a site in the main zone of the Bushveld Complex where the upper mottled anorthosite of the main zone crops out. Initial interest in the particular site followed investigations by Hattingh (1983) in which he found antipodal magnetization polarities. Palaeomagnetic sampling and investigations were followed by detailed petrological and mineralogical studies, with particular reference to the ore minerals.

In order to fulfil one of the main objectives of this study, i.e. to see whether a meaningful correlation exists between the petrology and palaeomagnetic results of this site, a summary of the main mineralogical characteristics of the magnetic minerals and palaeomagnetic characteristics of the three rock types will be presented:

7.1 (a) The upper mottled anorthosite:

Minerals in the anorthosite which could contribute to the magnetic properties of the rock, are the following:

Magnetic mineral	General comments
(i) Microscopic interstitial magnetite grains, virtually pure magnetite in composition, c. 500 micron in diameter.	Multidomain grains, Curie temperature of c. 578°C, carry a TRM, magnetization partially destroyed due to deuteric alteration.
(ii) Submicroscopic hematite exsolutions (smaller than 10 micron in length) in interstitial ilmenite grains.	Single- or pseudo-single-domain, in peak coercivity range for hematite (Tarling, 1983). Shape anisotropy or magnetocrystalline anisotropy may be important. Curie point was not established.

	Exsolution above or below 600°C, may carry a CRM or a TRM.
(iii) Submicroscopic magnetite inclusions in plagioclase (5-20 micron X 10-350 micron).	Carry a TRM, Curie point of c. 578°C. Shape anisotropy important. Pseudo-single-domain range.
(iv) Microscopic to submicroscopic exsolutions of magnetite in pyroxene (5-50 X 50-80 micron).	Carry a CRM due to exsolution at low temperatures. Shape anisotropy may be important. Laths in pseudo-single- or multidomain range.
(v) Submicroscopic magnetite and hematite dust resulting from the breakdown of multidomain magnetite.	Submicroscopic hematite virtually non-magnetic (Hedley, 1968). Magnetite in sub-single-domain range, therefore superparamagnetic.

Palaeomagnetic results: The rock is characterized by a mean intensity of magnetization of 4 434 x 10^{-3}A.m^{-1}, and a mean susceptibility of 6,5 x 10^{-3}SI. The main components of remanence are the following: a consistent primary magnetization component (D = 17,33°, I = 67,75°) carried by magnetite, a secondary low coercivity component which is not present in all the specimens, and a third intermediate magnetization component with a direction which is antipodal to the the primary TRM.

7.1 (b) **The intrusive two-pyroxene gabbro:**

The possible carriers of remanence in the gabbro are the following:

Magnetic mineral	General comments
(i) Submicroscopic hematite exsolutions (smaller than 10 micron in length)in ilmenite.	As in 7.1(a).
(ii) Microscopic to submicroscopic magnetite exsolutions in pyroxene (c. 5 X 10-15 micron).	As in 7.1(a).
(iii) Scarce submicroscopic magnetite inclusions in plagioclase.	As in 7.1(a).
(iv) Submicroscopic magnetite and hematite blebs resulting from the breakdown of larger magnetite grains.	As in 7.1(a)

Palaeomagnetic results: The rock has a mean intensity of magnetization of 611 x $10^{-3}A.m^{-1}$ and a mean susceptibility of 1,6 x 10^{-3}SI. Data suggest that the same consistent primary magnetization component carried by magnetite in the anorthosite is present in this rock. The primary magnetization component in the gabbro has the following direction, D = 9,34°, I = 58,70°. Furthermore, a superimposed low coercivity secondary component of magnetization is present, as well as a third intermediate component with an intermediate blocking temperature and coercivity spectrum which overlaps with that of the primary component.

7.1 (c) **The fine-grained norite:**

The norite is characterized by the following magnetic minerals:

Magnetic mineral	General comments
(i) Microscopic chromite poikilitically enclosed by orthopyroxene (c. 20 micron in diameter).	Ferrous chromite with Ti-rich zones, may contribute to the remanence.
(ii) Submicroscopic magnetite exsolutions in orthopyroxene (c. 20 micron in diameter).	Multidomain or pseudo-single-domain.
(iii) Possible ilmeno-hematite exsolved from chromite (Ramdohr, 1980).	Hematite exsolutions single- or pseudo-single-domain. Probably in peak coercivity range.
Not observed: (iv) Possible submicroscopic magnetite inclusions in plagioclase.	Would carry a TRM.

Palaeomagnetic results: The norite is characterized by a very low mean intensity of magnetization of 16 x 10^{-3}A.m^{-1}, and a mean susceptibility of 0,3 x 10^{-3}SI. A soft secondary component of magnetization is present in some specimens, as well as an intermediate component (NRM group C), which is removed at low to intermediate alternating fields. A third secondary magnetization component, which corresponds with NRM group B, with D = 171,20^{o} and I = -80,52^{o}, was also identified. This magnetization component has a blocking temperature of c. 500^{o}C, and is antipodal to the primary magnetization direction in the mottled anorthosite and gabbro.

Specimens from all three rock-types exhibited an ability to acquire a reversed magnetization to that of their primary magnetization directions.

Comparison of the magnetic characteristics and chief ore mineralogy of the two-pyroxene gabbro and the mottled anorthosite indicates a strong similarity between the two rock-types. Firstly, they carry a mutual primary magnetization direction which has been identified as a TRM carried by magnetite. Since both rocks contain magnetite in the form of laths in plagioclase and pyroxene, the conclusion is that this form of magnetite represents the high coercivity component. The latter is in accordance with the findings of Hattingh (1983). As already pointed out, the relative number of laths in the plagioclase of the gabbro is much less than that of the anorthosite, hence the difference in intensity of magnetization. Thus, the high intensity of magnetization, the high coercivity and mean magnetic susceptibility as well as the stable nature of the magnetization component points to the primary magnetite inclusions in plagioclase being the carrier of this TRM. Numerous previous workers have attributed these characteristics to the shape anisotropy and domain configurations of such laths. The indications in this investigation are however that these laths are actually not single-domain but pseudo-single-domain.

Indications are that an intermediate coercivity component of magnetization is present in the gabbro as well as in the mottled anorthosite. This magnetization component may be a VRM or a CRM carried by hematite. Magnetite, as exsolutions in pyroxene, may however also contribute to this intermediate magnetization component. The antipodal nature of this intermediate secondary magnetization to that of the primary TRM, is characteristic.

Thermal demagnetization indicated that the magnetization of the anorthosite and gabbro is not destroyed at temperatures of 578^{o}C. Furthermore, RRM-like, spurious behaviour of certain specimens was observed at temperatures above 578^{o}C. Thus there is an indication that a carrier of magnetization with a Curie temperature higher than 578^{o}C, is present in these rocks, and it is a possibility that ilmeno-hematite could be this carrier.

Further similarities between the magnetic features of the above two rocks is that they both contain a very low coercivity component. This magnetization component, which is not present in all specimens, is

probably carried by euhedral multidomain magnetite (which has been partly broken down), in the anorthosite. In the gabbro, the soft component of magnetization could be carried by multidomain magnetite exsolutions in pyroxene. The soft secondary magnetization component of both the mottled anorthosite and the gabbro may represent a VRM.

The characteristic low intensity of magnetization and low median demagnetization field of the norite suggests that it contains very little pseudo-single- or single-domain magnetite. This is supported by mineralogical evidence. The Fe-rich nature of the chromite and the associated Ti-rich phase in the norite could lead to complicated magnetic behaviour during magnetic cleaning. Ilmeno-hematite, which exsolved from chromite, is a possible carrier of a secondary magnetization component. This component was destroyed at temperatures of c. 500°C, and is roughly antipodal to the primary magnetization direction associated with laths in plagioclase in the anorthosite and gabbro.

The spurious behaviour of certain specimens from all three rock-types during palaeomagnetic investigations, must be linked directly to their magnetic mineral associations, and the relative quantities of these minerals. Since specimens from these rocks exhibited the ability to change the polarity of their magnetization directions, the explanation for this behaviour must lie in their mutual magnetic components. The possible minerals which could be responsible for this unusual behaviour, are the following:

1. Magnetite: (a) Laths in plagioclase.
   (b) Exsolutions in pyroxene.
   (c)Submicroscopic magnetite in ilmeno-hematite.
2. Hematite as exsolutions in ilmenite.

To assist in the explanation of the polarity changes, the following summary of the spurious magnetic behaviour of the three rock-types during palaeomagnetic investigations, and the associated magnetic minerals which could be responsible, is presented:

Firstly, the mottled anorthosite contains a large number of primary magnetite laths in plagioclase, as well as magnetite exsolutions in pyroxene. Lesser ilmeno-hematite occurs. The acquisition of a reversed remanence by the mottled anorthosite was observed in two specimens, which had been cleaned at high alternating fields, and were in storage for an 18 months period. In the case of these specimens, two observations are relevant. Firstly, a major part of the magnetization of the specimens had been destroyed prior to their spontaneous reversal in inclination, and secondly, this reversal may be time-dependent.

The two-pyroxene gabbro contains less magnetite laths in plagioclase than the anorthosite, and comparable amounts of magnetite in pyroxene. However, ilmeno-hematite represents the most common ore mineral assemblage in this rock. A change in sign of the inclination of three gabbro specimens was observed, and as in the case of the anorthosite, these specimens had been subjected to high AF strengths prior to their reversal in inclination. Furthermore, a specimen from the gabbro underwent a spontaneous reversal in inclination whilst in storage in a field-free space. In this case, the major magnetization component carried by magnetite, had already been destroyed, since a temperature of 580^{o}C had been reached during heating of the specimen. This is an indication that hematite must be involved in this unusual behaviour.

The following is important regarding the norite; virtually no magnetite laths in plagioclase are present, and minor magnetite exsolutions in pyroxene occur. In terms of the relative quantities of magnetic minerals, it follows that some mineral other than magnetite, must influence the remanence of the rock strongly.

A change in polarity of two norite specimens was observed during repeated NRM measurements. Thus, in this case, a reversal in inclination of a specimen can take place without the partial destruction of the magnetization components. This suggests that the dominant magnetic carrier in the previous two rocks, viz. magnetite, does not dominate the remanence of the norite. Furthermore, the polarity change, towards the same polarity as that of the primary TRM carried by magnetite laths, at temperatures approaching the Curie

point of magnetite, is significant. Characteristically, norite specimens which are subjected to magnetic cleaning, display an ability to acquire an RRM during AF cleaning, or an RRM-like effect during thermal demagnetization, at temperatures above 580°C.

At this stage it is necessary to consider the ilmeno-hematite intergrowths. Although the ilmenite does not fall in the self-reversing fields identified by Carmichael (1961), Uyeda (1958) and Westcott-Lewis and Parry (1971), Balsley and Buddington (1958) found that all members of the ilmenite-hematite series, irrespective of whether they were optically homogeneous or intergrowths of the two phases, were reversely magnetized (Figure 18(b)). Furthermore, Merrill and Grommè (1969) found that the final composition of ilmenite-hematite does not limit self-reversal, since the self-reversal mechanism is somehow related to a negative exchange interaction between a Ti disordered phase and a Ti ordered phase. Findings of Merrill (1975) support this mechanism. Such a mechanism is, according to Cahn (1967) and Morgan and Smith (1981), somehow related to repeated exsolutions of hematite from ilmenite, which is especially prominent in rocks which have had a long cooling history.

Thus, if hematite is responsible for the observed reversals in magnetization direction, more than one phase of hematite exsolutions may be present in the ilmenite of these rocks. The mechanism could involve the ordering and disordering of Fe and Ti ions in the ilmeno-hematite lattice, which could result in an antiparallel superexchange coupling between the two phases (Ishikawa and Syono, 1963).

Another possibility is that minute magnetite grains are associated with the hematite exsolutions in ilmenite. Such a mechanism would involve magnetostatic exchange interactions between two closely intergrown magnetic minerals which have different Curie points.

The most likely possibility which could account for the observed inclination-reversals, is an interaction between magnetite laths in plagioclase, or magnetite in pyroxene, and ilmeno-hematite. This mechanism could involve one of the following: the antiparallel coupling between two magnetization carriers, namely magnetite and

hematite, with different Curie points; interaction between magnetite and hematite, in which case it would imply that the hematite has a reversed TRM; or either of the above to produce an intermediate-coercivity secondary magnetization component carried by hematite which is reversed with respect to the TRM of the magnetite. Since no magnetization component could be identified at temperatures above 600°C, no evidence exists for a reversed TRM carried by hematite. It thus seems more likely that hematite probably carries a CRM.

The specimen from the two-pyroxene gabbro which underwent a spontaneous partial reversal in inclination in a field-free space during stepwise thermal demagnetization, demonstrates that hematite must be involved in the process, since the TRM of magnetite would have been destroyed during heating to temperatures above 580°C. Thus evidence points to the fact that hematite has the ability to readily follow other magnetic carriers parasitically.

This investigation indicates a correlation between features such as the intensity of remanence of the magnetic minerals in these rocks, their relative abundance, their oxidation-exsolution features and domain states, and their compositions. A correlation between the polarity of the major remanent component in the rocks, and the carrier of this magnetization component, was found. Other carriers of magnetization were also linked to specific magnetization components. The partial self-reversal of magnetization which was observed in a specimen, and the ability of certain specimens to undergo a spontaneous polarity reversal, is probably related to exsolutions of hematite in ilmenite. The relative quantities of the respective carriers of magnetization seem to determine the polarity of these rocks and impart different magnetic signatures to them. Although the possibility of a geomagnetic field reversal to account for the differences in polarity between the anorthosite-gabbro unit and the norite cannot be excluded, evidence obtained from this investigation suggests that the observed magnetic polarity difference between the norite and the anorthosite-gabbro unit at this sampling site, is due to a partial self-reversal of magnetization, which is a result of the specific magnetic mineralogy of the different rock-types.

8. ACKNOWLEDGEMENTS:

The writer wishes to express her gratitude to all those who assisted her during this study. Particular thanks are due to the following people and institutions:

1. The University of Pretoria and the Institute for Geological Research on the Bushveld Complex for the use of their facilities and for financial support.

2. The Chief Director of the Geological Survey of South Africa for the use of the palaeomagnetic laboratory; and special thanks to Mr. Manfred Hauger and Ria Blom for their support.

3. My supervisors, Dr. P.J. Hattingh and Prof. C.P. Snyman for their patience and guidance.

4. Colleagues and friends for all their assistence during the duration of this study, and Pat Eriksson in particular for his help with the diagrams.

A special word of appreciation is due to my family; I would like to thank my husband, Mike, and my parents in particular for all their support and encouragement.

9. REFERENCES:

ADE-HALL, J. M., AND WATKINS, N. D. (1970). Absence of correlations between petrology and natural remanence polarity in Canary Island lavas. Geophys. J. R. astr. Soc., 19, 351-360.

ADE-HALL, J. M., AND WILSON, R. L. (1969). Opaque petrology and natural remanence polarity in Mull (Scotland) dykes. Geophys. J. R. astr. Soc., 18, 333-352.

BALSLEY, J. R., AND BUDDINGTON, A. F. (1954). Correlation of reverse remanent magnetism and negative anomalies with certain minerals. J. Geomag. Geoelectr., 6, 176-181.

BALSLEY, J. R., AND BUDDINGTON, A. F. (1958). Iron titanium oxide minerals, rocks, and aeromagnetic anomalies of the Adirondack area, New York. Econ. Geol., 53, 777-805.

BANERJEE, S. K. (1972). Iron-titanium-chromite a possible new carrier of remanent magnetization in lunar rocks. Proc. Third Lun. Sc. Con., (Suppl. 3., Geochim. Cosmochim. Acta), 3, 2337-2342.

BECK, M. E., Jr. (1966). The effect of magmatic differentiation on the magnetic properties of diabase sheets of southeastern Pennsylvania. United States Geol. Survey Professional Paper, 550 D, D, 109-116.

BERGH, H. W. (1970). Paleomagnetism of the Stillwater Complex, Montana. In: Runcorn, S. K. (ed), Palaeogeophysics, Academic Press, London, 143-158.

BUDDINGTON, A. F., AND LINDSLEY, D. H. (1964). Iron-titanium oxide minerals and synthetic equivalents. J. Petrol., 5, 310-357.

BUTCHER, A. R. (1985). Magnetite compositions, 17-24. In: Annual Report, Institute for Geological Research on the Bushveld Complex, University of Pretoria, 107pp.

BUTTON, A. (1978). Diapiric structures in the Bushveld, north-eastern Transvaal. Econ. Geol. Res. Unit, Univ. Witwatersrand, Johannesburg. Inf. Circ., 123, 6pp.

CAHN, J. W. (1967). Spinodal decomposition. Trans. Met. Soc. A.I.M.E., 242, 166-180.

CARMICHAEL, C. M. (1961). The magnetic properties of ilmenite-hematite crystals. Proc. Royal Soc. London, Ser. A., 263, 508-530.

CHAMPION, D. E., AND CHRISTIANSEN, R. L. (1984). Occurrences of self-reversing remanent magnetization in pyroclastic deposits of Mt.Shasta, California. Eos, 65, 861.

CISOWSKI, S. M. (1980). The relationship between the magnetic properties of terrestrial igneous rocks and the

composition and internal structure of their component Fe-oxides grains. Geophys. J. R. astr. Soc., 60, 107-122.

COE, R. S. (1979). The effect of shape anisotropy on TRM direction. Geophys. J. R. astr. Soc., 56, 369-383.

COLLINSON, D. W. (1983). Methods in rock magnetism and palaeomagnetism. Techniques and instrumentation. Chapman and Hall Ltd., London, 503pp.

COX, A. (1980). Stochastic models for the polarity bias of geomagnetic reversals. Eos, 61, 222.

COX, A., AND DOELL, R. R. (1960). Review of palaeomagnetism. Bull. Geol. Soc. Am., 71, 645-768.

CREER, K. M., AND ISPIR, Y. (1970). An interpretation of the behaviour of the geomagnetic field during polarity transitions. Phys. Earth Planet. Int., 2, 283-293.

DANCHIN, R. V., AND d'OREY, F. (1972). Chromian spinel exsolution in ilmenite from the Premier Mine, Transvaal, South Africa. Contrib. Mineral. Petrol., 35, 43-52.

DAVIS, K. E.(1981) . Magnetite rods in plagioclase as the primary carrier of stable NRM in ocean floor gabbros. Earth Planet. Sci. Lett., 55, 190-198.

DAY, R. (1975). Some curious thermomagnetic curves and their interpretation. Earth Planet. Sci. Lett., 27, 95-100.

DAY, R. (1977). TRM and its variation with grain size. J. Geomag. Geoelectr., 29, 233-265.

DODSON, R. (1980). The distribution of the nondipole field as a function of the source geometry. Eos, 61, 221.

ENGELBRECHT, J. P. (1986). Die Bosveld Kompleks en sy vloergesteentes in die omgewing van Nietverdiend, wes-Transvaal. Ph.D. thesis, Univ. Pret. (unpubl), 327 pp.

EVANS, M. E., AND McELHINNY, M. W. (1969). An investigation of the origin of stable remanence in magnetite-bearing igneous rocks. J. Geomag. Geoelectr., 21, 757-773.

EVANS, M. E., McELHINNY, M. W., AND GIFFORD, A. C. (1968). Single domain magnetite and high coercivities in a gabbroic intrusion. Earth Planet. Sci. Lett., 4, 142-146.

EVERITT, C. W. F. (1962). Self-reversal of magnetization in a shale containing pyrrhotite. Phil. Mag., 7 (77), 831-842.

FISHER, R. A. (1953). Dispersion on a sphere. Proc. Royal Soc. London, Ser. A., 217, 295-305.

FLEET, M. E., BILCOX, G. A., AND BARNETT, R. L. (1980).

Oriented magnetite inclusions in pyroxenes from the Grenville Province. Can. Min., 18, 89-99.

FORD, W. E. (1932). Dana's textbook of Mineralogy, 4th Ed. John Wiley and Sons, Inc., New York, 851 pp.

FULLER, M., WILLIAMS, I., AND HOFFMAN, K. A. (1979). Paleomagnetic records of geomagnetic field reversals and the morphology of the transitional fields. Rev. Geophys. Space Phys., 17, 179-203.

GALLAGHER, K. J., FEITKNECHT, W., AND MANNWEILER, U. (1968). Mechanism of oxidation of magnetite to γ- Fe_2O_3. Nature, 217, 1118-1121.

GORTER, E. W. (1957). Chemistry and magnetic properties of some ferrimagnetic oxides. Adv. Phys., 6, 336-361.

GOUGH, D. I., AND VAN NIEKERK, C. B. (1959). A study of the palaeomagnetism of the Bushveld Gabbro. Phil. Mag., 4 (37), 126-135.

GROENEVELD, D. (1968). The Bushveld Igneous Complex in the Stoffberg area, Eastern Transvaal, with special reference to the magnetite seams. D.Sc. thesis, Univ. Pret. (unpubl.), 169pp.

HAGGERTY, S. E. (1976a). Opaque mineral oxides in terrestrial igneous rocks. In: Rumble, D. (ed), Oxide minerals. Min. Soc. Am., Short Course Notes, no.3, Hg101-Hg276.

HAGGERTY, S. E. (1976b). Oxidation of opaque mineral oxides in basalts. In: Rumble, D. (ed), Oxide minerals. Min. Soc. Am., Short Couse Notes, no.3, Hg1-Hg98.

HALGEDAHL, S., AND FULLER, M. (1980). Magnetic domain observations of nucleation processes in fine particles of intermediate titanomagnetite. Nature, 288, 70-72.

HALLS, H. C. (1976). A least-squares method to find a remanence direction from converging remagnetization circles. Geophys. J. R. astr. Soc., 45, 297-304.

HALLS, H. C. (1979). Separation of multicomponent NRM: combined use of difference and resultant magnetization vectors. Earth Planet. Sci. Lett., 43, 303-308.

HARGRAVES, R. B., AND PETERSON, N. (1971). Notes on the correlation between petrology and magnetic properties of basaltic rocks. Zeitschrift für Geophys., 37, 367-382.

HARGRAVES, R. B., AND YOUNG, W. M. (1969) . Source of stable remanent magnetism in Lambertsville diabase. Am. J. Sc., 267, 1161-1177.

HATTINGH, P. J. (1983). A palaeomagnetic investigation of the layered sequence of the Bushveld Complex. D.Sc. thesis, Univ. Pret. (unpubl), 177pp.

HATTINGH, P. J. (1986a). The palaeomagnetism of the main zone of the eastern Bushveld Complex. Tectonophys., 124, 271-295.

HATTINGH, P. J. (1986b). The palaeomagnetism of the main zone in the western Bushveld Complex. Earth Planet. Sci. Lett., 79, 441-452.

HEDLEY, I. G. (1968). Chemical remanent magnetization of the FeOOH, Fe_2O_3 system. Phys. Earth Planet. Int., 1, 103-121.

HELLER, F. (1980). Self-reversal of natural remanent magnetisation in the Olby-Laschamp Lavas. Nature, 284, 334-335.

HOFFMAN, K. A. (1975). Cation diffusion processes and self-reversal of thermoremanent magnetization in the ilmenite-haematite solid solution series. Geophys. J. R. astr. Soc., 41, 65-80.

HOFFMAN, K. A. (1982). The testing of geomagnetic reversal models: recent developments. Phil. Trans. R. Soc. Lond., A 306, 147-159.

HOFFMAN, K. A., AND DAY, R. (1978). Separation of multi-component NRM: a general method. Earth Planet. Sci. Lett., 40, 433-438.

HOFFMAN, K. A., AND SHIVE, P. N. (1982). Self-reversal of natural Ti-rich titanomagnetites by low temperature oxidation. Eos, 63, 306.

ISHIKAWA, Y., AND SYONO, Y. (1963). Order-disorder transformations and reverse thermoremanent magnetism in the $FeTiO_3$-Fe_2O_3 system. Phys. Chem. Solids, 24, 517-528.

KADZIALKO-HOFMOKL, M., AND KRUCZYK, J. (1976). Complete and partial self-reversal of natural remanent magnetization of basaltic rocks from Lower Silesia, Poland. Pure and Applied Geophysics, 114, 207-213.

KEIL, K., AND FRICKER, P. E. (1974). Baddeleyite (ZrO_2) in gabbroic rocks from Axel, Heiberg Island, Canadian Arctic Archipelago. Amer. Mineral., 59, 249-253.

KIRSCHVINK, J. L. (1980). The least-squares line and plane and the analysis of palaeomagnetic data. Geophys. J. R. astr. Soc., 62, 699-718.

KRETZ, R. (1963). Distribution of magnesium and iron between orthopyroxene and calcic pyroxene in natural mineral assemblages. Jour. Geol., 71, 773-785.

LARSEN, E. E., AND STRANGWAY, D. W. (1966). Magnetic polarity and igneous petrology. Nature, 212, 756-757.

LEE, C. A. (1981). Post-deposition structures in the Bushveld Complex mafic sequence. J. geol. Soc. London, 138, 327-341.

LINDSLEY, D. H. (1976). The crystal chemistry and structure of oxide minerals as exemplified by the Fe-Ti oxides. In: Rumble, D. (ed), Oxide Minerals. Min. Soc. Am., Short Course Notes, no. 3, L1-L88.

LOMBAARD, B. V. (1934). On the differentiation and relationships of the rocks of the Bushveld Complex. Trans. Geol. Soc. S. Afr., 37, 5-52.

LOWRIE, W., AND FULLER, M. (1971). On the alternating field demagnetization characteristics of multidomain thermoremanent magnetization in magnetite. J. Geophys. Res., 76, 6339-6349.

McELHINNY, M. W. (1964). An improved method for demagnetising rocks in alternating magnetic fields. Geophys. J. R. astr. Soc., 10, 369-374.

McELHINNY, M. W. (1973). Palaeomagnetism and plate tectonics. Cambridge Univ. Press, 358pp.

MERRILL, R. T. (1975). Magnetic effects associated with chemical changes in igneous rocks. Geophys. Surv., 2, 277-311.

MERRILL, R. T., AND GROMMÉ, C. S. (1969). Nonreproducible self-reversal of magnetization in diorite. J. Geophys. Res., 74, 2014-2024.

MOLYNEUX, T. G. (1970). A geological investigation of the Bushveld Complex in Sekhukhuneland and part of the Steelpoort Valley, Eastern Transvaal with particular reference to the oxide minerals. D.Sc. thesis, Univ. Pret. (unpubl), 125pp.

MOON, T. S. (1984). Single domain reversal. Eos, 65, 861.

MOORE, A. C. (1968). Rutile exsolution in orthopyroxene. Contrib. Mineral. Petrol., 17, 233-236.

MORGAN, G. E., AND BRIDEN, J. C. (1981). Aspects of Precambrian palaeomagnetism, with new data from the Limpopo Mobile belt and Kaapvaal Craton of Southern Africa. Phys. Earth Planet. Int., 24, 142-168.

MORGAN, G. E., AND SMITH, P. P. K. (1981). Transmission electron microscope and rock magnetic investigations of remanence carriers in a Precambrian metadolerite. Earth Planet. Sci. Lett., 53, 266-240.

MURTHY, G. S., EVANS, M. E., AND GOUGH, D. I. (1971). Evidence of single domain magnetite in the Michikamau anorthosite. Can. J. Earth Sci., 8, 361-370.

NASLUND, H. R. (1987). Lamellae of baddeleyite and Fe-Cr-spinel in ilmenite from the Basistoppen sill, East Greenland. Can. Min., 25, 91-96.

NIENABER-ROBERTS, C. J. (1986). A note on the needlelike inclusions in plagioclase from the Bushveld Complex. Ann. geol. Surv. S. Afr., 20, 55-58.

NISHIDA, J., AND SASAJIMA, S. (1974). Examination of self-reversal due to N-type magnetization in basalt. Geophys. J. R. astr. Soc., 37, 453-460.

O'REILLY, W. (1976). Magnetic minerals in the crust of the earth. Earth Rep. Prog., Phys., 39, 857-908.

O'REILLY, W., AND BANERJEE, S. K. (1967). The mechanism of oxidation in titanomagnetites: A magnetic study. Min. Mag., 36, 29-37.

OWENS, W. H. (1974). Mathematical model studies on factors affecting the magnetic anisotropy of deformed rocks. Tectonophys., 24, 115-131.

PHILLIPS, F. C. (1963). An introduction to crystallography. Longmans, Green and Co. Ltd., London, 340pp.

PHILLIPS, J. D. (1977). Time variation and asymmetry in the statistics of geomagnetic reversal sequences. Jour. Geophys. Res., 82, 835-843.

PIPER, J. D. A. (1977). Magnetic stratigraphy and magnetic-petrologic properties of Precambrian Gardar Lavas, South Greenland. Earth Planet. Sci. Lett., 34, 247-263.

RAAL, F. (1965). The transition between the Main and Upper Zone of the Bushveld Complex in the Western Transvaal. M.Sc. thesis, Univ. Pret. (unpubl), 59pp.

RAMDOHR, P. (1980). The ore minerals and their intergrowths. Second Ed., Volume 2. Pergamon Press, Oxford, 1207pp.

SCHARLAU, T. A. (1972). Petrographische und petrologische untersuchungen in der Haupt-Zone des östlichen Bushveld-Komplexes, District Groblersdal/ Transvaal. Dissertation, Johann Wolfgang Goethe Universität zu Frankfurt am Main.

SCHMIDTBAUER, E. (1971). Magnetization and lattice parameters of Ti substituted Re-Cr spinels. J. Phys. Chem. Solids, 32, 71-76.

SCHULT, A. (1968). Self-reversal of magnetization and chemical composition of titanomagnetites in basalts. Earth Planet. Sci. Lett., 4, 57-63.

SHARPE, M. R. (1981). The chronology of magma influxes to the eastern compartment of the Bushveld Complex as

exemplified by its marginal border groups. J. geol. Soc. London, 138, 307-326.

SHARPE, M. R. (1982). The floor contact of the eastern Bushveld Complex: Field relations and petrography. Inst. geol. Res. Bushveld Complex, Univ. Pret., Res. Rep. 36, 43pp.

SHARPE, M. R. (1985). Strontium isotope evidence for preserved density stratification in the main zone of the Bushveld Complex, South Africa. Nature, 316, 119-126.

SHARPE, M. R., AND CHADWICK, B. (1982). Structures in Transvaal Sequence rocks within and adjacent to the eastern Bushveld Complex. Trans. geol. Soc. S. Afr., 85, 29-41.

SOFFEL, H. C. (1971). The single-domain (multi-domain) transition in intermediate titanomagnetites. J. Geophys., 37, 451-470.

SOUTH AFRICAN COMMITTEE FOR STRATIGRAPHY (S.A.C.S.).(1980). Stratigraphy of South Africa, Part 1 : Lithostratigraphy of the Republic of South Africa, South West Africa/ Namibia and the Republic of Bophuthatswana, Transkei and Venda. Geol. Surv. S. Afr. Hb. 8, 690pp.

STACEY, F. D. (1963). The physical theory of rock magnetism. Adv. Phys., 12, 46-133.

TARLING, D. H. (1971). Principles and applications of Palaeomagnetism. Chapman and Hall Ltd., London, 164pp.

TARLING, D. H. (1983). Palaeomagnetism. Principles and applications in Geology, Geophysics and Archaeology. Chapman and Hall Ltd., London, 379 pp.

THORPE, A. N., MINKEN, J. A., SENFTLE, F. E.,ALEXANDER, C., BRIGGS, C., EVANS, H. T., Jr., AND NORD, G. L. (1977). Cell dimensions and antiferromagnetism of lunar and terrestrial ilmenite single crystals. J. Phys. Chem. Solids, 38, 115-123.

TIVEY, M., AND JOHNSON, H. P. (1981). Characterization of viscous remanent magnetization in single- and multi-domain magnetite grains. Geophys. Res. Lett., 8, 217-220.

TRUKHIN, V. I., ZHILYAEVA, V. A., SAVRASOV, D. I., SAFROSHKIN, V. YU., AND BUBNOV, A. V. (1984). Self-reversal of thermoremanent magnetization in rocks from Yakutian kimberlite pipes. Physics Solid Earth, 20, 849-857.

TUCKER, P. AND O'REILLY, W. (1980a). The acquisition of thermoremanent magnetization by multidomain single-crystal titanomagnetite. Geophys. J. R. astr. Soc., 60, 21-36.

TUCKER, P., AND O'REILLY, W. (1980b). The laboratory simulation of deuteric oxidation of titanomagnetites: effect on magnetic properties and stability of thermoremanence.

Phys. Earth Planet. Int., 23, 112-133.

UYEDA, S. (1955). Magnetic interaction between ferromagnetic minerals contained in rocks. J. Geomag. Geoelectr., 7, 9-36.

UYEDA, S. (1958). Thermo-remanent magnetism as a medium of palaeomagnetism, with special reference to reverse thermo-remanent magnetism. Japanese Jour. Geophys., 2, 1-23.

VADKOVSKII, V. N., GURARII, G. Z., AND MAMIKON'YAN, M. R. (1980). Analysis of the process of geomagnetic field reversal. Physics Solid Earth, 16, 506-516.

VAN ZYL, J. P. (1970). The petrology of the Merensky Reef and the associated rocks on Swartklip 988, Rustenburg District. Geol. Soc. S. Afr. Spec. Publ. 1, 80-107.

VERHOOGEN, J. (1956). Ionic ordering and self-reversal of magnetization in impure magnetites. Jour. Geophys. Res., 61, 201-209.

VERHOOGEN, J. (1962). Oxidation of iron-titanium oxides in igneous rocks. Jour. Geol., 70, 168-181.

VON GRUENEWALDT, G. (1970). On the phase-change orthopyroxene-pigeonite and the resulting textures in the Main and Upper Zones of the Bushveld Complex in the eastern Transvaal. Geol. Soc. S. Afr. Spec. Publ. 1, 46-58.

VON GRUENEWALDT, G. (1971). A petrographical and mineralogical investigation of the rocks of the Bushveld Igneous Complex in the Tauteshoogte-Roossenekal area of the eastern Transvaal. D.Sc. thesis, Univ. Pret. (unpubl), 228pp.

VON GRUENEWALDT, G. (1973). The main and upper zones of the Bushveld Complex in the Roossenekal area, Eastern Transvaal. Trans. Geol. Soc. S. Afr., 76, 207-227.

VON GRUENEWALDT, G. (1976). Sulfides in the upper zone of the eastern Bushveld Complex. Econ. Geol., 71, 1324-1336.

VON GRUENEWALDT, G., SHARPE, M. R., AND HATTON, C. J. (1985). The Bushveld Complex: Introduction and Review. Econ. Geol., 80, 803-812.

WATKINS, N. D., AND HAGGERTY, S. E. (1965). Some magnetic properties and the possible petrogenetic significance of oxidized zones in an Icelandic olivine basalt. Nature, 206, 797-800.

WATKINS, N. D., AND HAGGERTY, S. E. (1967). Primary oxidation variation and petrogenesis in a single lava. Contrib. Mineral. Petrol., 15, 251-271.

WATSON, G. S. (1956). A test for randomness of directions. Mon. Not. R. Astr. Soc., Geophys. Suppl., 7, 289-300.

WESTCOTT-LEWIS, M. F., AND PARRY, L. G. (1971). Thermoremanence in synthetic rhombohedral iron-titanium oxides. Aust. J. Phys., 24, 735-752.

WILLIAMS, C. T. (1978). Uranium-enriched minerals in mesostasis areas of the Rhum layered pluton. Contrib. Mineral. Petrol., 66, 29-39.

WILSON, R.L., AND WATKINS, N.D. (1967). Correlation of petrology and natural magnetic polarity in Columbia Plateau basalts. Geophys. J. R. astr. Soc., 12, 405-424.

ZIJDERVELD, J. D. A. (1967). A.c. demagnetization of rocks: analysis of results. In: Collinson, D. W., Creer, K. M. and Runcorn, S. K. (ed), Methods in Palaeomagnetism, 254-286.